

MAY 1990

VOLUME 21

NUMBER 1

NEWSLETTER

INDEX

	<u>page</u>
From the Editor's Desk	i
Conference Schedule	ii
International Symposium on Polymeric Microspheres	iii
FAX Numbers & Membership List	iv, v

CONTRIBUTIONS

J M Asua	1
J Barton	3
D C Blackley	8
F Candau	10
M C Croucher	103
M S El-Aasser	13
A P Gast	24
A L German	27
F K Hansen	31
A Klein	13
Do Ik Lee	79
J Lyklema	33
M Nomura	35
C Pichot	36
I Piirma	39
G W Poehlein	44
G Reiss	63
R L Rowell	71
W B Russel	76
F Saunders	79
V T Stannett	82
K Tauer	85
J W Vanderhoff	13
J A Waters	100
M Winnik	103

FROM THE EDITOR'S DESK

CONTRIBUTIONS

We are please to welcome several new contributors to this bumper edition of the IPCG Newsletter: Jaroslav Barton, Ton German and Klaus Tauer. Members will enjoy reading their excellent contributions and look forward to their future participation in the Group's activities. Gary Poehlein's contribution for the last Newsletter arrived too late and was held over until this one.

MEMBERSHIP

Vivian Stannett has officially retired from his Camille Dreyfus Professorship (of which he is now Emeritus) and is writing up the PhD thesis material of his last PhD student. Despite several letters, Dr Leonardo Rios has failed to respond to the offer of membership of the IPCG.

FAX NUMBERS & MEMBERSHIP LIST

An updated list of the FAX numbers is enclosed, as is the current membership list.

DISTRIBUTION OF NEWSLETTER

We are all most grateful to Pete Sperry and Christian Pichot, who are now distributing the Newsletter in North America and Europe respectively. I will look after the Pacific distribution.

CONFERENCES

Please note that the ACS Divisions of Polymer Materials Science and Colloid and Surface Chemistry will cosponsor a Special Symposium on Polymer Latexes in honor of Robert M Fitch. It will focus on Latex Particle Nucleation and Particle Morphology is to be held 14-19 April, 1991 in Atlanta, Ga. It is being organized by Mohamed El-Aasser. *Abstracts are due 1 September, 1990.* The next Gordon Research Conference on Polymer Colloids will be held 1-5 July, 1991 at Tilton, New Hampshire. Again the Chair is Mohamed El-Aasser.

Note, too, the Internation Symposium on Polymeric Microspheres that is to be held 24-27 October, 1991 at Fukui University, Fukui, Japan. This is a cooperative venture between EPI, Lehigh; LMO, CNRS France; and PPT, McMaster University (see notice piii).

NEXT NEWSLETTER

Please forward your contributions to me by 30 September, 1990.

DH Napper
Editor

CONFERENCE SCHEDULE

1990

<u>Conference</u>	<u>Location</u>	<u>Date</u>
64th Colloid and Surface Science Symposium	Lehigh	18-20 June
33rd IUPAC Polymers (MACRO 90)	Montreal	8-13 July
200th ACS National Meeting	Washington	26-31 August
Faraday Discussion 'Colloid Stability'	Bristol	10-13 September

1991

201st ACS National Meeting -Latex Particle Nucleation and Morphology (honoring R M Fitch)	Atlanta	14-19 April
Gordon Research Conference Polymer Colloids	Tilton	1-5 July
7th International Conference Colloid Surfaces	Compiègne	7-12 July
Polymeric Microspheres Symposium	Fukui	24-27 Oct



FUKUI UNIVERSITY

9-1, BUNKYO 3-CHOME
FUKUI-SHI 910, JAPAN

Dear International Polymer Colloids Group Members:

CALL FOR PAPERS
for
INTERNATIONAL SYMPOSIUM ON POLYMERIC MICROSPHERES
OCTOBER 24 - 27, 1991
FUKUI UNIVERSITY, FUKUI, JAPAN

We are planning to organize an international symposium entitled "International Symposium on Polymeric Microspheres" at Fukui University under the sponsorship of the Ministry of Education, Japan. This symposium will be held during the period of October 24-27, 1991 in cooperation with Emulsion Polymers Institute, Lehigh University, U.S.A., McMaster Institute for Polymer Production Technology, McMaster University, CANADA and Laboratoire des Materiaux Organiques, CNRS, FRANCE.

The topics to be covered are:

- (1) Kinetics and Mechanism - Particle formation and growth in
 - (a) Preparation of organic polymer microspheres by emulsion, dispersion and other alternative polymerizations, and
 - (b) Preparation of inorganic polymer microspheres, for example, by alkoxide method.
- (2) Reactor Models and Simulation.
- (3) Characterization and its New Technique on
 - (a) Interfacial properties and morphology of polymeric microspheres,
 - (b) Dispersion properties.
- (4) Application of Polymeric Microspheres.

Registration Fee:

includes a copy of proceedings and reception.

- | | | |
|----------------------------------|-------|------------|
| (1) Active participants/Students | ----- | ¥20,000yen |
| (2) Non-active participants | ----- | ¥50,000yen |

The number of papers is limited to about 40, including invited papers due to limitation of time, and the paper acceptable is only for oral presentation. Some financial support for travel and local expenses will be available for the Member of International Polymer Colloids Group who belongs to an university or other nonprofit organization. The first circular will be distributed around the end of May, 1990. However, we hope that those who are interested in submitting a paper or attending the symposium write their intention to:

Professor Mamoru Nomura
Department of Materials Science and Engineering,
Fukui University, Fukui, Japan

at their earliest convenience.

Sincerely yours,

Mamoru Nomura
Organizer

Secretary: D.H. Napper
 School of Chemistry
 University of Sydney
 NSW 2006 AUSTRALIA

IPCG

INTERNATIONAL POLYMER COLLOIDS GROUP

IPCG Membership FAX (Telecopier) Numbers

J M	Asua	34-43-21-2236
D R	Bassett	1-304-747-5570
D C	Blackley	44-1-700-4272
F	Candau	33-88-41-4099
M	Croucher	1-416-822-6984
J S	Dodge	1-216-933-0509
A S	Dunn	44-61-200-4484
M S	El-Aasser	1-215-758-5423
V I	Eliseeva	7-095-230-2332
A P	Gast	1-415-725-7294
A L	German	31-40-44-2576
J W	Goodwin	44-272-25-1295
A	Hamielec	1-416-528-5114
F K	Hansen	47-2-45-5441
H	Kast	49-621-609-2502
Do Ik	Lee	1-517-638-7510
J	Lyklema	31-83-708-4141
S	Muroi	81-462-21-7212
D H	Napper	61-2-692-3329
M	Nomura	81-776-26-7448
R H	Ottewill	44-272-25-1295
R	Pelton	1-416-521-1350
C	Pichot	33-72-72-8080
I	Piirma	1-216-375-5290
G W	Poehlein	1-404-894-3120
G	Riess	33-89-59-9859
W B	Russel	1-609-258-6744
F L	Saunders	1-517-636-6558
P R	Sperry	1-215-592-3377
V T	Stannett	1-919-737-3465
P J	Stenius	46-820-8998
D C	Sundberg	1-603-862-3564
K	Takamura	1-519-332-5933
R E	Uschold	1-302-695-3645
A	Vrij	31-30-52-1877
T G M	van de Ven	1-514-398-7249
J W	Vanderhoff	1-215-758-5423
J A	Waters	44-753-69-4665
M	Winnick	1-416-978-8775

NORTH AMERICA

Dr D R Bassett
Technical Center
Union Carbide Corporation
South Charleston
West Virginia 25303 USA

Dr M Croucher
Xerox Research Centre of Canada
2660 Speakman Drive
Mississauga Ontario
CANADA L5K 2L1

Dr J S Dodge
B F Goodrich
Chemical Division Technical Centre
Avon Lake Ohio 44012
USA

Dr M S El-Aasser
Emulsion Polymer Institute
Lehigh University
111 Research Drive Bldg A
Bethlehem PA 18015-4732 USA

Dr A F Gast
Department of Chemical Engineering
Stanford University
Stanford
California 94305-5025 USA

Dr R M Fitch
5020 Windy Point Rd
Racine WI 53402
USA

Dr A E Hamielec
Department of Chemical Engineering
McMaster University
Hamilton Ontario
CANADA L8S 4L7

Dr A Klein
Department of Chemical Engineering
Whitaker Laboratory No.5
Lehigh University Bethlehem
Pennsylvania 18015 USA

Dr I M Kreiger
Olin Building
Case-Western Reserve University
Cleveland Ohio 44106
USA

Dr R Pelton
Department of Chemical Engineering
McMaster University
Hamilton Ontario
CANADA L8S 4L7

Dr I Piirma
Institute of Polymer Science
University of Akron
Akron Ohio 44325-3909
USA

Dr G W Poehlein
Centennial Research Building 282
Georgia Institute of Technology
Atlanta Georgia 30332-0370
USA

Dr R L Rowell
Dept of Chemistry GRC-T102
University of Massachusetts
Amherst MA 01003
USA

Dr F L Saunders
Dow Chemical Co
Central Research 1712 Building
Midland Michigan 48640
USA

Dr K Takamura
BASF Canada
PO Box 3077
453 Christina St, South
Sarnia Ontario CANADA

Dr W B Russel
Department of Chemical Engineering
Princeton University
Olden St Princeton
New Jersey 08544 USA

Dr P R Sperry
Exploratory Polymer Research
Rohm & Haas Co
727 Norristown Rd Spring House
Pennsylvania 18901 USA

Dr V T Stannett
Department of Chemical Engineering
North Carolina State University
Box 5035 Raleigh
North Carolina USA

Dr J W Vanderhoff
Emulsion Polymers Institute
Lehigh University
111 Research Drive Bldge A
Bethlehem PA 18015-4732 USA

Dr T G M van de Ven
Pulp & Paper Building
Dept of Chem McGill University
3420 University St Montreal PQ
CANADA H3A 2A7

Dr D C Sundberg
Department of Chemical Engineering
Kingsbury Hall
University of New Hampshire Durham
New Hampshire 03824 USA

Dr R Uschold
Fabricated Products Department
Du Pont Experimental Station
Exp Stat 1/207 Wilmington
Delaware 19806 USA

Dr M Winnik
Department of Chemistry
University of Toronto
Ontario M5S 1A1
CANADA

Dr C F Zukoski
Department of Chemical Engineering
113 Roger Adams Laboratory
1209 W. California St
Urbana IL 61801 USA

Dr Do Ik Lee
Dow Chemicals
Designed Latex Research 1604 Bldg
Midland Michigan 48674
USA

REST OF THE WORLD

Dr A L German
Eindhoven University Technology
Department of Polymer Chemistry
PO Box 513
5600 MB Eindhoven
NETHERLANDS

Dr A S Dunn
Department of Chemistry
UMIST
PO Box 88
Manchester M60 1QD
ENGLAND

Dr A Vrij
Riksuniversiteit te Utrecht
van't Hoff Laboratorim
Postbus 80 501 Padualaan B
3508 TB Utrecht
NETHERLANDS

Dr C Pichot
CNRS Laboratoire des Materiaux
Organiques BP 24
69390 Vernaison
FRANCE

Dr D C Blackley
London School Polymer Technology
Polytechnic of North London
Holloway Rd
London N7 8DB
ENGLAND

Dr D H Napper
Department of Physical Chemistry
University of Sydney
Sydney NSW
AUSTRALIA 2006

Dr F Candau
(CRM-EAHP) Institute Charles Sadron
6 Rue Boussingault
Strasbourg Cedex 67083
FRANCE

Dr F K Hansen
University of Oslo
PO Box 1033
Blindern
N-0315 Oslo 3
NORWAY.

Dr G Riess
Ecole Nationale Supérieure
de Chimie de Mulhouse
3 rue A Werner
68093 Mulhouse CEDEX
FRANCE

Dr H Kast
EDM-E100 BASF Aktiengesellschaft
D-6700 Ludwigshafen
WEST GERMANY

Dr J Barton
Polymer Institute
Slovak Academy of Science
Dubravsk Cesta
842 36 Bratislava
CZECHOSLOVAKIA

Dr J G H Joosten
DSM Dept FA - GF
P.O.Box 18 6160
MD Geleen
NETHERLANDS

Dr J Lyklema
Laboratory for Physical &
Colloid Chemistry
Dreijenplein 6
6703 HB Wageningen
NETHERLANDS

Dr J M Asua
Grupo de Ingeniería Química
Facultad de Ciencias Químicas
Universidad del País Vasco
Apto 1072, 20080 San Sebastian
SPAIN.

Dr J Ugelstad
Institutt for Industriell Kemi
Norges Tekniske Høgskole
7034 Trondheim-Nth
NORWAY

Dr J W Goodwin
School of Chemistry
University of Bristol
Cantock's Close
Bristol BS8 1TS
ENGLAND

Dr K Tauer
Institut für Polymerchemie
'Eirich Correns'
Akademie der Wissenschaften DDR
Kantsrasse 55
TELTOW-DDR 1530

Dr M Nomura
Dept of Materials Science &
Engineering
Fukui University Fukui
JAPAN 910

Dr P J Stenius
Ytkemiska Institutet
Box 5607 S-114 86
Stockholm
SWEDEN

Dr R H Ottewill
School of Chemistry
University of Bristol
Cantock's Close
Bristol BS8 1TS
ENGLAND

Dr S Muroi
Japan Research Centre
Grace Japan K K
100 Kaneda Atsugi
Kanagaira 243
JAPAN

Dr V I Eliseeva
Institute of Physical Chemistry
Academy of Sciences of the USSR
Leninsky Prospekt 31
V-31 Moscow
USSR

Mr J Waters
ICI Plc Paints Division
Wexham RD
Slough S12 5DS
ENGLAND

International Polymer Colloids Group Newsletter

Contribution from the Grupo de Ingeniería Química, Facultad de Ciencias Químicas, Universidad del País Vasco, Apdo. 1072, 20080 San Sebastián, Spain.

Reported by José M. Asua

Entry and Exit Rate Coefficients in Emulsion Polymerization of Styrene

(José M. Asua and José C. de la Cal)

The rate coefficient for entry of radicals into the polymer particles and the radical exit rate coefficient were estimated in the seeded emulsion polymerization of styrene using data of the time evolution of the conversion during the approach to the steady-state values of n reported in the literature [1,2]. These data included experiments in which the concentration of polymer particles as well as the initiator concentration were varied. Two different seed particle sizes were used. Parameter estimation was carried out taking into account the variation of the particle size during polymerization. Good fitting of the experimental data was achieved. The dependence of k_a and k_d on the particle size was used in an attempt to discriminate between the models proposed in the literature for the entry and exit rate coefficients. It was found that the collisional model, the diffusional model and the colloidal model for the entry rate coefficient were incompatible with the assumption that desorption of radicals occurred through a diffusion mechanism with no additional resistance in the interphase. The results obtained were consistent with a model in which the entry of radicals into the polymer particles occurred by the propagational mechanism and the radicals desorbed from the polymer particles by diffusion. In addition, the values of k_a and k_d calculated using the equations derived from these mechanisms agreed with those estimated in this work from experimental data.

References:

- 1.- B.S. Hawlett, D.H. Napper and R.G. Gilbert, J. Chem. Soc., Faraday Trans. 1, 76, 1323 (1980) .
- 2.- J.A. Penboss, R.G. Gilbert and D.H. Napper, J. Chem. Soc., Faraday Trans. 1, 82, 2247 (1986).

Semicontinuous Seeded Emulsion Copolymerization of Vinyl Acetate and Methyl Acrylate

(Belén Urquiola, Gurutze Arzamendi, José R. Leiza, Aranzazu Zamora, José M. Asua, Joaquín Delgado¹, Mohamed S. El-Aasser¹ and John W. Vanderhoff¹.)

The semicontinuous seeded emulsion copolymerization of vinyl acetate and methyl acrylate was investigated. The effect of type of process (starved process vs. semi-starved process), type of feed (neat monomer addition vs. monomer emulsion addition), amount of seed initially charged in the reactor, and feed rate on the time evolution of the overall conversion, copolymer composition and polymer particle size was analyzed. It was found that, in the case of the starved process, both monomers, but mainly vinyl acetate, accumulated in the reactor. The preferential accumulation of vinyl acetate resulted in a drift of the copolymer composition. Both monomers accumulation and copolymer composition drift were reduced by increasing the amount of seed initially charged in the reactor and by decreasing the feed rate. For the semi-starved process, it was found that a vinyl acetate rich copolymer was formed when a low methyl acrylate feed was used, whereas a methyl acrylate rich copolymer was obtained at high methyl acrylate feed rates. For both starved process and semi-starved process, the total number of polymer particles, after an initial increase, reached a plateau value which was the same in all of the experiments carried out. These results were analyzed by means of a mathematical model developed for this system.

¹ Emulsion Polymers Institute, Lehigh University.

Polymer Colloids Group Newsletter

Contribution from the Department of Polymerization Reactions,
Polymer Institute of the Slovak Academy of Sciences,
842 36 Bratislava, Czechoslovakia

Reporter: J. Barton

On the Determination of the Locus of Initiation of the Acryl-
amide Polymerization in Inverse Microemulsion

(V. Vašková, J. Bartoň)

The inverse microemulsions are well-known as media for biologically active water-soluble compounds. They belong to non-traditional polymerization systems. Recently, polymerization of water-soluble monomers in such systems has been studied¹⁻⁴.

In order to contribute to the polymerization mechanism, we tried to estimate the locus of initiation. We have studied acrylamide (AAM) polymerization initiated by the water-soluble ammonium peroxydisulfate (APS), the partially - water-soluble 2,2'-azobisisobutyronitrile (AIBN), and/or the oil-soluble dibenzoyl peroxide (BP), in the presence of predominantly water-soluble inhibitor 2,2,6,6-tetramethyl-4-hydroxy-piperidine-1-oxyl (HTPO) or predominantly oil-soluble inhibitor 2,2,6,6-tetramethyl-4-stearoyloxy-piperidine-1-oxyl (STPO). From the results obtained, e.g. inhibition periods and the dependence of inhibition periods on the inhibitor concentration as well as measuring the decay of inhibitors by ESR method, the following conclusions could be made:

1. If APS for initiation of AAM polymerization has been used, the initiation reaction takes place in the water micropool. When the polymerization of AAM starts, HTPO is already completely deactivated. On the contrary STPO, which probably concentrates in the interlayer between water micropool and oil macrophase, practically does not react with primary radicals at all. No inhibition period was observed.

2. If AAM polymerization has been initiated by AIBN, the locus of initiation might be the interlayer. This could be supported by practically the same duration of the inhibition periods measured for the systems containing HTPD or STPD as well as by the fact that in the moment when the polymerization starts the concentration of both inhibitors in the systems is near to zero.
3. If the AAM polymerization has been initiated by BP, the inhibition periods measured are nearly the same for both inhibitors and they are longer than those when using AIBN instead of BP. Besides, the decay of both inhibitors is markedly slower. One could assume that also in this case the locus of the initiation is the interlayer. The initiator is transferred from the oil macrophase to the locus of initiation.

References:

1. F. Candau, J. S. Leong, R. M. Fitch, J. Polymer Sci., Polym. Chem. Ed., 23, 193 (1985).
2. M. T. Carver, U. Dreyer, R. Knoesel, F. Candau, R. M. Fitch, J. Polym. Sci., Part A, 27, 2161 (1989).
3. M. T. Carver, F. Candau, R. M. Fitch, J. Polym. Sci., Part A, 27, 2179 (1989).
4. V. Vašková, V. Juraničová, J. Bartoň, Makromol. Chem., in press.

Effect of Crosslinked Seed Polymer Particles on the Kinetics
of Emulsion Polymerization of Butyl Acrylate

(I. Capek)

A major problem in the kinetic investigation of the batch emulsion polymerization is the number and complexity of the reactions which should be taken into account. This disadvantage can be avoided to some extent by studying the seed emulsion polymerization. In seeded systems, mainly growth of polymer particles occurs. By two-stage polymerization method also the latex with interpenetrating polymer network can be prepared. The preparation involves making a seed latex of a crosslinked polymer (polymer 1) and then introducing into the reaction vessel the second monomer (monomer 2) alone or together with its cross-linking agent. Monomer 2 is then polymerized. Since no fresh (or small amount of) emulsifier is added during the second stage of the polymerization, it is assumed that no new nucleation takes place during monomer 2 polymerization. Here, the growth occurs on the already established latex particles. It has been claimed that this type of polymerization method the morphology of the resulting particles ranges from homogeneous through the simple domain type to the core-shell morphology. Among other criteria, the particle morphology depends on the miscibility of monomer 2 in polymer 1. The mutual compatibility of polymer 1 and 2, the crosslinked density of the networks and the relative hydrophilicities are also involved.

In order to clarify the polymerization mechanism of such systems we investigated the emulsion polymerization of butyl acrylate in the presence of simple or crosslinked poly(ethyl acrylate) particles. In the presence of poly(ethyl acrylate), poly(ethyl acrylate-co-hexamethylene diacrylate) or poly(ethyl acrylate), the rate of polymerization was found to be proportional to the 0.4, 0.6 or 0.55 order of magnitude with respect to the ammonium peroxodisulfate (initiator) concentration. These results show that the reaction order in the system with poly(ethyl acrylate) particles agrees very well with that proposed by the

micellar theory. The increase of the reaction order above 0.4 in the systems with crosslinked seed particles is claimed to a hindered termination of radicals in polymer particles. The presence of pendant unsaturated groups in the crosslinked polymer particles favours formation of "fixed" radicals. They grow in the presence of monomer. These radicals may terminate by the reaction with primary or oligomer radicals, which are very mobile, or by the monomolecular termination mechanism. In the range of high conversion the desactivation of these "fixed" radicals can proceed by the residual termination mechanism. Here bimolecular termination between "fixed" radicals may occur as a consequence of propagation.

In the presence of poly(ethyl acrylate), poly(ethyl acrylate-co-hexamethylene diacrylate) or poly(ethyl acrylate-co-divinylbenzene) particles the number of final (seed and new) polymer particles was found to be proportional to the 0.1, 0.15 or 0.07 order of magnitude with respect to the ammonium peroxydisulfate concentration. It is seen that new slight nucleation takes place during butyl acrylate polymerization. The trend of new nucleation was also supported by the ratio the number of final/seed particles.

In all runs the rate of polymerization increases only slightly with increasing monomer concentration. It indicates the formation of a monomer reservoir. Because the formation of monomer droplets was not proved, monomer was supposed to be located in the emulsifier micelles, water and seed polymer particles.

The decrease of the rate of polymerization with increasing anionic emulsifier concentration was observed. This unexpected behaviour was discussed in terms of the fall in the monomer concentration at the reaction sites as the number of particles increases, the low entry efficiency of radicals into polymer particles and the hydrophilicity of seed polymer particles.

References:

1. W. V. Smith, R. H. Ewart, J. Chem. Phys. 16, 592 (1948).
2. S. K. Soh, D.C. Sundberg, J. Polym. Sci., Polym. Chem. Ed. 20, 1345 (1982).
3. W. Funke, Brit. Polym. J. 21, 107 (1989).

Recent Publications:

1. On the Initiation Mechanism in Emulsion Polymerization Systems,
J. Bartoň, Makromol. Chem., Makromol. Symp. 31, 11 (1990).
2. Polymerization in Inverse Microemulsion,
V. Vašková, V. Juraničová, J. Bartoň,
Makromol. Chem., Macromol. Symp., 31, 201 (1990).
3. Effect of a bi- Unsaturated Monomer on the Emulsion Poly-
merization of Ethyl Acrylate,
I. Capek, J. Kostrubová, J. Bartoň,
Makromol. Chem., Macromol. Symp. 31, 213 (1990).

NOVEL AZO INITIATOR/STABILISERS FOR AQUEOUS EMULSION POLYMERISATION REACTIONS.
II. BEHAVIOUR AS POLYMERISATION INITIATOR/STABILISERS

D. C. Blackley, London School of Polymer Technology,
 The Polytechnic of North London, Holloway, London N7 80B.

Our previous contribution to the Polymer Colloid Group Newsletter was concerned with the preparation, decomposition kinetics and solution properties of a novel series of non-ionic azo initiators which are water-soluble and surface-active. This contribution is concerned with the polymerisation behaviour of these initiators. These initiator/stabilisers are of interest principally because they are capable of functioning as colloid stabilisers for the latices which form during aqueous emulsion polymerisation reactions initiated by them. They are therefore suitable for the initiation of aqueous emulsion polymerisation reactions in the absence of other colloid stabilisers. It will be recalled that we are making these azo initiator/stabilisers the subject of two further contributions to the Polymer Colloid Group Newsletter in response to several requests for further information concerning them which were received following a presentation about them which I gave to the 1989 Polymer Colloids Gordon Research Conference.

The initiator/stabilisers we have investigated are the di-esters of 4,4'-azobis-4-cyanopentanoic acid (4,4'-AB-4-CPA) and a range of fatty-alcohol ethoxylates based upon a mixture of cetyl and oleyl alcohols. The esterification reaction is carried out by reacting the diacid chloride of 4,4'-AB-4-CPA with the fatty-alcohol ethoxylate. It is presumed that esterification takes place via the terminal hydroxyl group of the fatty-alcohol ethoxylate. All the initiators of this type which have been prepared have been found to be capable of initiating the bulk polymerisation of styrene, the aqueous emulsion polymerisation of styrene in the presence of a conventional surfactant such as sodium dodecyl sulphate, and the emulsion polymerisation of styrene in the absence of conventional surfactants or other colloid stabilisers. It is notable that even the azo compounds of low degree of ethoxylation, which are at best very sparingly soluble in water, have been found to be effective as initiators for both types of emulsion polymerisation reaction.

Our interest in these compounds has been principally as initiators for aqueous emulsion polymerisation reactions in the absence of conventional surfactants or other colloid stabilisers. The products of this type of reaction are stable latices of small particle size. Using this type of initiator/stabiliser in the absence of conventional surfactants, it is possible to prepare stable latices which are presumably essentially non-ionic and of very low ionic strength. The colloid stability of these latices is presumably a consequence partly of the presence of undecomposed initiator/stabiliser adsorbed at the particle surfaces and partly of the presence of the decomposition products of the initiator/stabiliser adsorbed at the particle surfaces - the latter would also be expected to be surface-active and to be capable of conferring colloid stability upon hydrophobic sols. We have no information concerning the relative contributions to colloid stability from these two sources, but suspect that the principal contribution may come from the presence of undecomposed initiator/stabiliser. The particle sizes of the latices produced by these emulsion polymerisation reactions are small and uniform. Various shapes of conversion-time curve for this type of reaction have been observed. The shape appears to depend upon factors such as the temperature of the reaction and the degree of ethoxylation of the initiator.

A typical reaction system for the emulsion polymerisation of styrene at 50°C using these azo initiator/stabilisers in the absence of other colloid stabilisers comprises monomer 40 cm³, water 100 cm³ and initiator 1.1×10^{-3} mol. Under these

reaction conditions, the 30-, 45- and 60-mol ethoxylate initiators gave broadly similar conversion-time behaviour, whereas the 24-mol ethoxylate initiator gave a reaction system which polymerised less rapidly than did the other three reaction systems in this series. Thus the times required for 50% conversion of monomer to polymer using this type of reaction system at this temperature were found to be in the range 1 - 2 hours for the 30-, 45- and 60-mol ethoxylate initiators, but ca. 6 hours for the 24-mol ethoxylate initiator.

The observations summarised in the preceding paragraph relate to reaction systems which contained equimolar amounts of the various ethoxylate initiators. Because the degree of ethoxylation, and hence the molecular weight, varies from one initiator/stabiliser to another, the actual weights of initiator in these reaction systems varied, being directly proportional to the molecular weight. We also have results for the behaviour of reaction systems in which the weight of initiator/stabiliser was kept constant. A typical reaction system of this type for the emulsion polymerisation of styrene at 50°C using these azo initiator/stabilisers in the absence of other colloid stabilisers comprises monomer 40 cm³, water 100 cm³ and initiator 5 gm. Under these reaction conditions, the 24-, 30-, 45- and 60-mol ethoxylate initiators gave broadly similar conversion-time behaviour, whereas the 14-mol ethoxylate initiator gave a reaction system which polymerised very much more slowly than did the other four reaction systems in this series. Thus the times required for 50% conversion of monomer to polymer using this type of reaction system at this temperature were again in the range 1 - 2 hours for the 30-, 45- and 60-mol ethoxylate initiators. In the case of the reaction system which contained the 24-mol ethoxylate initiator, the conversion was less than 20% after 4 hours reaction.

As noted above, various shapes of conversion-time curve have been observed for reaction systems containing these azo initiator/stabilisers in the absence of other colloid stabilisers. The conversion-time curves obtained for reaction systems initiated and stabilised by the 45- and 60-mol ethoxylate initiators using the above reaction systems at 50°C resemble those for conventional emulsion polymerisation reactions, except that the region of constant rate extends in some cases to ca 80% conversion before a reduction in rate of polymerisation is observed. By contrast, the conversion-time curves obtained for reaction systems initiated and stabilised by the 24- and 30-mol ethoxylate initiators using the above reaction systems at 50°C differ from those for conventional emulsion polymerisation reactions. These curves can best be described as comprising two (in the case of the 24-mol ethoxylate initiator) or three (in the case of the 30-mol ethoxylate initiator) linear regions of progressively decreasing slope. Reactions initiated and stabilised by the 24- and 30-mol ethoxylate initiators using the above reaction systems at 50°C appear to differ from those for similar reactions initiated and stabilised by the 45- and 60-mol in at least two important respects:

- i) the conversion-time curves do not indicate a conventional nucleation period;
- ii) the rate of polymerisation decreases as the reaction proceeds, instead of increasing.

Several aspects of emulsion polymerisation reactions initiated by these azo compounds in the absence of other colloid stabilisers have been investigated, including the effects of initiator/stabiliser level, polymerisation temperature, and amount of aqueous phase present in the reaction system. Many unexpected results have been obtained which, taken as a whole, indicate that the azo compounds we have investigated comprise an interesting class of initiator/stabiliser whose behaviour as initiator/stabilisers for aqueous emulsions polymerisation reactions is complex.

POLYMER COLLOID GROUP NEWSLETTER

Contribution from the Institut Charles Sadron (CRM-EAHP)
6, rue Boussingault, 67083 Strasbourg Cédex

by

Françoise CANDAU

POLYMERIZATION OF ACRYLAMIDE IN A SWOLLEN LAMELLAR MESOPHASE
(in collaboration with G. Holtzscheler, J.C. Wittmann and D. Guillon,
Polymer, in press).

Polymerization of acrylamide (AM) in liquid crystalline phase swollen by large amounts of oil and water and showing long range smectic order has been investigated (Fig.1). The macroscopic properties of the systems during polymerization were followed by viscometry, turbidimetry and ^1H NMR experiments. The microscopic structures were analyzed by small angle X-ray diffraction and optical microscopy.

The results give clear evidence of a polymerization-induced structural change from the initial swollen lamellar phase to a final homogeneous dispersion of spherical particles. The polymerization of acrylamide immediately promotes phase separation and transfer of monomer from the organized mesophase to a disordered isotropic phase (Fig.2). A specific feature of the system investigated here is that the final state is a single phase, namely, an isotropic, clear and stable latex, whereas in some other studies, phase separation was observed throughout the reaction.

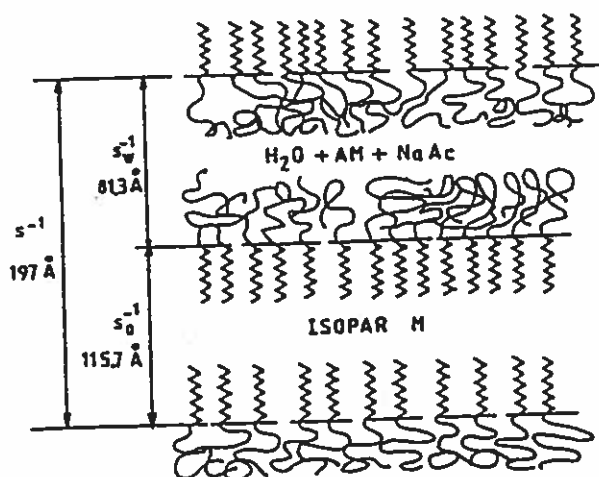


FIGURE 1. Schematic model of the lamellar phase. Composition of the system (wt/wt). Isopar M : 41.5% ; surfactant blend (Arlacel 83 + G 1086) : 22.1% ; acrylamide : 14.2% ; water 20.1% ; sodium acetate 2.1%

Several factors are responsible for the structural change observed during the above polymerization. First, these swollen and fluid four-component systems have flexible and fluctuating interfaces, much more labile than the rigid layers of concentrated ($C_s = 0.7$) and viscous binary or one-phase component(s). In the former case, the layers are only flat at scales smaller than the persistence length of the film and can easily undergo deformations. In addition, highly curved local defects might be present as reported

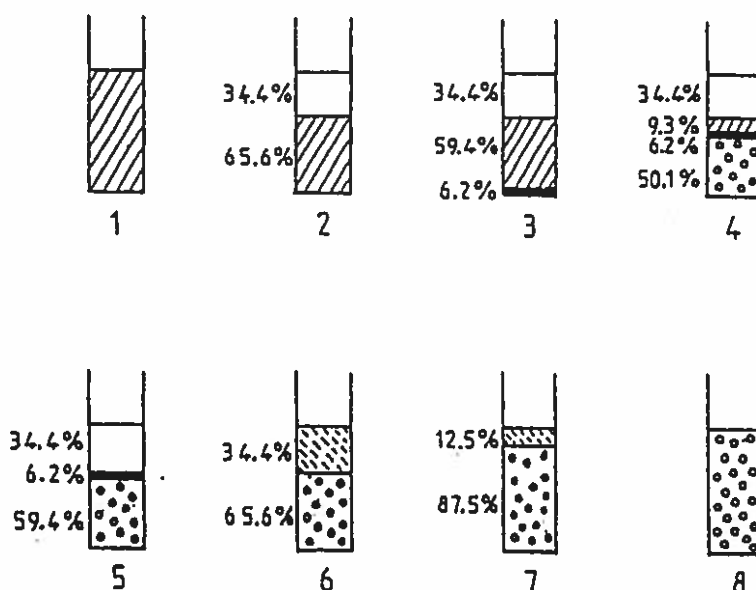


FIGURE 2. Schematic drawings showing the evolution of the system during the polymerization of acrylamide in the absence of stirring.

□ isotropic phase ; ▨ lamellar phase ; — turbid ring

◉◉ isotropic polymerized latex ; ▨▨ turbid phase

1) Initial lamellar system ($s^{-1} = 197 \text{ \AA}$) ; 2) Phase separation ; 3-5) Polymerization of the lower phase ; 6-7) Polymerization of the upper phase ; 8) Final latex.

for similar birefringent microemulsions⁽¹⁾. Repulsive undulation forces of entropic origin were shown to be at the origin of the stability of hyper-swollen lamellar phases.

The second important factor involved in the structural modification comes from the monomer itself. Thorough studies of acrylamide microemulsions by light scattering, viscometry and conductivity have revealed the strong influence of this monomer on the interfacial properties of the systems. In particular, a notable extension of the one-phase domain in the phase diagram was observed, indicating that AM acted as a cosurfactant and was partially located between the surfactant molecules, thus increasing the flexibility of the film.

The existence of fluctuating membranes containing a significant part of the monomer permits one to understand the results. There is no need to invoke the entropy loss during polymerization and the energy of confinement of a high molecular weight polymer in a restricted layer thickness of 80 Å. Indeed, the simple effect of polymerization on the interfacial energy of the systems seems to be the key parameter. As soon as the polymerization starts, the monomer consumption from the layers induces a change in the film curvature energy, which destabilizes the system and gives rise to a shift in the phase diagram. A two-phase equilibrium forms between a lamellar phase with zero curvature and an upper isotropic phase with a spontaneous curvature which can be either bicontinuous or of globular type. Both phases contain all of the components, which shows that the monomer is not the only component expelled from the lamellar phase.

The diagrams of Figure 2 show an important feature of the process, namely the coexistence of one latex phase with two reservoir phases of lamellar and microemulsion like types. One can speculate that the polymerization starts in the upper microemulsion phase in a similar way to that described elsewhere⁽²⁾. Gravity forces due to the very large difference in density between polymer (≈ 1.39) and monomer (1.12) would cause the newly formed polymer particles to settle at the bottom of the flask. As polymerization proceeds, the volume of the lower latex phase grows at the expense of that of the reservoir lamellar phase. The composition and volume of the upper reservoir microemulsion is maintained constant at the equilibrium (saturation) level by diffusion of components from the lamellar phase, whose volume and periodicity shrink with time. After the total disappearance of the lamellar phase (step 5 in Fig.2), the composition of the upper phase is no longer maintained at the saturation level; the phase becomes turbid and unstable, until complete polymerization has taken place. Finally, when all of the monomer has reacted, an optically transparent isotropic and stable latex is produced with a particle size of 74 nm as shown from quasi-elastic light scattering experiments.

It should be noted that this mechanism is very reminiscent of that reported for conventional emulsion polymerization, where a monomer reservoir phase exists in the form of polydisperse macroscopic droplets. The original feature of the acrylamide polymerization in lamellar phase lies in the fact that, all through the polymerization reaction, the monomer is located in the aqueous phase of a microemulsion. This is the reason for the small particle size produced by such a process.

REFERENCES

- (1) J.M. di Meglio, M. Dvolaitzky and C. Taupin
J. Phys. Chem. 89, 871 (1985).
- (2) C. Holtzscheler and F. Candau
J. Colloid Interface Sci. 125, 97 (1988).

RECENT PUBLICATIONS

- (1) Inverse microlatexes : mechanism of formation and characterization.
F. CANDAU and M.T. CARVER
in "Structure and Reactivity in Reverse Micelles" (M.P. Pileni Ed.) Elsevier Science Publ., Amsterdam, chap. 19, p.361 (1989).
- (2) Polymerization in inverse emulsions and microemulsions.
F. CANDAU
in "An Introduction to Polymer Colloids" (F. Candau and R. Ottewill Eds.). NATO ASI Series, D. Reidel Publ., Dordrecht, chap. 3, p.73 (1989).
- (3) Mechanism and kinetics of the radical polymerization of acrylamide in reverse micelles.
F. CANDAU
in "Radical Polymerization in Heterogeneous Systems" (J. Barton Ed.). Makromol. Chem. Makromol. Symp., Hüthig Wepf Verlag, Basel, Heidelberg, New York, 31, 27 (1990).

Contribution to the International Polymer Colloids Group Newsletter

E.S. Daniels, V.L. Dimonie, M.S. El-Aasser, A. Klein,
O.L. Shaffer, C.A. Silebi, E.D. Sudol, and J.W. Vanderhoff

*Emulsion Polymers Institute, Lehigh University
Mountaintop Campus, Building A, 111 Research Drive
Bethlehem, Pennsylvania 18015-4732 U.S.A.*

The titles of our current research projects are given in the enclosed Contents of our Graduate Research Progress Reports, No. 33, January, 1990. Copies of any of these reports can be obtained by contacting Debra Nyby at the above address. Summaries of progress in several research areas are presented.

1. Interfacial Phenomena Controlling Particle Morphology of Composite Latexes (Yi-Cherng Chen)

A mathematical model based on a thermodynamic analysis was derived to describe the free energy changes corresponding to various morphologies possible in composite latex particles. Some of these are depicted in Figure 1.1. Seeded batch emulsion polymerizations were carried out at 70°C using monodisperse polystyrene latex as seed. The surface polarity of the seed particles was estimated by contact angle measurements at the latex 'film'/water interface with octane as the probe fluid. Methyl methacrylate and ethyl methacrylate were polymerized in a second stage seeded polymerization in the presence of a nonionic stabilizer, nonylphenol polyethylene oxide (Igepal Co-990). Two types of initiator (potassium persulfate and azobisisobutyronitrile (AIBN)) were used to vary the second stage polymer/water interfacial tension. Values obtained for the interfacial tension of polymer/second stage monomer solutions versus the aqueous phase, measured by the drop-volume method under conditions similar to those prevailing during the polymerization, correlated well with the particle surface polarity and the observed particle morphology. The results showed that, rather than the bulk polymer hydrophilicity, the particle surface polarity is the controlling parameter in determining which phase is 'inside' or 'outside' the composite particles. The variation of the polymer phase interfacial tension with polymer concentration was also estimated.

The experimentally measured interfacial tensions were used to determine the thermodynamically preferred morphology as a function of the polymer volume ratio. The predicted morphologies were in good agreement with the observed morphologies of the composite particles (Y.C. Chen, V.L. Dimonie, and M.S. El-Aasser, *J. Appl. Polym. Sci.*, accepted).

A similar approach was applied to study the development of particle morphology during the course of seeded polymerizations which resulted in particles possessing varied morphologies. Based on the interfacial tensions, the relative stabilities (based on free energies) of possible particle morphologies were calculated as a function of the conversion of the second stage monomer. The mechanism of change in particle morphology was proposed. Results suggest that the development of particle morphology is affected by the diffusivity of the polymer chains. This phenomenon was found to agree with the observed particle morphologies. When the composite latex particles were swollen with toluene, the particle morphology approached the thermodynamically favored configuration (Y.C. Chen, V.L. Dimonie, and M.S. El-Aasser, submitted to *Macromolecules*).

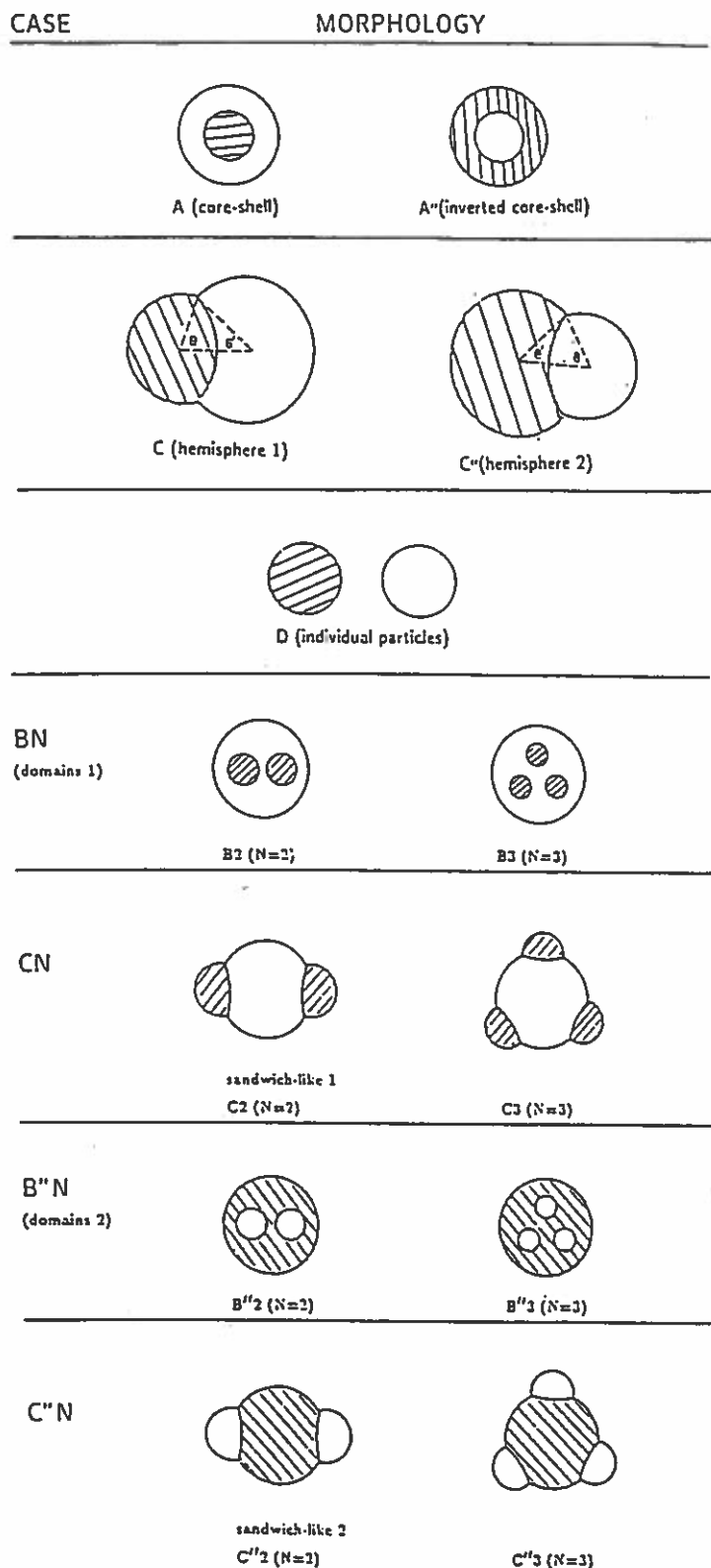


Figure 1.1: Various morphological structures of composite latex particles; shaded areas polymer 1, open areas polymer 2.

Recently, we have studied the effect of surfactant on composite latex particle morphology. Composite particles were prepared by seeded batch emulsion polymerization (polystyrene seed and methyl methacrylate monomer) at 70°C using persulfate initiator and various surfactants. When Pluronic F-108 (poly(ethylene oxide-propylene oxide)), a nonionic surfactant, was used, the final particle morphology showed that the PMMA was partially covered by the polystyrene. However, when Igepal Co-990 was used under the same conditions, the reverse morphology was found (polystyrene partially covered by the PMMA). The measured polymer (in monomer)/aqueous phase interfacial tensions were consistent with the observed morphologies. The development of particle morphology during the course of polymerization was also observed by electron microscopy and agreed with the thermodynamic predictions.

2. Modification of Poly(Vinyl Alcohol) in the Emulsion Polymerization of Vinyl Acetate (Neal J. Earhart, Hubertus T. Kroener, Henry Yue)

During emulsion polymerizations using poly(vinyl alcohol) (PVA) as emulsifier, the oligomeric radicals formed in the aqueous phase can grow until they precipitate from the aqueous phase and nucleate latex particles or react with the solute PVA to form PVA macroradicals which then add vinyl acetate and generate graft copolymers. Indirect evidence for grafting reactions of PVA and vinyl acetate in the aqueous phase during the emulsion copolymerization of 50/50 vinyl acetate/n-butyl acrylate was indicated by the change in the rates of individual monomer consumption as predicted by the disparate copolymerization reactivity ratios ($r_1 = 0.05$ and $r_2 = 5$). The initial polymerization rate of vinyl acetate was greater than that of n-butyl acrylate up to 25-35% conversion; then, the butyl acrylate polymerized preferentially until it was depleted, followed by the remaining vinyl acetate (see Figure 2.1A).

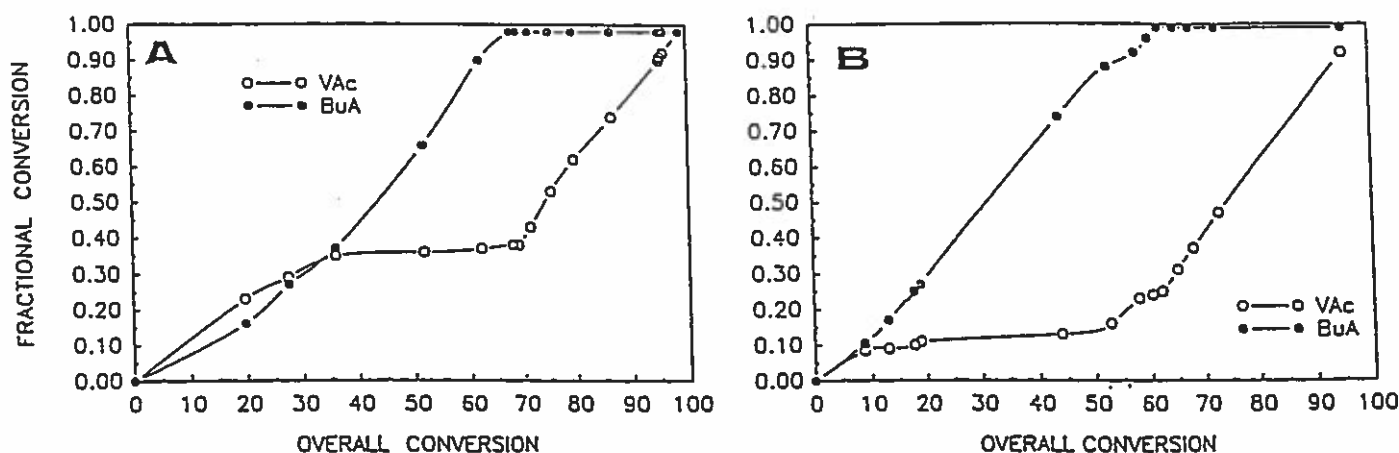


Figure 2.1: Fractional conversion versus overall conversion for the emulsion copolymerization of 50:50 (by wt.) VAc/n-BuA using 10% PVA based on total monomer: A) fully hydrolyzed PVA; and B) PVA modified to 82% hydrolysis by grafting VAc.

The extent of grafting was shown to affect the PVA concentration in the aqueous phase depending upon its initial degree of hydrolysis. The serum solids of the latex using the partially hydrolyzed PVA (87%, Vinol 205, Air Products) decreased during the course of the polymerization, while it increased during the polymerization when the fully hydrolyzed PVA (98%, Vinol 107) was used, confirming that the fully hydrolyzed PVA can be grafted to a greater extent and still remain water-soluble (see Table 2.1). A limited amount of vinyl acetate can be grafted onto

the PVA and yet maintain water-solubility. This amount was determined by Fourier Transform Infrared Spectroscopy and found to correspond to approximately 82% hydrolysis.

Fully (98%) and partially (87%) hydrolyzed PVAs of similar molecular weight, as well as the PVAs modified by grafting of vinyl acetate to the degree corresponding to 82% hydrolysis, were used in vinyl acetate/n-butyl acrylate copolymerizations. When the fully and partially hydrolyzed PVAs were modified to possess the same degree of hydrolysis (i.e., 82%) they performed similarly in terms of kinetics and latex particle size in batch polymerizations. The individual rates of monomer consumption were no longer affected by the presence of the modified PVA and followed the rates expected based on reactivity ratios (see Figure 2.1B).

Table 2.1: Percent Solids and Composition of the Latex Serum Prepared With 10% Vinol 205 and Vinol 107 as Determined by FT-IR

Latex	Reaction Time (min)	% Solids of Serum	Overall Degree of Hydrolysis	%PVAc Grafted in the Serum
L205/10-a	0	3.42	88.0	0.00
	5	2.98	83.0	5.02
	15	2.80	81.9	6.11
	40	2.72	81.8	6.18
	Final	360	2.71	81.9
L107/10-a	0	3.23	98.0	0.00
	5	3.25	92.2	5.85
	15	3.36	85.1	13.88
	120	3.38	82.0	16.00
	Final	360	3.40	81.9

The mechanism of PVA modification was investigated with respect to the grafting sites on PVA chains and the degree of grafting. NMR analysis of PVA modified in model reactions was used to identify the sites and mechanism of vinyl acetate grafting on PVA. The mechanism of grafting was postulated to be hydrogen abstraction from the PVA backbone. The ^{13}C NMR spectra of the reaction products of PVA and potassium persulfate initiator show new peaks at: 100 ppm assigned to the quaternary carbon in the 1,1 diglycol unit; 63.9 ppm (CH group) and 49.0 and 39.8 ppm (CH_2 group) due to the shift of the signal of the carbon atoms adjacent to the newly created 1,1 diglycol and 1,2,3 triglycol units. The NMR spectra show that the methyl group of the unhydrolyzed acetate groups are not involved in radical reactions and the proton abstraction takes place at the methine and methylene carbons of the PVA backbone, the former site being preferred.

3. Polymerization of Reactive Surfactants (M. Belen Urquiola)

Reactive surfactants, which contain a polymerizable group, can irreversibly bind to polymer particles increasing greatly the latex stability. The extent of their participation in homopolymerization or copolymerization reactions with other monomers will determine their role in particle nucleation and stabilization during an emulsion polymerization process.

A reactive surfactant of the type sodium alkyl allyl sulfosuccinate (TREM LF-40, Henkel)

has been used. The homopolymerization of the reactive surfactant in solution was followed using ^{13}C NMR and the effect of surfactant concentration on the polymerization rates was also determined. It was found that the rate of polymerization is proportional to $[M]^{(0.25-0.35)}$, where $[M]$ is the concentration of surfactant. This result was unexpected in that solution polymerization rates are typically directly proportional to the first power of the monomer concentration. The interaction between TREM LF-40 and the persulfate initiator was then investigated. However, no specific interaction was found that could explain these unusual polymerization rates. The tendency of allyl groups to participate in chain transfer reactions is well known, and this could act to slow down the polymerization. Therefore, chain transfer through the allyl group could be the reason for the unusual polymerization rates.

Emulsion copolymerizations of the reactive surfactant TREM LF-40 with monomers having widely different water solubilities were studied at 60°C . These monomers are given in Table 3.1. The evolution of the conversion of both the reactive surfactant and the monomer was measured and the results are given in Figure 3.1. In these polymerizations the molar ratio of TREM LF-40 to monomer was 0.4/1 in all cases (0.25M TREM LF-40, CMC = 1.2mM), potassium persulfate (8.5mM) was the initiator with sodium bicarbonate buffer (22mM). To varying degrees the reactive surfactant participates preferably in the copolymerization as indicated by the high rates of polymerization while significant amounts of monomer were present. These are compared to the rate of homopolymerization of the reactive surfactant in Figure 3.1 (bottom right); the rate of polymerization of the TREM LF-40 in the copolymerization only approaches that of the homopolymerization after the monomer has been largely consumed. It should be pointed out that the copolymerizations with BA and MA both resulted in the formation of latex particles while that with VAc resulted in the formation of a water soluble polymer. In the latter case the proportion of TREM LF-40 units in the polymer chain is greater, as indicated by the polymerization kinetics, thus maintaining the hydrophilicity of the formed polymer. Reactivity ratios of the TREM LF-40 with the monomers will be determined in the future.

Table 3.1: Water Solubilities of the Monomers

Monomer	Water Solubility (g monomer/ 100 g water)
Butyl Acrylate	0.14
Vinyl Acetate	2.50
Methyl Acrylate	5.60

4. Associative Polymers: An Investigation Into the Fundamental Thickening Mechanism in Latex Dispersions (Richard D. Jenkins)

We are probing the interrelationships among colloidal stability, dispersion rheology, and the adsorption behavior of model associative polymers whose structure consists of linear water-soluble poly(ethylene glycol) backbones of molecular weight 16600-100400 that have been capped with hydroxyl, dodecyl, or hexadecyl endgroups. A minimum amount of model associative polymer (O(0.5%)) is required to flocculate the dispersion by bridging; a certain degree of networking among the associative polymers is needed to span the distance between particles. Restabilization occurs at larger concentrations of associative polymer (O(1-2%)), and a homogeneous network of associative polymer and latex particles forms, i.e. an "infinite floc". Molecular areas of adsorption of the associative polymer on monodisperse polystyrene latex particles, calculated from

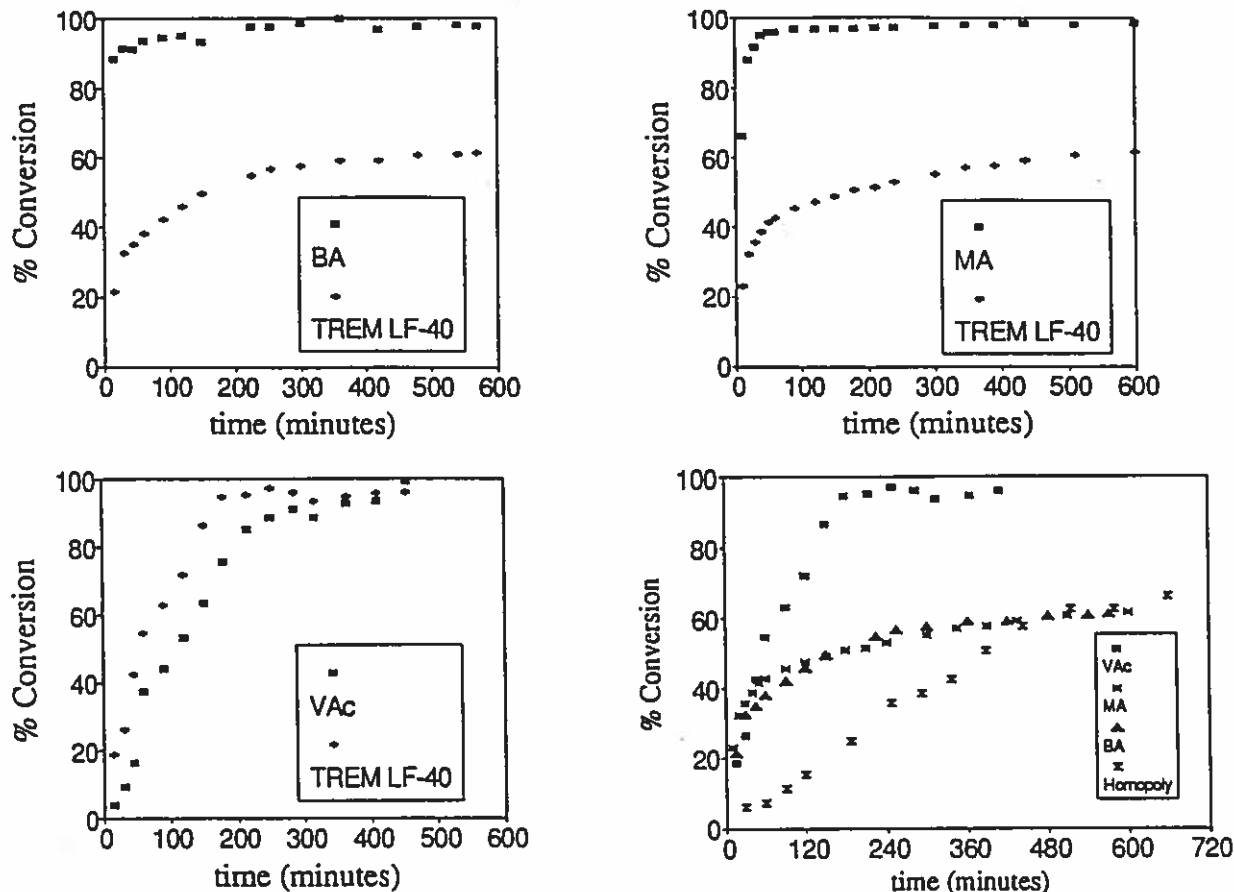


Figure 3.1: Copolymerization conversion histories of TREM LF-40 with: top left) butyl acrylate; top right) methyl acrylate; and bottom left) vinyl acetate; bottom right) comparison of the rate of consumption of the TREM LF-40 to that in homopolymerization.

the adsorption isotherms that were obtained (Figure 4.1) using a modified serum replacement technique, suggest that this restabilization coincides with full coverage of the particles surface by the associative polymer. The details of the adsorption isotherm provide insight into the structure of the adsorbed layer. At low polymer concentration in the serum (less than 30 ppm), the amount of associative polymer adsorbed is nearly the same regardless of hydrophobe type. Hence, the backbone of the model polymer adsorbs to polystyrene, which was expected since poly(ethylene oxide) does adsorb to polystyrene, and since the diisocyanates in the urethane linkages that connect the poly(ethylene oxide) blocks in the backbones of the model polymers are also slightly hydrophobic. At large polymer concentrations, the adsorption isotherms for the thickeners with the hydrophobic endgroups show a dramatic increase in the adsorbed amount of polymer that correspond to a change in conformation of the adsorbed layer from a planar to a bristle-like conformation. This change in conformation promotes better packing of hydrophobes on the particle surface and enhances expulsion of the hydrophobic endgroups of the associative polymer by the aqueous phase. Because the areas of adsorption are large (on the order of 2000-20,000 Å²/molecule, depending on particle size, hydrophobe length, and thickener molecular weight), and because the molecular area of adsorption increases as the size of the latex particle increases, the polymer conformation on the surface probably consists of loops and trains, with one of the hydrophobic endgroups firmly anchoring the associative polymer, and one hydrophobic endgroup extending out into the dispersion medium.

As reported previously [Jenkins, R.D., Silebi, C.A., and El-Aasser, M.S., Polym. Mater.

Sci. & Eng., 61, 629 (1989)], solutions of model associative polymer with hexadecyl hydrophobic endgroups exhibit dramatic shear-thickening in their steady shear viscosity profiles (Figure 4.2). The magnitude of this enhancement in solution viscosity decreases with increasing polymer molecular weight and concentration. To understand this shear thickening phenomenon from a molecular point of view, we have modelled the rheological properties of the model associative polymer solutions with Yamamoto network theory. In our model, the stress supported by a rubber-like network of finitely extendable polymer chains, constructed from physical entanglement junctions that continuously rupture and reform, depend upon the change in the free energy of the polymer chains in the network on extension. Calculations of the steady shear viscosity show that a decrease in the configurational entropy of the chains in the network during simple shear produces a restoring force that resists flow, and thereby produces the observed shear-thickening.

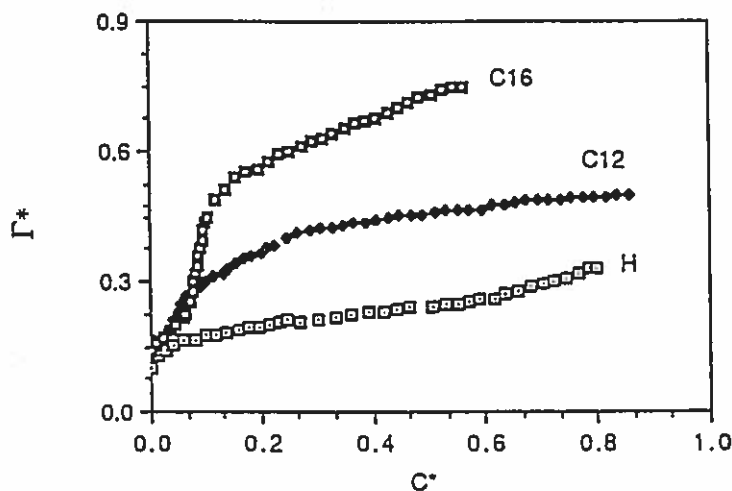


Figure 4.1: Typical adsorption isotherms of model associative polymer on polystyrene latex particles. Γ^* is a dimensionless variable related to the amount of associative polymer adsorbed on a unit area of latex surface, and c^* is a dimensionless variable related to the concentration of associative polymer in the latex serum. The molecular weight of associative polymer is 67,000.

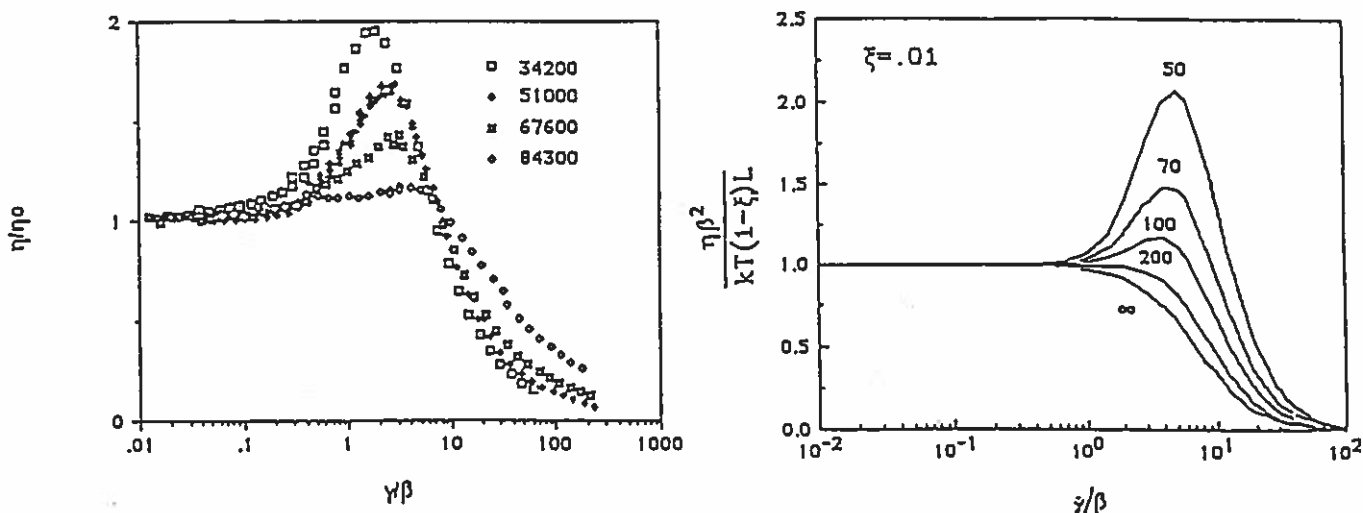


Figure 4.2: Comparison of shear-thickening/shear-thinning steady shear viscosity profiles of 1% model associative polymers with hexadecyl endgroups from (left) experimental measurements and (right) statistical mechanical network theory.

5. Preparation of Rocket Propellant by Emulsification (Tom. W. Hawkins)

Solid rocket propellant consists of a dispersion of solid oxidizer particles in a continuous polymer matrix. Presently, fabrication of this composite is time consuming and expensive for large rocket motors and an alternative route of preparation has been explored using model systems. This alternative employs emulsification of liquid, model oxidizer salt mixtures in monomer mixtures capable of low temperature polymerization. Recent results demonstrate the viability of this novel approach since cured model emulsion propellants containing 75 vol% dispersed phase have been prepared which display physical properties (i.e., maximum stress, initial modulus, and maximum strain) comparable to typical carboxy-terminated polybutadiene-based (CTPB) solid propellant.

Two polymerization routes were studied for cure of model emulsion propellant. The first is the step-wise reaction of hydroxy-terminated butadiene macromer with isocyanates (isophorone diisocyanate, IPDI, and prepolymer derivatives) to form a polybutadiene-based polyurethane continuous phase. This type of polyurethane is an industry standard for current solid propellant production. The second route is the free radical initiated chain polymerization of methacrylate-terminated butadiene macromer with styrene monomer. Isocyanate-cured model emulsion propellants displayed physical properties at unacceptably low values. Chain extension of the polyurethane with difunctional, isocyanate-capped hexadecanediol improved properties, but not enough to compare favorably to CTPB solid propellants. Attempts to chain extend the polyurethane with tetrafunctional, isocyanate-capped prepolymer from N,N,N',N'-tetrakis(2-hydroxypropanol)ethylene diamine resulted in unacceptable formation of gel early in the emulsification process.

The free radical initiated chain polymerization of methacrylate-terminated butadiene macromer (MW \approx 2000 dalton) with a reactive diluent monomer, styrene, provided a polymer matrix for cured model emulsion propellant displaying physical properties comparable to CTPB solid propellant (see Table 5.1). The superiority of the chain polymerized butadiene macromer/styrene matrix over the step polymerized butadiene macromer/isocyanate matrix is a reflection of the effect of liquid, internal phase volume on the physical properties of cured emulsion. For both chain and step polymerized matrices the relative maximum stress follows Nielsen's equation for an elastomer containing a disperse phase which bears no load. Also the relative initial modulus is found to follow an isostrain model in which the modulus of the disperse phase is negligible. Such behaviors dictate that the polymer matrix for cured emulsion propellant must be considerably stronger than that for typical solid propellant (see Table 5.2).

Table 5.1: Model Emulsion Propellant Properties Compared to Standard Propellant Properties

PROPERTY	MODEL EMULSION PROPELLANT*	STANDARD PROPELLANT
STRESS _{max} (psi)	53 - 65	60 - 100
MODULUS _{ini} (psi)	778 - 950	400 - 2000
STRAIN _{max} (%)	49 - 59	35 - 150

* continuous phase composition comprised of methacrylate-terminated butadiene macromer with styrene in 60/40 wt ratio, respectively, with sorbitan monooleate (8.8 wt%) and 30 mM dilauroylperoxide; disperse phase volume fraction of 75% (ammonium chloride solution).

Table 5.2: Model Emulsion Propellant Properties Compared to Continuous Phase Properties

PROPERTY	STEP POLYMERIZED CONTINUOUS PHASE*	CHAIN POLYMERIZED CONTINUOUS PHASE**
STRESS _{max} (psi)	41	1,112
MODULUS _{ini} (psi)	50	11,645
STRAIN _{max} (%)	146	133

* hydroxy-terminated butadiene macromer/IPDI (1.4/1.0, NCO/OH) and sorbitan trioleate (8.8 WT%)

** methacrylate-functional butadiene macromer/styrene (60/40, WT) and sorbitan monooleate (8.8 WT%)

Papers Recently Presented

The following papers were presented at the Annual Meeting of the American Institute of Chemical Engineers held in San Francisco, CA, November 1989:

"Phase Compositions of Styrene Oil-in-Water Microemulsions", J.S. Guo, M.S. El-Aasser, E.D. Sudol, H.J. Yue, and J.W. Vanderhoff.

"Effect of Mass Transfer in Miniemulsion Copolymerization", M.S. El-Aasser, V.S. Rodriguez, C.A. Silebi, and J.M. Asua.

Recent Publications

"Emulsion Polymerization", M.S. El-Aasser in *Scientific Methods for the Study of Polymer Colloids and Their Applications*, F. Candau and R.H. Ottewill, Eds., Kluwer Academic Publishers, Netherlands, 1-34, 1990.

"Preparation of Uniform Nonspherical Latex Particles", J.W. Vanderhoff, H.R. Sheu, and M.S. El-Aasser in *Scientific Methods for the Study of Polymer Colloids and Their Applications*, F. Candau and R.H. Ottewill, Eds., Kluwer Academic Publishers, Netherlands, 529-565, 1990.

"Dilute Phase Behavior of Cetyl Alcohol, Sodium Lauryl Sulfate, and Water", R.J. Goetz and M.S. El-Aasser, *Langmuir*, **6**, 132-136 (1990).

"A New Approach for the Estimation of Kinetic Parameters in Emulsion Polymerization Systems. I. Homopolymerization Under Zero-One Conditions", J.M. Asua, M.E. Adams, and E.D. Sudol, *J. Appl. Polym. Sci.*, **39**, 1183-1213 (1990).

"Miniemulsion Copolymerization of Vinyl Acetate and Butyl Acrylate. IV. Kinetics of the Copolymerization", J. Delgado, M.S. El-Aasser, C.A. Silebi, and J.W. Vanderhoff, *J. Polym. Sci.: Part A: Polym. Chem.*, 28, 777-794 (1990).

"Uniform Nonspherical Latex Particles as Model Interpenetrating Polymer Networks", H.R. Sheu, M.S. El-Aasser, and J.W. Vanderhoff, *J. Polym. Sci.: Part A: Polym. Chem.*, 28, 653-667 (1990).

"Phase Separation in Polystyrene Latex Interpenetrating Polymer Networks", H.R. Sheu, M.S. El-Aasser, and J.W. Vanderhoff, *J. Polym. Sci.: Part A: Polym. Chem.*, 28, 629-651 (1990).

"The Determination of Particle Size Distribution of Submicrometer Particles by Capillary Hydrodynamic Fractionation (CHDF)", J. DosRamos and C.A. Silebi, *J. Coll. Int. Sci.*, 135, 165-177 (1990).

"An Analysis of the Separation of Submicron Particles by Capillary Hydrodynamic Fractionation (CHDF)", J. DosRamos and C.A. Silebi, *J. Coll. Int. Sci.*, 133, 302-320 (1990).

"Preparation of Highly Sulfonated Polystyrene Model Colloids", J.H. Kim, M. Chainey, M.S. El-Aasser, and J.W. Vanderhoff, *J. Polym. Sci.: Part A: Polym. Chem.*, 27, 3187-3199 (1989).

"Dielectric Properties of Cleaned and Monodisperse Polystyrene Latexes in Microwaves", F. Henry, C. Pichot, A. Kamel, and M.S. El-Aasser, *Coll. Polym. Sci.*, 267, 48-59 (1989).

Recent Ph.D. Dissertations and M.S. Reports

"Structured Latex Particles with Hydrophilic Polymer Cores", Ph.D. Dissertation by Jong M. Park.

"Inverse Emulsion Polymerization of Acrylamide in a Tubular Reactor", Ph.D. Dissertation by Thomas A. Bash.

"Preparation and Characterization of Acrylate Latexes Containing Dicarboxylic Acid Comonomer", Ph.D. Dissertation by Michele R. Lock.

"Preparation of High-Molecular-Weight Copolymers as Fuel Additives", M.S. Report by Iris Segall.

"Miniemulsion Copolymerization of Vinyl Acetate and Butyl Acrylate in a Tubular Reactor", M.S. Report by Scott A. Adamec.

"Ultraviolet Light Curing of Water-Based Inks", M.S. Report by Kyungsun Emily Min.

Copies of the Abstracts are available upon request.

CONTENTS

	Page		Page
Emulsion Polymer Institute Staff	1	Interfacial Mass Transport of Monomers Into Latex Particles Stabilized With Mixed Surfactants and Water-Soluble Polymers (J.I. Kim)	129
PREPARATION OF POLYMER COLLOIDS		Coagulation Studies of Polystyrene Latexes (J. Wydlia)	136
Preparation and Characterization of Monodisperse Porous Polymer Particles (C.M. Cheng)	5	Effect of Eluan Composition on Separation Factor in Capillary Hydrodynamic Flow Fractionation (CHDF) (J. Venkatesan)	148
The Morphology of Microscopic Composite Particles Prepared By A Two-stage Polymerization (S. Shen)	24	POLYMERIZATION KINETICS, REACTOR DESIGN AND CONTROL	
Particle Morphology In Seeded Composite Latexes (Y.C. Chen)	33	Modeling and Control of Latex Particle Size Distribution in Emulsion Polymerization (A. Spod)	154
The Dilute Phase Behavior of Cetyl Alcohol, Sodium Lauryl Sulfate and Water (R.J. Goetz)	51	Inverse Emulsion Polymerization of Acrylamide in a Tubular Reactor (T. Bash)	157
Batch and Semicontinuous Polymerization Utilizing Miniemulsions (P.L. Tang)	62	Development and Evaluation of a 2L Rotating-Cylinder Reactor for Use in Preparing Large-Particle-Size Latexes (C.M. Cheng)	165
Polymerization of Styrene O/W Microemulsions (J.S. Guo)	67	APPLICATIONS OF POLYMER COLLOIDS	
Preparation and Characterization of Acrylic Latexes Containing Dicarboxylic Acid Comonomers (M.R. Lock)	83	Preparation of Rocket Propellants by Emulsification (T.W. Hawkins)	171
Grafting Reactions of Poly(vinyl alcohol) During the Emulsion Copolymerization of Poly(vinyl acetate-co-butyl acrylate) (M.J. Barham)	88	Associative Thickeners: An Investigation into Their Thickening Mechanism (R.D. Jenkins)	180
Grafting Reactions of Poly(vinyl alcohol) During The Emulsion Copolymerization of Vinyl Acetate (H.T. Kroemer)	90	Structure and Breakup of Flocs Subjected to Fluid Stresses (M. Durall)	201
CHARACTERIZATION OF POLYMER COLLOIDS		Preparation of High-Molecular-Weight Copolymers As Fuel Additives (I. Segall)	204
Electrokinetic, Optical and Rheological Study of Ordered Polymer Colloids (Y.P. Lee)	100	Structured Latex Particles With Hydrophilic Polymer Cores (J.M. Park)	205
Polymerization of Reactive Surfactants (M.B. Urquola)	109	Preparation of Water-Absorbent Polymers By Inverse Suspension Polymerization (Y.S. Chang)	215
Preliminary Evaluation of Diphenyl Ether Disulfonate Surfactants In Emulsion Polymerization (E.S. Daniels)	115	DISSERTATIONS AND THESIS TITLES	
		RECENT PUBLICATIONS	
			233
			238

STANFORD UNIVERSITY
STANFORD, CALIFORNIA 94305-5025

DEPARTMENT OF CHEMICAL ENGINEERING

Contribution to Polymer Colloids Newsletter
Current Research Projects
Alice P. Gast

Colloidal Crystal Morphology and Orientation

with Yiannis Monovoukas

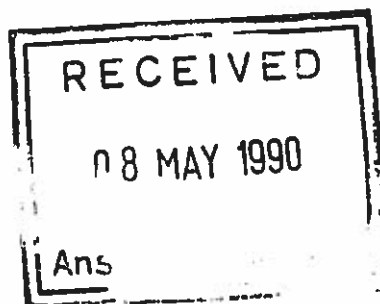
We have made microscopic observations of colloidal crystals grown in thin capillary cells. Observation between crossed polarizers reveals striations and polarization-dependent crystal colors. We employ dynamical diffraction theory to account for the depolarization of diffracted light in colloidal crystals and to correct Bragg diffraction wavelengths and intensities. Using Jones calculus, we predict crystal colors and intensities transmitted through crossed polarizers. We construct theoretical conoscopic images that provide a summary of the effects of crystal orientation on diffraction wavelength and intensity. Both striated and unstriated high volume fraction face centered cubic crystals often orient with the (110) planes parallel to the cell walls. We show that striated crystals are twin fcc structures by determining the relative orientation between successive bands. We illustrate that as the volume fraction and cell thickness decrease, the tendency of the suspensions to crystallize with the (111) planes parallel to the cell walls increases while the number density of striated crystals decreases.

We measure light attenuation anisotropies, resulting from coherent and incoherent scattering from a suspension of polystyrene microspheres, using a rotary polarization modulator polarimeter. Measured anisotropies are in excellent agreement with dynamical diffraction predictions. These measurements provide a new means to quantify crystal orientation in thin cells.

Aggregation of Colloidal Suspensions in Electric Fields

with Paul M. Adriani

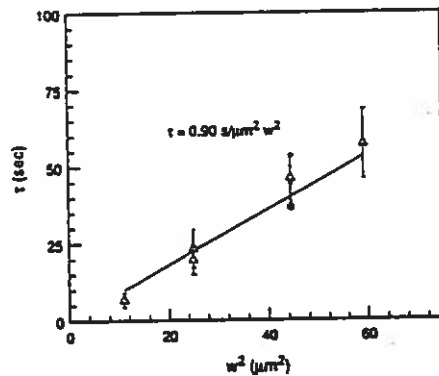
Predictions of electrorheological suspension properties rely on knowledge of the particle interaction forces. We deduce interaction forces experimentally from observations of field-induced aggregation in dilute suspensions. We investigate reversible chain formation, induced by a high frequency electric field, in dilute nonaqueous suspensions of sterically stabilized, one micron poly[methyl methacrylate] (PMMA) latices. Optical microscopy and digital image analysis provide the chain length distribution. We employ electrophoresis to measure a particle charge sufficient to inhibit field induced aggregation. Equilibrium predictions of chain aggregation incorporating a screened Coulombic repulsion and field induced dipole attraction agree well with experimental observations near the onset of aggregation; at elevated field strengths aggregation becomes diffusion limited.



Surface Diffusion of Adsorbed Proteins

with Robert D. Tilton

With a combination of total internal reflection fluorescence and fluorescence recovery after pattern photobleaching, we measure the lateral mobility of eosin-isothiocyanate labeled bovine serum albumin (BSA) irreversibly adsorbed to poly(methylmethacrylate) (PMMA) surfaces from aqueous solution. We probe lateral mobility over distances of several micrometers by photobleaching and monitoring fluorescence of the adsorbed fluorophore with the interference fringe pattern formed by intersection of two coherent laser beams at the point of total internal reflection at the solid-liquid interface. The rate of fluorescence recovery after photobleaching reveals the rate of adsorbed protein transport, and the period of the fringes determines the characteristic length for transport. As illustrated in the figure below, corresponding to a surface coverage of 0.60 area fraction, the second order dependence of the fluorescence recovery times on the fringe period demonstrates that adsorbed BSA migrates by surface diffusion. There exists a heterogeneity of adsorbed states such that 40% of the adsorbed proteins are mobile, while the remaining proteins are immobilized. BSA surface diffusion is time-independent over 7 hours, but is concentration-dependent; the self-diffusion coefficient decreases by approximately one order of magnitude from its infinite dilution limit of $D_0 = (5.6 \pm 0.5) \times 10^{-8} \text{ cm}^2/\text{s}$ as the surface coverage is increased to 0.69 area fraction.



Fluorescence recovery times scale with the square of the fringe half-period, indicative of diffusive transport.

Associating Block Copolymers in Dilute Solution

with Kathleen Cogan and Jennifer Raeder

When linear diblock copolymers are dissolved in a solvent selective for one block they can form spherical micelles, semicrystalline aggregates, or extended micellar or vesicular structures. We have been studying two such systems, one with an ionic and one with a nonionic insoluble block, dissolved in cyclopentane. From light-scattering studies we have found that micelles from these systems are extremely sensitive to trace amounts of water in the cyclopentane. In addition, the ionic polymer is sensitive to ionic impurities in the aqueous phase. Controlling water and salt contents allows us to manipulate the sizes and shapes of the structures formed in these systems.

We have used small-angle x-ray scattering to probe the structure of the micelles, and compare the structures to those predicted for a multi-arm star polymer. The scaling behavior, depicted in a logarithmic plot of scattered intensity versus scattering vector, provides information regarding concentration profiles within the polymer structures. Beyond the flat Guinier Region, scattering from single chains decays with a slope related to the Flory swelling exponent. For star-like structures, the slope approaches -4 as the density profile approaches that of a solid sphere. Furthermore, asymptotic scaling exponents indicate arms are stretched in micelles with higher aggregation numbers. In the figures below, we show results for the two systems. In figure 1, we show that a longer tail block remains as single chains in solution, whereas the more symmetric polymer forms very dense micelles. In figure 2, we see that an increase of aggregation number, induced by addition of water, causes scaling to deviate from single chain behavior.

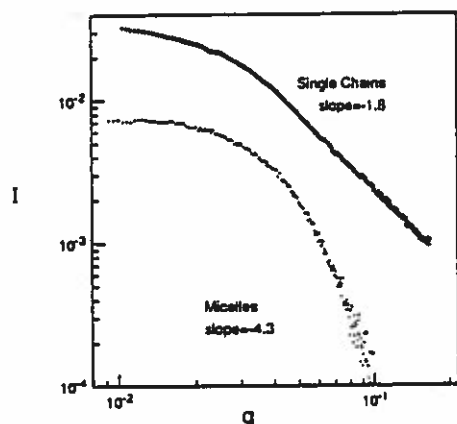


Fig. 1. PMAA/PBMA solutions: --- 4/92 slope of -1.8 at high q indicates single chains. - - - 6/42 slope of -4.3 indicates compact spherical micelles. We expect this slope to approach -2.0 at large enough q to probe semi-dilute single chain within the arms.

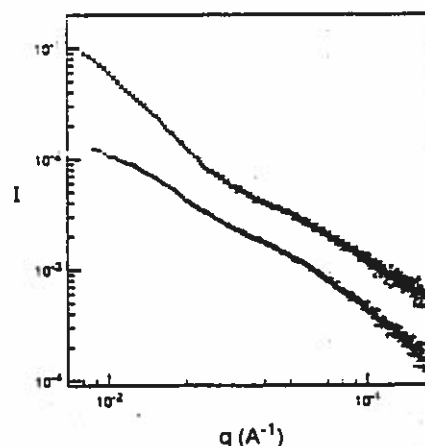


Fig. 2. PEO/PS = 65/80 solutions: (+) unsaturated and (x) unsaturated with water. Deviations from single chain scattering profiles become more pronounced as aggregation number increases at higher water behavior contents.

Kinetic aspects of the Emulsion Polymerization of Butadiene

Pierre A. Weerts, Anton L. German*

Laboratory of Polymer Chemistry, Eindhoven University of Technology,
P.O. Box 513, 5600 MB Eindhoven, The Netherlands

Introduction. Despite the enormous industrial importance of polybutadiene-containing polymers prepared by emulsion polymerization, very little is known about the kinetic behaviour of butadiene in emulsion polymerization systems. Since 1984 the typical behaviour of this monomer has been studied in our polymer group.^{1,2,3,4)} Some interesting kinetic aspects on *ab initio* polymerizations have been found, which will be discussed below. Further research will be focused on seeded experiments, in order to obtain more detailed kinetic information.

Interval II analysis. The kinetics in interval II was analysed by making a double logarithmic plot of the average rate per particle (R_p/N) versus particle diameter at an arbitrarily chosen conversion, viz. 90 % (d_{90}). This plot is analogous to the well-known Ugelstad plot of $\log \bar{n}$ vs. $\log \alpha'$,⁵⁾ where $\alpha' = \rho_i v / N k_t$ with ρ_i is the rate of radical production in the aqueous phase, v the volume of a monomer-swollen particle, N the particle number density, and k_t the rate coefficient for bimolecular termination within the particles. Obviously, R_p/N is equivalent to \bar{n} . Since $N = V/v$, with V the total volume of polymer per unit volume of aqueous phase, it is easily seen that $\alpha' \propto v^2 \propto d^6$. At constant $[\Pi]$ (implying a constant ρ_i), $\log \alpha'$ can thus be replaced by $\log d_{90}$ (or $\log d$).

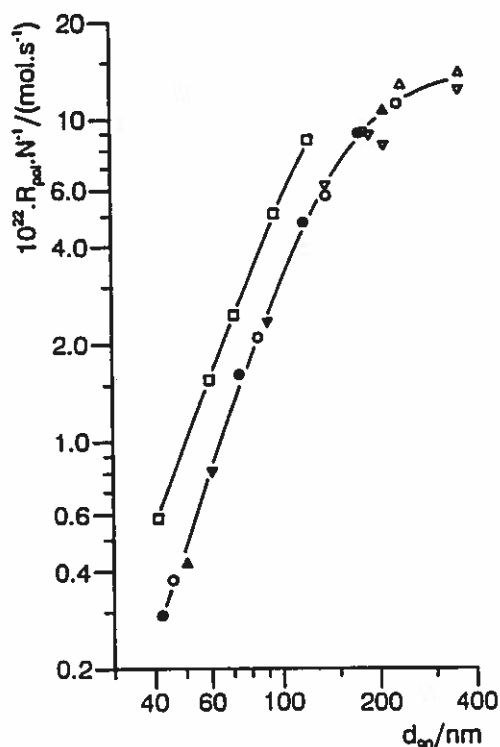


Figure 1. Average rate per particle R_p/N vs. the volume-average diameter d_v at 90 % conversion (d_{90}), for polymerizations with dresinate 214 (open symbols) and sodium dodecyl-sulfate (full symbols). The final particle size was varied by changing the emulsifier concentration (\circ), cation concentration (Δ), or monomer/water ratio (∇). Data of Wendler et al.⁶⁾ for polymerizations at 70°C (\square).

In our experiments the final particle diameter was varied by changing the type and concentration of emulsifier (sodium dodecylsulfate and the commercial emulsifier dresinate 214 were used), the cation concentration, or the monomer/water ratio (Figure 1). It is obvious that interval II kinetics is internally consistent, and also strongly dependent on particle size.

Figure 1 also contains data points taken from the work of Wendler et al.⁶⁾ for butadiene emulsion polymerizations at 70°C, where particle size was varied by changing the amount of bis(isopropoxythiocarbonyl)disulfane (also known as diproxid or dixie), a chain transfer agent which decreases colloidal stability by introducing polar end-groups that reduce emulsifier adsorption.⁷⁾ Agreement with our results is excellent, given the temperature difference of 8°C.

Using the (probably inaccurate) value for $k_p = 100 \text{ L.mol}^{-1}.\text{s}^{-1}$ reported by Morton et al.⁸⁾ at 62°C, and $C_M = 5.6 \text{ mol.L}^{-1}$,⁴⁾ a value of $4.7 \cdot 10^{-22} \text{ mol.s}^{-1}$ for R_p/N would result if $\bar{n} = 0.5$. Given this rough estimate of a Smith-Ewart case 2 situation, it is evident that values for $\bar{n} < 0.5$ are realistic.

Interval III analysis. Since the monomer concentration within the particles is decreasing continuously in interval III, it is convenient to remove C_M from the rate equation and write the expression in terms of the fractional conversion in interval III, x , with $x = (C_M^0 - C_M)/C_M^0$ and C_M^0 the initial monomer concentration within the particles:⁹⁾

$$-\frac{d\ln(1-x)}{dt} = \frac{k_p \bar{n} C_M^0 N}{N_A n_M}$$

where n_M is the number of moles of monomer per unit volume of water present at the beginning of interval III.

For the simple zero-one system with $\bar{n} < 0.5$, where bimolecular termination is not rate determining, it is easily shown that:¹⁰⁾

$$\bar{n} = \frac{\rho}{2\rho + k}$$

where ρ is the rate coefficient for radical entry and k the rate coefficient for exit (desorption). During interval III ρ may be considered unchanging to within a good approximation, since the swollen particle diameter is almost constant. On the other hand, k may depend on other factors than particle size; however, a reasonable starting point is to assume k to be constant, and then to check if this is consistent with the data. Several limiting cases can be distinguished:

Smith-Ewart case 2, with $k \ll \rho$: $\bar{n} = 0.5$
 Smith-Ewart case 1, with $k \gg \rho$: $\bar{n} \approx \rho/k$

Plotting $-\ln(1-x)$ vs. reaction time (Figures 2 and 3) gives straight lines up to a weight fraction of polymer w_p (equivalent to the *ab initio* conversion) of 0.85 or higher, for all polymerizations with $d_{90} < 175 \text{ nm}$.

Since the bimolecular termination rate coefficient varies significantly with w_p , termination cannot be rate-determining because $-\ln(1-x)/dt$ is constant for

$0.60 < w_p < 0.85$ under all conditions investigated. The approximation of instantaneous termination is thus valid, and $\bar{n} < 0.5$.

Furthermore, Figures 2 and 3 show that the product of $k_p \bar{n}$ is constant within each experiment; it would be highly fortuitous if k_p and \bar{n} would counter-balance under all experimental conditions, so it is apparent that k_p and \bar{n} are both constant in interval III. This further implies that k_p is not diffusion controlled, at least for $w_p < 0.85$; this is to be expected given the low glass transition temperature of (emulsion) polybutadiene ($T_g = -86^\circ\text{C}$).

The pseudo-first-order termination rate coefficient may start to become sufficiently small for very large particles as to become rate-determining, consistent with the non-linearity of $-\ln(1-x)$ observed for polymerizations with $d_{90} > 175$ nm (e.g. the polymerization with 8.1 g.L^{-1} dresinate 214 in Figure 3, with $d_v = 180$ nm at 90 % conversion). At a relatively low w_p of ca. 0.7, the interval III rate $-\text{dln}(1-x)/\text{dt}$, and thus \bar{n} , begin to increase. Termination is no longer instantaneous, yet the initial steady state suggests a zero-one behaviour at lower w_p . If we assume the initial $\bar{n} = 0.5$, an estimation for $k_p = 180 - 200 \text{ L.mol}^{-1}.\text{s}^{-1}$ is obtained. Although intuitively not unreasonable this assumption is not necessarily correct, since the initial \bar{n} can still be < 0.5 . Furthermore, the particle size distributions of these latexes are narrow, but not monodisperse, which complicates a proper interpretation. Therefore, this estimate of k_p should be regarded as a lower limit of its true value.

It is obvious that the system is kinetically dominated by a first-order radical loss process, whose nature is as yet uncertain. However, chain transfer/desorption processes involving polybutadiene, C_{12} -thiol (used as chain transfer agent), emulsifier, and the Diels-Alder dimer 4-vinyl-1-cyclohexene, were all refuted on experimental grounds. Desorption of monomeric species seems a reasonable explanation, given the rather low estimate of the propagation rate coefficient, in combination with the moderate aqueous phase solubility of butadiene at saturation pressure, viz. 40 mmol.L^{-1} at 62°C .¹¹⁾ If true, k may indeed be constant in interval III, according to the transfer/diffusion model developed by Nomura.¹²⁾

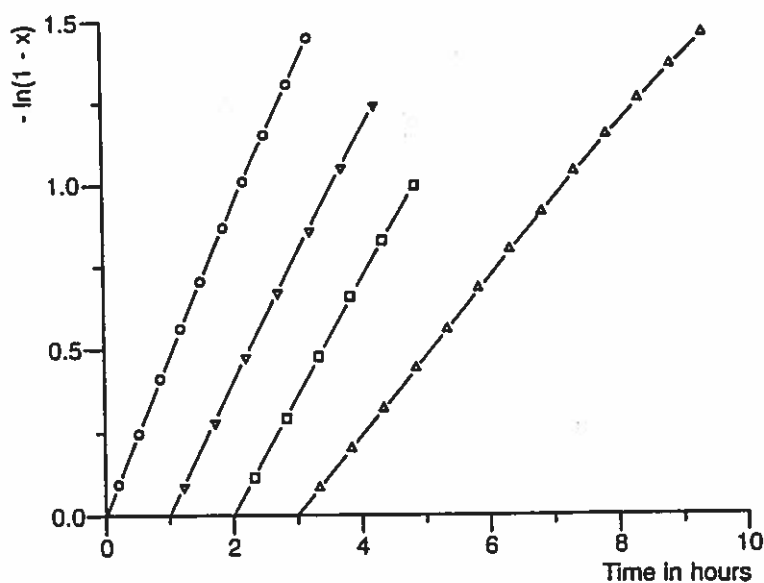
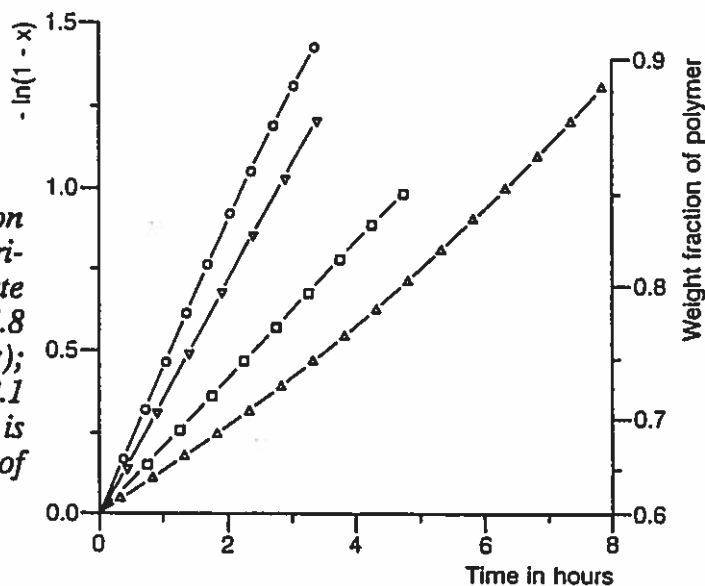


Figure 2. $-\ln(1-x)$ vs. Reaction time in interval III, for polymerizations with different sodium dodecylsulfate concentrations $C_E = 64.8 \text{ g.L}^{-1}$ (O); $C_E = 32.4 \text{ g.L}^{-1}$ (∇); $C_E = 16.2 \text{ g.L}^{-1}$ (\square); $C_E = 8.1 \text{ g.L}^{-1}$ (Δ). For convenience the zero-point is shifted one hour along the x-axis.

Figure 3. $-\ln(1-x)$ vs. Reaction time in interval III, for polymerizations with different dresinate 214 concentrations $C_E = 64.8 \text{ g.L}^{-1}$ (○); $C_E = 32.4 \text{ g.L}^{-1}$ (▽); $C_E = 16.2 \text{ g.L}^{-1}$ (□); $C_E = 8.1 \text{ g.L}^{-1}$ (△). On the right axis is indicated the weight fraction of polymer w_p



References

- 1 P.A. Weerts, J.L.M. van der Loos, A.L. German, *Makromol. Chem.* **190**, 777 (1989)
- 2 P.A. Weerts, J.L.M. van der Loos, A.L. German, *Polym. Comm.* **29**, 278 (1988)
- 3 P.A. Weerts, J.L.M. van der Loos, A.L. German, *Makromol. Chem.*, submitted
- 4 P.A. Weerts, A.L. German, R.G. Gilbert, *Macromolecules*, submitted
- 5 J. Ugelstad, P.C. Mörk, J.O. Aasen, *J. Polym. Sci.: Part A-1* **5**, 2281 (1967)
- 6 K. Wendler, N. Karim, M. Fedtke, *Plaste Kautsch.* **30**, 247 (1983)
- 7 K. Wendler, H. Elsner, W.D. Hergeth, M. Fedtke, *Plaste Kautsch.* **32**, 128 (1985)
- 8 M. Morton, P.P. Salatiello, H. Landfield, *J. Polym. Sci.* **8**, 215 (1952)
- 9 D.R. James, D.C. Sundberg, *J. Polym. Sci., Polym. Chem. Ed.* **18**, 903 (1980)
- 10 R.G. Gilbert, D.H. Napper, *J. Macromol. Sci., Rev. Macromol. Chem. Phys.* **C23**, 127 (1983)
- 11 C.D. Reed, J.J. McKetta, *J. Chem. Eng. Data* **4**, 294 (1959)
- 12 M. Nomura, in "Emulsion Polymerization", edited by I. Piirma, Academic Press, New York 1982

CONTRIBUTION TO POLYMER COLLOID GROUP NEWSLETTER SPRING 1990

from

FINN KNUT HANSEN
UNIVERSITY OF OSLO, DEPT. OG CHEMISTRY
P.O. BOX 1033 BLINDERN, 0315 OSLO 3, NORWAY

Dr. Geir Fonnum, now at Dyno Industrier, finished his thesis last year on the Synthesis and Characterization of Associative Thickeners. Some years ago we felt that there is too little (public) knowledge about the connection between structure and properties of associative thickeners, and Dr. Fonnum, with his main education in synthetic organic chemistry, set out to start filling this gap. The work was performed at the Department of Organic Chemistry at NTH, and has been a success. Although not revolutionary, it has initiated our continued work in this field. Dr. Fonnum will present some of the results on the ACS meeting at Lehigh this summer, and it eventually will be published. Below is given a brief summary of some of the work.

Hydrophobic groups at the ends of the polymers.

The importance of the polymer's hydrophobic endgroups are shown in figure 1. The figure show the viscosity/shear rate profile of dispersions thickened by the HMPCs 1a-c of Table 1. These thickeners are identical apart from the hydrophobic ends. The most striking effect is the enormous differens in thickening efficiency. By increasing the endgroup chain length from 11 to 17 carbon atoms, latex viscosity is increased 200 times, also pseudoplasticity becomes more expressed.

Hydrophobic groups in the interior of the polymers.

The influence of hydrophobic parts at the interior of the polymers has been investigated by using different diisocyanates but keeping the same end groups. The thickeners (2a-d) are synthesized with the diisocyanates of toluene, hexamethylene, methylene bis(4-cyclohexyle) and dodecamethylene. The thickeners' rheological behaviour are shown in fig. 2. There are only small differences in rheology between these; the thickener that exhibits the highest viscosity is the one synthezied from the least hydrophobic monomer, toluenediisocyanate.

Thickening mechanism

Bielman et al. have suggested that the thickening mechanism is based on the formation of a three-dimensional network in the solution. Bridging between micelles may still occur by small impurities of PEG in PEG monomethyl ether, but our result should be taken into account in the thickening mechanism.

The associative thickeners can be compared to nonionic ethoxylated surfactants. They both contain alifatic or aromatic hydrophobic parts and a hydrophilic ethylene oxide and their properties are related to association in solution. Like the surfactants there seems to be an increase in associative ability when the hydrophobic ends become larger. However, when the ethylene-oxide part is shorter, we obtain less efficcient thickeners. This is probably a result of smaller hydrodynamic radius of the aggregate that the thickeners make in water.

The different rheological properties we observe can be explained by regarding the system as a dynamic network with a network relaxation time determined by the average time one association lasts. At high shear rates the aggregates are broken down (destroyed) faster than they can rebuild and pseudoplasticity arise. The average lifetime of an association is larger the larger the size of the hydrophobic ends.

Table 1.

The chemical composition of associative thickeners with the structure A-PEG-B-PEG-B-PEG-A where A is a mono-urethane, B a di-urethane and PEG is polyethylene glycol (degree of polymerization, $n=135$).

A = $R^a\text{NHCO}$
B = $R^b(\text{NHCO})_2$

No.	R^a	R^b	Mn
1a	$C_{17}H_{35}$	C_6H_{12}	9900
b	$C_{14}H_{29}$	"	"
c	$C_{11}H_{23}$	"	"
2a	$C_{18}H_{37}$	C_7H_6	22400
b	"	C_6H_{12}	22500
c	"	$C_{13}H_{22}$	22700
d	"	$C_{12}H_{24}$	22700

Figure 1.

Associative thickeners with different hydrophobic endgroups. The rheology of an acrylic dispersion with 1.9 w% thickener 1a-c. The hydrophobic ends are in a heptadecyl, in b tetradecyl and in c undecyl.

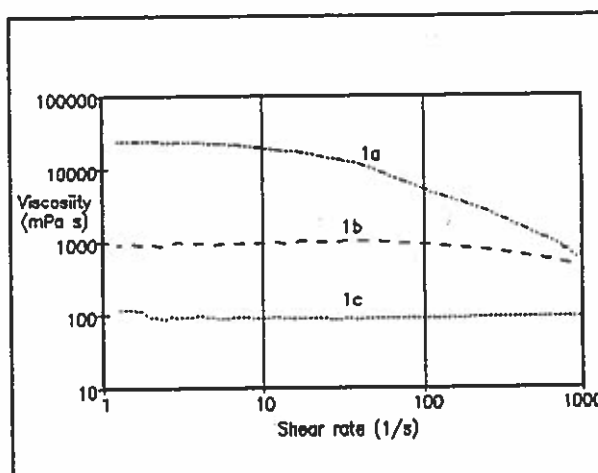
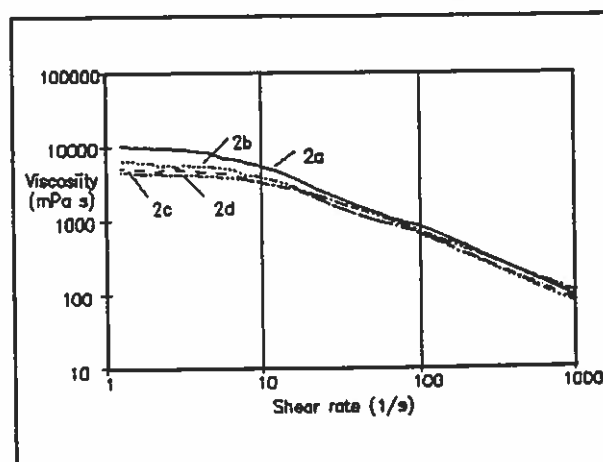


Figure 2.

Changing the hydrophobic parts in the middle of the polymer. The rheology of an acrylic dispersion with 0.38 w% thickeners 2a-d. The thickeners are synthesized from toluene.



Polymer Colloid Group Newsletter

Contribution from the Department of Physical and Colloid Chemistry,
Wageningen Agricultural University, Dreijenplein 6, 6703 HB Wageningen, The
Netherlands

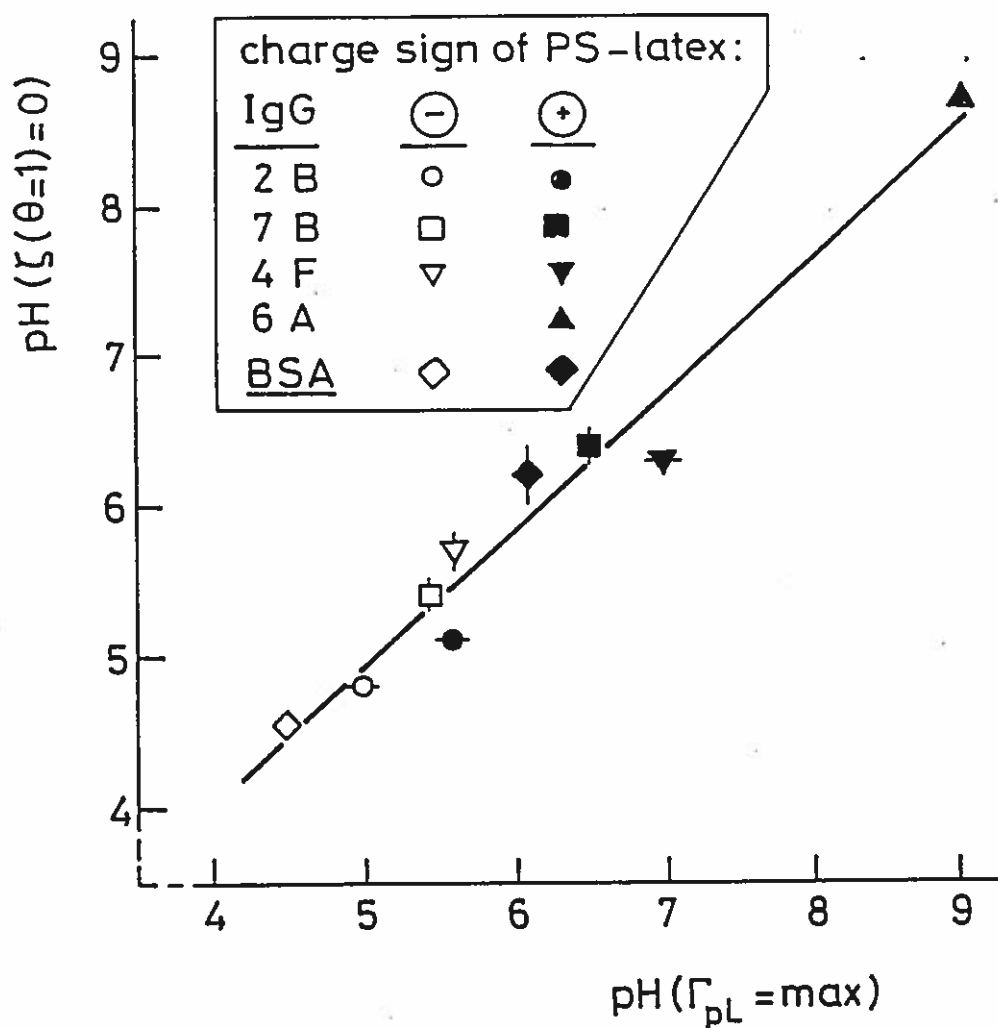
Protein Adsorption Maxima

A.V. Elgersma, W. Norde, J. Lyklema

In a preceding Newsletter of the Polymer Colloid Group (NL 18 (1987) #2, 24-25) we reported on the using of latices as adsorbents for proteins. Such systems are of great relevance for a number of applications, including the preparation of various immunochemical tests. Academically, their interest derives from their suitability as model systems to study the adsorption of biopolymers in general, and proteins in particular. Here, we report on new insights regarding the pH-dependence of protein adsorption.

In previous investigations (see W. Norde and J. Lyklema, *Colloid Surfaces* 38(1989)1; W. Norde, *Adv. Colloid Interface Sci.* 25(1986)267) it was found for BSA and HPA that the plateau adsorption Γ_{pl} , if plotted as a function of pH passed through a maximum at or nearby the i.e.p. of the protein. This phenomenon was found for several latices, for glass, silica, silver iodide and polyoxymethylene crystals. We concluded that the maximum was a property of the protein, rather than that it would be attributable to the nature of the adsorbent or, for that matter, to the protein-adsorbent interaction. Our interpretation was that at the i.e.p. the protein had the greatest conformational stability, so that it would retain most of the three-dimensional conformation it had in the dissolved state. At pH-values above or below the i.e.p., there is a net negative or positive charge on the protein, resulting it to undergo some structural alterations, resulting in thinner adsorbed layers, that is, in lower values for Γ_{pl} .

Recent systematic studies, conducted with a variety of proteins (BSA and four monoclonal immunoglobulins) on positively and negatively charged latices lead us to revisit our insight. As the figure demonstrates, there is a perfect on-to-one relationship between the pH of maximum adsorption and the isoelectric point of the protein-covered latex, called pH ($\zeta(\theta=1)=0$).



Relation between the isoelectric point of the protein-polystyrene latex complex and the pH where Γ_{pL} reaches its maximum value. The isoelectric point ranges of the four IgG monoclonals 2B, 7B, 4F and 6A are 4.8-5.1, 5.2-6.0, 6.9-7.3 and 8.7-9.3, respectively. Data from Ph.D. thesis A.V. Elgersma, Agricult. Univ. Wageningen, Netherlands (1990).

From the above, it is inferred that maximum conformational stability of (adsorbed) proteins is not reached at the i.e.p. of (bulk) protein, but at the i.e.p of the protein-latex complex. Isoelectricity is determined by the sum of the charges of the protein, the latex and co-adsorbed low molecular weight ions. For a number of conditions the co-adsorption is about equal to the charge on the latex. If that is the case, Γ_{pL} attains its maximum at the i.e.p. of the protein in solution. We have now concluded that this is not always the case.

The above observation sheds new light on the co-uptake of ions and its relation to the conformational stability of biopolymers.

by Mamoru Nomura

Department of Materials Science and Engineering, Fukui University,
Fukui, Japan

We are now studying the kinetics of emulsion polymerization initiated by oil-soluble initiators. The paper entitled "Kinetics of Emulsion Polymerization Initiated by Oil-soluble Initiators" has been published in "Makromol. Chem. Rapid Commun. 10, 581-587 (1989). Its abstract will be shown below.

In spite of many experimental and theoretical investigations so far carried out, the quantitative understanding of the kinetics and mechanism of the emulsion polymerization initiated by oil-soluble initiators has not been satisfactory. The aim of this paper is therefore to clarify the particle growth mechanism by examining the factors and their effect on the average number of radicals per particles.

From Fig. 1, where the events and rates which affect the concentration of N_n particle are shown, we have:

$$\frac{dN_n}{dt} = \left(\frac{r_{ip}}{2N_T}\right)N_{n-2} + \left(\frac{\rho_A}{N_T}\right)N_{n-1} + k_f(n+1)N_{n+1} + \left(\frac{k_{tp}}{v_p}\right)(n+2)(n+1)N_{n+2} - \left[\left(\frac{r_{ip}}{2N_T}\right) + k_f n + \left(\frac{\rho_A}{N_T}\right) + \left(\frac{k_{tp}}{v_p}\right)n(n-1)\right]N_n \quad (1)$$

Further, the following steady-state radical balance in the water phase must be considered.

$$\rho_A = k_a(R_w^*)N_T = r_{iw} + \sum k_{fn}N_n - 2k_{tw}(R_w^*)^2 \quad (2)$$

where $r_{ip} = 2k_{df}f_p[I]_p v_p N_T$ and $r_{iw} = 2k_{df}f_w[I]_w$.

The average number of radicals per particle can be calculated by

$$\bar{n} = (N_1 + 2N_2 + \dots + nN_n + \dots)/N_T \quad (3)$$

Since we are interested in the range where \bar{n} is less than unity, only N_0, N_1, N_2, N_3, N_4 and N_5 were considered in Eqs.(1) to (3). The resulting six differential equations were integrated simultaneously with Eq.(2) and the steady state values of N_1 to N_5 were introduced into Eq.(3) to obtain \bar{n} . Fig. 2 plots the calculated value of \bar{n} against $\alpha_p = (r_{ip} v_p / k_{tp} N_T)$ with varying $m = (k_f v_p / k_{tp})$ for the case where the oil-soluble initiator used is completely insoluble in water ($K = ([I]_w / [I]_p v_p N_T) = 0$) and also no radical termination occurs in the water phase ($\gamma = (2k_{tw} k_{tp} / k_a^2 N_T v_p) = 0$).

Fig. 3 shows a plot of \bar{n} versus α_p for $\gamma=0, K=0.05$, which corresponds to the case where AIBN is used as an initiator. From these figures, We can conclude that the initiator dissolved in the water phase is responsible for realizing the region of $\bar{n}=0.5$ in the emulsion polymerization initiated by oil-soluble initiators.

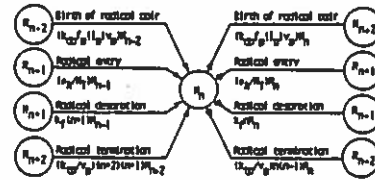


Fig. 1 Events for N_n

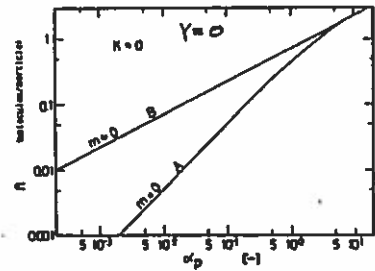


Fig. 2 \bar{n} vs. α_p at $K=0$

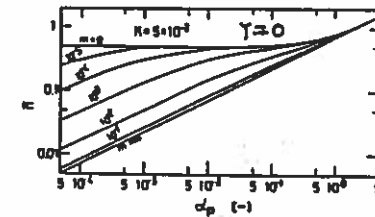


Fig. 3 \bar{n} vs. α_p at $K=0.05$

CONTRIBUTION TO POLYMER COLLOID
GROUP NEWSLETTER
FROM CNRS/LYON

(SUBMITTED BY C. PICHOT)

Properties of polystyrene colloids prepared in the presence of zwitterionic sulfobetaine emulsifiers (C. Graillat, B. Dumont (LMO), C. Pichot, V. Vintenon (UM CNRS-bioMérieux)).

Much work has been investigated on the mode of action of these surfactants when they are used either as emulsifiers in emulsion polymerization, or as poststabilizers. From interfacial measurements, it was recently found that they exhibit strong adsorption energies at the styrene-water interface (particularly in the case of the N-N dodecyl dimethylammonio propane sulfonate (NC₁₂) : 36 KJ/mole instead of 21 KJ/mole for SDS), what suggests that the sulfobetaines are strongly adsorbed onto the monomer-swollen particles. Moreover, from emulsion polymerization kinetics, it was also found that latex particles, at the end of the nucleation stage, were more narrowly distributed with sulfobetaines than with SDS. However, numbers of particles were notably smaller (depending upon the type of sulfobetaine), which could indicate that more coagulation would occur during the nucleation step ; therefore repulsive forces conferred by the dipole coming from the zwitterion would be less efficient than ionic groups (SO₄⁻) for stabilizing the nucleating particles.

More data have been collected on the electrophoretic behaviour of polystyrene latexes covered with these emulsifiers definitively confirming that the zwitterion (which behaves like inner salt) does not significantly affect the mobility of the particles in comparison to that conferred by residual charges or ionic emulsifiers. It appears that sulfobetaines would stabilize latex particles through a mechanism which is not well understood, involving the presence of a dipolar moment in the double layer.

Rheological studies on polystyrene latexes poststabilized with sulfobetaine surfactants have been also continued in a large domain of volumic fractions and ionic strengths, and the results are currently interpreted on the basis of various models. It was particularly found that the use of an alkyl sulfamidobetaine (with a low CMC) allowed to obtain high concentrations of small size latexes with low viscosity. Experiments carried out under dynamic regime (with a Rheometrics equipment) seem to indicate that latex particles covered with sulfobetaine were weakly associated.

Using NC12 as zwitterionic surfactant, it was also shown that the potassium persulfate/sodium metabisulfite was an efficient initiator system, especially for producing latexes (in a large range of size) having the same particle size but exhibiting various surface (SO₄⁻ + SO₃⁻) charge density.

**Studies on styrene-acrylonitrile grafting onto polybutadiene latexes
(P. Mathey - J. Guillot (LMO))**

During emulsion polymerization, dienic structure of butadiene leads to the formation of a network by crosslinking on the residual double bonds. Investigation on swelling of polybutadiene particles and films, by the styrene acrylonitrile mixture, was carried out in order to get more information on polymer structure and behaviour in the presence of monomers. A thermodynamic approach, according to Flory and al, has permitted to determine several parameters such as the average number of butadiene units between the crosslinking points which represent the crosslinking density. Results were compared with data from simulation of butadiene emulsion polymerization : a good agreement between experiments and simulation were observed. The interaction parameter between acrylonitrile and polybutadiene was determined. Swelling of films by monomer mixtures of various compositions has shown solvation of styrene as a function of comonomer composition. This variable has an importance on the final structure of the ABS particle, prepared by emulsion polymerization of styrene/acrylonitrile onto a polybutadiene seed. Thermodynamic data were used to explain variations in the ABS particles structure, such as different distribution of internal and external grafting of copolymer SANS. Grafting reaction kinetics was also compared with simulation.

**Kinetic studies in emulsion polymerization of 2-ethyl-hexylacrylate
(T. Desroches - C. Pichot - J. Guillot (LMO))**

Emulsion polymerization behaviour of 2 ethyl hexyl acrylate (EHA) has been examined in the presence of SDS. The constant propagation rate was first determined from kinetic study of the emulsion copolymerization of EHA with styrene at various comonomer feed composition ; the obtained value has been found lower than for acrylates having lower alkyl group. Parallely, the nucleation mechanism has been investigated by following the particle size distribution change with conversion through transmission electron microscopy. This work was extended to the emulsion copolymerization of EHA with a polar monomer, the methylmethacrylate, using a batch process. The composition of the water-polymer interface of the particles has been examined using the soap titration method so as to access to the particle structuration. Moreover, the composition and glass transition temperature were determined as a function of conversion and a good agreement has been observed with stimulated data based on a program taking actual kinetic parameters and partition coefficients into account.

**Studies on film formation in styrene-butylacrylate copolymer latexes
(cooperative work with Y. Chevallier - C. Graillat (LMO) - M. Joanicot -
K. Wong (Rhône-Poulenc) - L. Rios (UNAM Mexico) B. Cabane (CEN Saclay)).**

Recent data have been obtained by SANS on the film formation process when an aqueous dispersion of soft latex particles is spread onto a substrate. It has been found that ordering of particles in latex films is strongly affected by the surface coverage. When the latexes are covered by copolymerized polyacrylic acid, particles retain their structure and the final film exhibits honey-comb like morphology. On the contrary, when the latexes are covered by a surface-active-agent (such as a zwitterionic emulsifier), the particle structure is not kept except the particles are well stabilized, and a first order transition of the colloidal dispersion towards the film phase is observed during the drying process. This phenomenon is associated with expulsion of the surface active agent and the film structure is disordered.

RECENT PAPERS :

- Structure - properties relationships in styrene-butyl acrylate emulsion copolymers. I-Synthesis and characterization of latex. A. CRUZ - C. MONNET - C. PICHOT - L. RIOS - J. GUILLOT - B. SCHLUND - Polym., 60, October, 1872 (1989).
- Structure-properties relationships in styrene-butyl acrylate emulsion copolymers. II-Thermo mechanical properties. Experimental results and simulation. A. CRUZ - B. SCHLUND - C. PICHOT - J. GUILLOT - Polymer, 60, October, 1883 (1989).
- Colloidal and rheological properties of polystyrene latexes stabilized with various amphoteric sulfobetaine surfactants. C. PICHOT - B. DUMONT - C. GRAILLAT - P. DEPRAETERE - A. GUYOT - Preprints, Londres PRI, Paper 13, (1989).
- Copolymer latex morphology. J. GUILLOT - A. GUYOT - C. PICHOT - Chap. livre "Scientific methods for preparation of polymer colloids and their applications". Edit. R.H. OTTEWILL, F. CANDAU, NATO ASI Series, Kluwer Academic Publishers (1989), page 97.

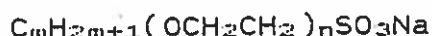
POLYMER COLLOIDS GROUP NEWSLETTER CONTRIBUTION

Submitted by Irja Piirma, The University of Akron,
Akron, Ohio, USA, 44325-3909

Emulsion Polymerization of Styrene using Electrosteric
Stabilization

Reported by An-Min Sung

An investigation has been carried out to evaluate the stabilizing behavior of polyoxyethylated surfactants having an ionic head at the end of the molecule. Surfactants of the AVANEL S™ series (PPG industries, Inc.) were chosen. Their general structure is as follows:



where $m = 12 - 15$, and n is either 3, 7, 9, or 15, and they are named S30, S70, S90, and S150, respectively.

Emulsion polymerizations of styrene were carried out using the same molar concentration of surfactant ($3.6 \times 10^{-5} \text{ mol}$) under controlled ionic strength (0.15). A redox initiator combination, diisopropylbenzene hydroperoxide - tetraethylene pentamine was utilized.

The results shown in Figures 1 and 2 suggest that an increase in the ethylene oxide chain length actually decreases the stabilizing efficiency of this surfactant in styrene emulsion polymerization. Samples of these different latices were filtered and coagulated in test tubes using increasing amounts of electrolyte, $MgSO_4$. It was found that the coagulation of latices stabilized with surfactants S30, S70, and S90 showed a dependence of time, which the latex S150 did not. Further, the first three latices were not peptizable, but the S150 latex could be peptized either by heating or by diluting the flocculated latex. These results indicate that the stabilization mechanism changes from primarily electrostatic to entropic steric stabilization as the ethylene oxide chain length increases to fifteen units.

Emulsion polymerizations of styrene were also carried out at constant amounts of surfactant ($7.1 \times 10^{-3} \text{ mol}$) under different ionic strengths for different surfactants. From the results shown in Figures 3 and 4, it is apparent that an increase in the ethylene oxide chain length results in a decreased sensitivity of the dispersion to the presence of electrolyte. These results agree with the previous coagulation tests, and seem to indicate that the stabilization mechanism of these surfactants changes from electrostatic to steric stabilization as the ethylene oxide chain length increases.

Fig. 1 Rate of polymerization of styrene versus ethylene oxide chain length in surfactants at same concentration (molar)

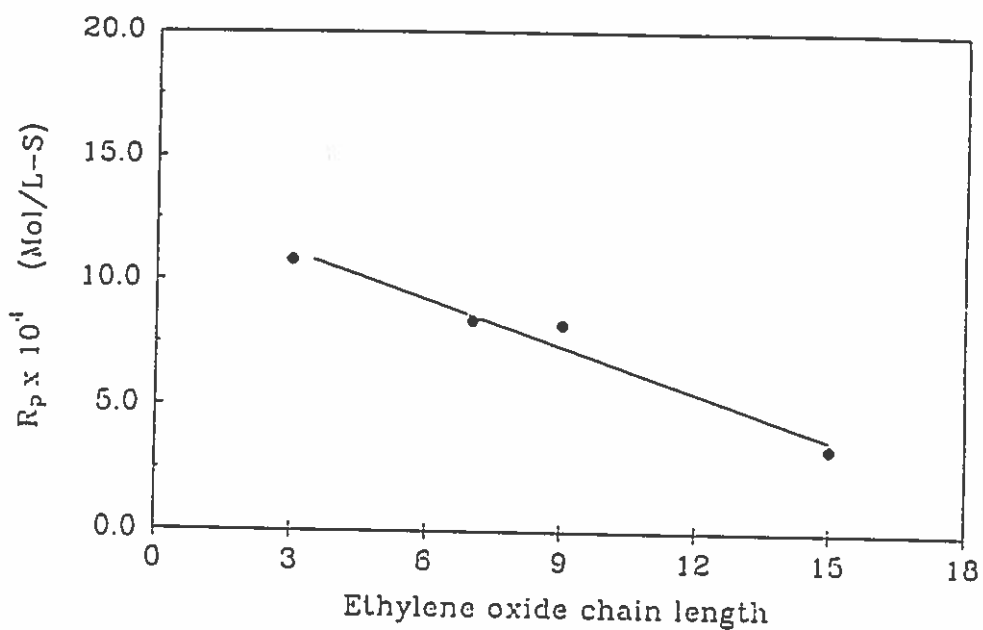


Fig. 2 Number of particles from DLS versus ethylene oxide chain length in surfactants at same concentration (molar)

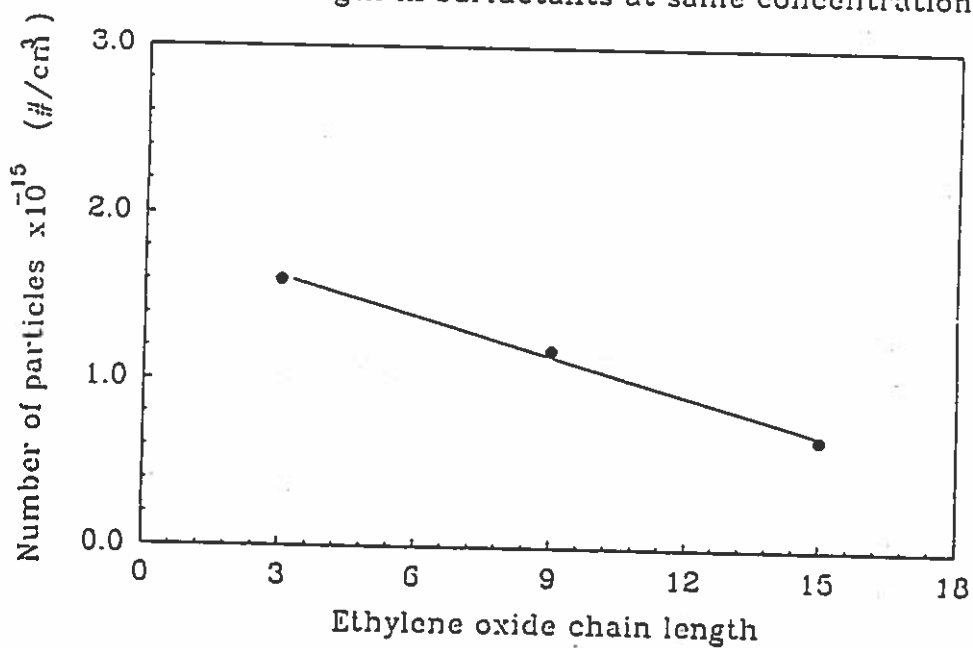


Fig. 3 Rate of polymerization of styrene versus ionic strength for different surfactants at same concentration (molar)

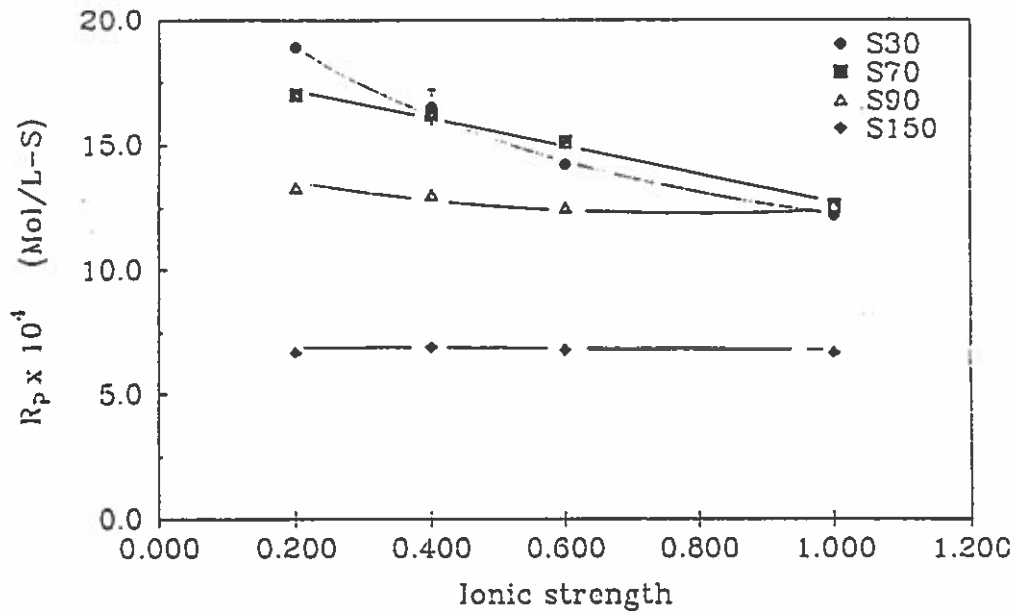
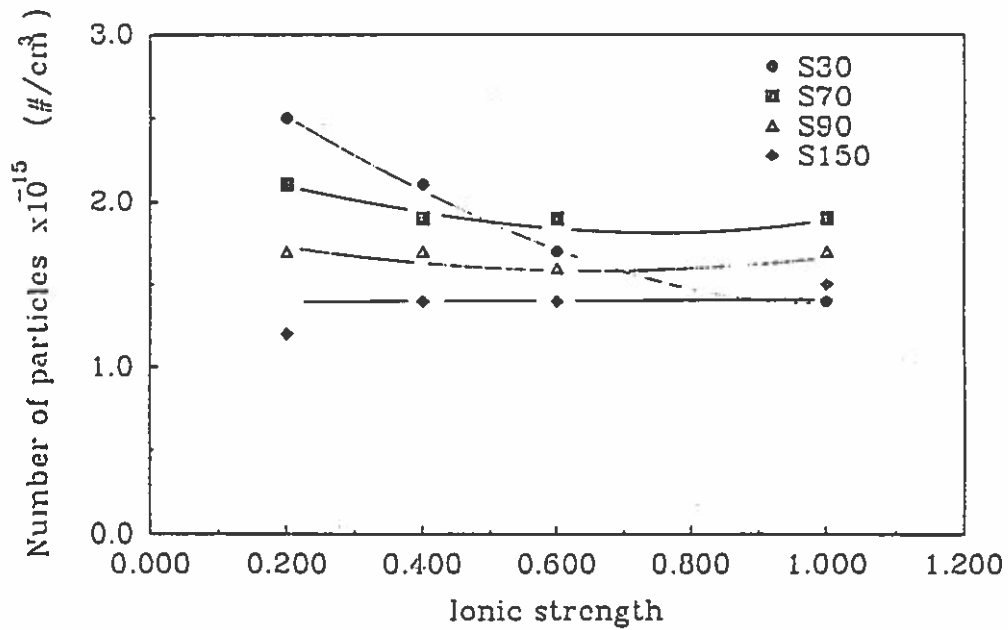


Fig. 4 Number of particles from DLS versus ionic strength for different surfactants at same concentration (molar)

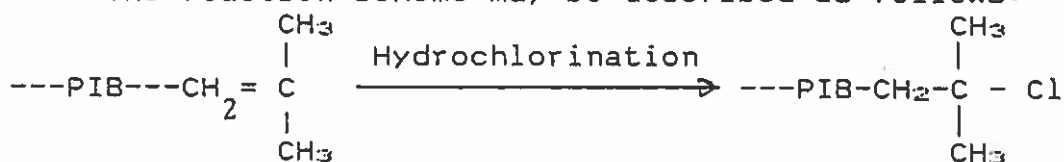


Synthesis of Amphipathic Block Copolymers based on Polyisobutylene and Polyoxyethylene

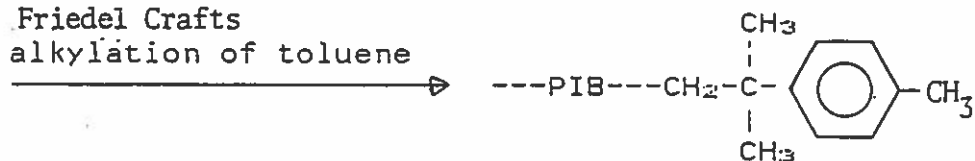
Reported by Bidulata Sar

Triblock copolymers of polyisobutylene (PIB) and polyoxyethylene (POE) have been prepared and characterized. A new method, a coupling technique, was used to synthesize these triblock copolymers. The method comprises the synthesis of monoarm polyisobutylene molecules carrying one terminal benzyl bromide end group and their coupling with the potassium salt of POE. In this manner a series of PIB-b-POE-b-PIB triblock copolymers have been obtained.

The reaction scheme may be described as follows:



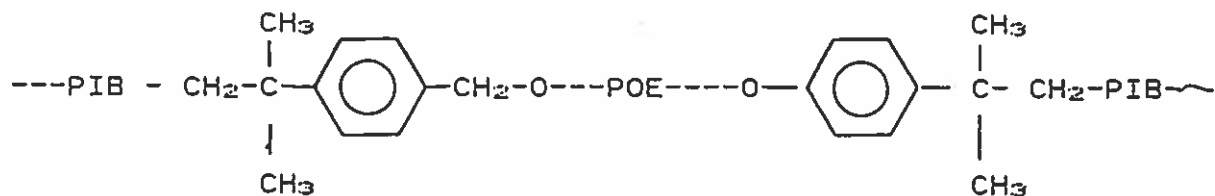
Friedel Crafts
alkylation of toluene



bromination



Coupling with KO-----POE-----OK gives



Quantitative hydrochlorination of various (Amoco) polybutenes was achieved by bubbling HCl gas through their methylene chloride solution. The structure of the hydrochlorinated product was confirmed by H^1NMR . Friedel Crafts alkylation of toluene by tertiary chloro-ended polyisobutylene was carried out to synthesize toluene ended PIB. Further bromination of the toluene ended PIB generated a benzylbromide ended PIB. The reaction was quantitative, and the structure was verified by H^1NMR . The benzyl bromide ended PIB was then coupled with the potassium salt of POE. After purification essentially a PIB-b-POE-b-PIB triblock was isolated. The products of several different synthesis were characterized by H^1NMR , UPC, UV, and IR. These block copolymers will be used to stabilize emulsion polymerizations of a variety of monomers.

Emulsion Copolymerization of Butadiene and Acrylonitrile
Reported by Samuel Laferty

A study of the variables controlling the kinetics of the copolymerization of butadiene and acrylonitrile is being conducted. The parameters under investigation so far are initiator levels, and surfactant types and levels.

KINETIC ANALYSIS OF SEEDED EMULSION POLYMERIZATION OF VINYL ACETATE

David M. Lange and Gary W. Poehlein
School of Chemical Engineering
Georgia Institute of Technology
Atlanta, GA 0100

INTRODUCTION

Hayashi et al. (1989) have published a considerable amount of data on the seeded emulsion polymerization of vinyl acetate in the absence of additional emulsifier. The results show that new particles are formed if the concentration of seed particles is not adequate to capture all of the free radical oligomers initiated in the aqueous phase. One series of experiments involved measuring particle concentrations and sizes as a function of time and conversion for the same recipe.

The purpose of this paper is to present a kinetic analysis of this data. The data obtained were from a seeded batch system in which secondary nucleation occurred early in the reaction. This provided a second relatively monodisperse population of particles in addition to the latex seed. An additional feature of this system is the large sizes of both particle populations. If typical emulsion polymerization kinetics apply, this system would possess a large α' value (α' is a dimensionless parameter used in emulsion polymerization kinetics (Uglestad et al. (1967))).

The unusual features of this system provide additional information on vinyl acetate emulsion polymerization. First, the data obtained at high α' values allows estimation of a capture constant (k_c) for vinyl acetate. Secondly, the initial formation of a second population of particles yields conditions used for competitive growth experiments. Thus competitive growth of particles may also be examined for vinyl acetate with these data.

EXPERIMENTAL

Experimental details are given by Hayashi et al. (1989). The recipe used for the experiments considered in this paper was as follows:

Deionized water	240.0g
KPS (initiator)	1.44g
Distilled VAC	80.0g

Seed particles (number) $5.5 \times 10^{10}/g$ - latex

(Diameter = $0.4 \mu m$)

Seven parallel experiments were carried out with this recipe. These reactions were stopped at different times and the reaction mixture analyzed for monomer conversion and particle concentrations and sizes. The results are shown in Table 1. The number concentrations of the two particle populations do not change after the early part of the reactions.

Table 1: DATA FROM VINYL ACETATE SEEDED POLYMERIZATION

Time (min)	Overall Conversion	D_{seed} (nm)	N_{seed} ($\times 10^{15} \frac{particles}{l-H_2O}$)	D_{new} (nm)	N_{new} ($\times 10^{15} \frac{particles}{l-H_2O}$)
0	0.0	400	7.4	0	0
10	18.8	780	7.4	400	1.32
20	39.1	950	7.4	490	1.29
30	71.4	1010	7.4	590	1.34
40	90.2	1180	7.4	650	1.34
50	99.2	1190	7.4	670	1.38

UGLESTAD THEORY ANALYSIS

The kinetics of emulsion polymerization with a monodisperse particle population involves a radical balance; on the particles and the aqueous phase which lead to the following relationships due to Stockmayer (1957), O'Tolle (1965) and Ugelstad et al. (1967).

$$1. \quad \bar{n} = \frac{a}{4} \left(\frac{I_m(a)}{I_{m-1}(a)} \right)$$

$$2. \quad \alpha = \alpha' + \bar{m} - Y \alpha^2$$

where: $a = (8\alpha)^{1/2}$

$$\alpha = \frac{\rho A v_p}{N k_{tp}}$$

$$m = \frac{k_d v_p}{k_{tp}}$$

$$\alpha' = \frac{\rho_i v_p}{N k_{tp}}$$

$$Y = \frac{2k_{tw} k_{tp} N}{v_p k_a^2}$$

A solution to Equations 1 and 2 can be plotted in the form of $\log \bar{n}$ vs $\log \alpha'$ with Y as a variable parameter and m fixed as shown in Figure 1. Please note that the \bar{n} value is not influenced by Y unless α' is large. Most emulsion polymerization kinetic studies involve small values of α' where the parameter m is important.

The vinyl acetate data shown in Table 1, however, involve relatively low concentrations of large particles where α' is larger. These data were analyzed to obtain the polymerization rates of each particle population. The rate data were then used to calculate values of \bar{n} for each particle population as a function of time.

The two different particle populations present a problem in estimating Y . The emulsion polymerization kinetic analysis presented earlier considers only a single monodisperse particle population. An initial assumption would be to consider this system monodisperse and calculate α' and various dimensionless parameters using average values of particle volume and \bar{n} . With these assumptions, the \bar{n} - α' data is superimposed on the solution plot in Figure 1. Two data points are shown for data obtained at lower conversions in interval III (higher conversions were not considered due to gel-effect uncertainties). The termination constant used in the calculations was adjusted for the gel-effect. Both data points fall on a line representing a constant $Y_{\text{monodisperse}}$ value of approximately 10^{-1} . With this value of Y , the radical capture rate constant k_c was found to be $2.46 \times 10^{-12} \text{ cm}^3/\text{sec}$.

A second proposed method for dealing with the two particle populations is to assume the radical absorption rate into each particle population is either proportional to surface area or can be modeled on the basis of continuum diffusion theories. Both cases were used in this study. The population of particles formed by secondary nucleation are referred to as "new" particles in the nomenclature.

Plotting $n^{-\alpha}$ data for the two particle populations on the solution plot with constant m_{seed} set to zero and varying Y_{seed} allows estimation of the defined Y . This allows for estimation of k_a and k_c based on the seed growth ($k_a = Nk_c$). A similar method is used for the new particle population. It should be noted that Y in these individual cases are different since they are based on individual populations. The individual Y values would not be related to $Y_{monodisperse}$. Results are shown on Figure 2 for two sample times. The data points for the two different absorption theories overlap. Hence these data cannot help to resolve the question concerning models of radical transport. These results are used to calculate values of k_c which are displayed in Table 2. Values of k_c estimated for styrene are also shown in Table 2 for comparison. The larger k_c values for the vinyl acetate system in comparison to styrene are supported by the aqueous-phase termination considerations proposed by Hawkett et al. (1985). In their analysis of aqueous-phase termination they concluded that increasingly water soluble monomers should produce less aqueous-phase termination. Decreasing aqueous-phase termination should produce a larger value of k_c for the system. If the aqueous - phase termination hypothesis of Hawkett et al. is correct, it would support the observed results since vinyl acetate has a greater water solubility than styrene, .35M vs 0.004M.

Table 2: k_c Estimates

System	k_c
Monodisperse Assumption	$2.46 \times 10^{-12} \frac{cm^3}{s}$
Based on Seed Particles	$6.75 \times 10^{-12} \frac{cm^3}{s}$
Based on New Particles	$2.98 \times 10^{-12} \frac{cm^3}{s}$
Styrene Polymerization (Feeney (1986))	$5.5 \times 10^{-13} - 5.5 \times 10^{-16} \frac{cm^3}{s}$
Styrene Polymerization (Uglestad (1978))	$2.5 \times 10^{-12} - 2.5 \times 10^{-14} \frac{cm^3}{s}$

COMPETITIVE GROWTH

Vanderoff et al. (1956) considered the tendency of the particle size distribution of polydisperse latexes to sharpen during polymerization. The

$$\frac{dv_p \text{ unswollen}}{dt} = k D_p^c \text{ unswollen} \quad (3)$$

where $v_p \text{ unswollen}$ is the unswollen particle volume or polymer volume, $D_p \text{ unswollen}$ is the unswollen particle diameter, k is a constant, and c is an exponent determined from experimental data.

Emulsion polymerization with two different size seed particle populations initially present were conducted to examine competitive growth effects. Conditions were adjusted to prevent secondary particle nucleation and the different size particles were allowed to compete for resources (monomer, radicals, etc.) during the polymerization. At the end of reaction the resulting average diameters of both seed populations were obtained.

Integration of equation 3 provides

$$D_b^{3-c} - D_{b_0}^{3-c} = D_a^{3-c} - D_{a_0}^{3-c} = \frac{2(3-c)}{\pi} \int_0^t k(t) dt \quad (4)$$

Rearranging yields
$$\frac{D_b}{D_a} = \frac{1}{\gamma} [\gamma^{3-c} + \alpha^{3-c} - 1]^{\frac{1}{3-c}}$$

with

$$\alpha = \frac{D_{b_0}}{D_{a_0}} \quad (5)$$

$$\gamma = \frac{D_a}{D_{a_0}}$$

Figure 3 demonstrates the effect of different values of c on the particle size ratio. If $c < 3$ then the particle size distribution will sharpen during reaction and if $c > 3$ the particle size distribution will broaden. Data from competitive growth experiments may be plotted on Figure 5 to estimate the value of c . Styrene emulsion polymerization was found to produce values of c in the range of 0 to 1 for smaller particles. A value of $c = 2.5$ was found to apply to large particles (> 150 nm).

In this seeded study of vinyl acetate, a second relatively monodisperse population of particles is nucleated at the start of the polymerization (as observed by SEM). Thus, unintentionally, the particle size-time data for both particle populations allows competitive growth analysis of this vinyl acetate system. The particle size data were smoothed

polymerization (as observed by SEM). Thus, unintentionally, the particle size-time data for both particle populations allows competitive growth and corresponding values plotted on Figure 3. A value of c in the range of 2.75 fit the data. Particles in the same size range in styrene polymerization produce a similar value of 2.5 for c .

SUMMARY

The data for Hasashi et al. can be used for kinetic analysis by several techniques. The calculated radical capture rates constants can only be considered approximate because of the assumptions necessary to complete the calculations. A more complete paper, with additional input from Hayashi and coworkers, is being prepared.

BIBLIOGRAPHY

- Feeney, P. J., PhD Dissertation, Department of Physical Chemistry, University of Sydney, Sydney, Australia (1986)
- Hansen, F. K., and Uglestad, J., *J. Polym. Sci.: Polym. Chem. Ed.*, **16**, 1953, (1978)
- Hawket, B. S., Napper, D. H., and Gilbert, R. G., *J. Polym. Sci.: Polym. Chem. Ed.*, **19**, 3173 (1981)
- Hayashi, S., Komatsu, A., and Hirai, T., *J. Polym. Sci.: Part A: Polym. Chem.*, **27**, 157, (1989)
- O'Toole, J. T., *J. Appl. Polym. Sci.*, **9**, 1291 (1965)
- Stockmayer, W. H., *J. Polym. Sci.*, **24**, 314 (1957)
- Uglestad, J. Mork P. C., and Aasen, J. O. *J. Polym. Sci., A-1*, **5**, 2281, (1967)
- Vanderhoff, J. W. Vitkuske, J. F., Bradford, E. B., and Alfredy, T., *J. Polym. Sci.*, **20**, 225 (1956)

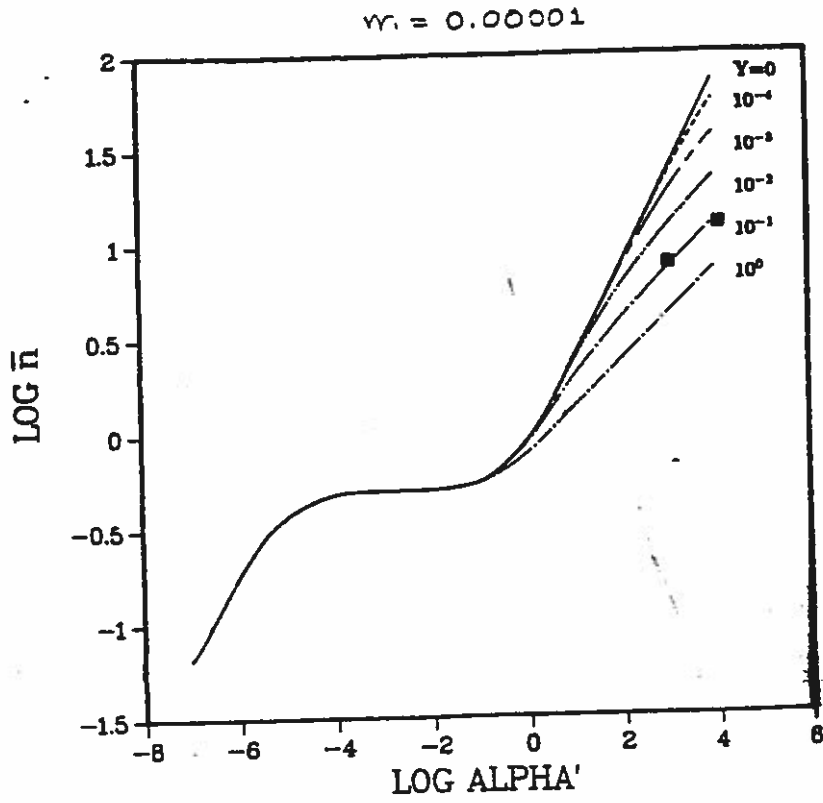


Figure 1. Estimation of Y for system assuming particles are monodisperse.

ESTIMATION OF Y

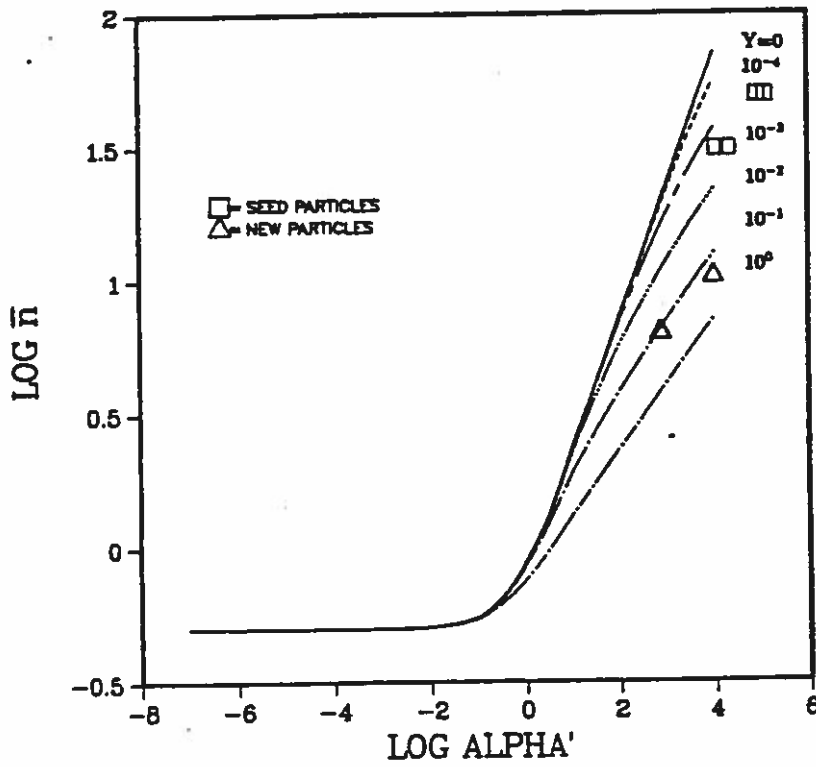


Figure 2 Estimation of Y_{seed} and Y_{new} . Data based on radical absorption proportional to surface area and radical absorption modeled on continuum mechanics are both plotted.

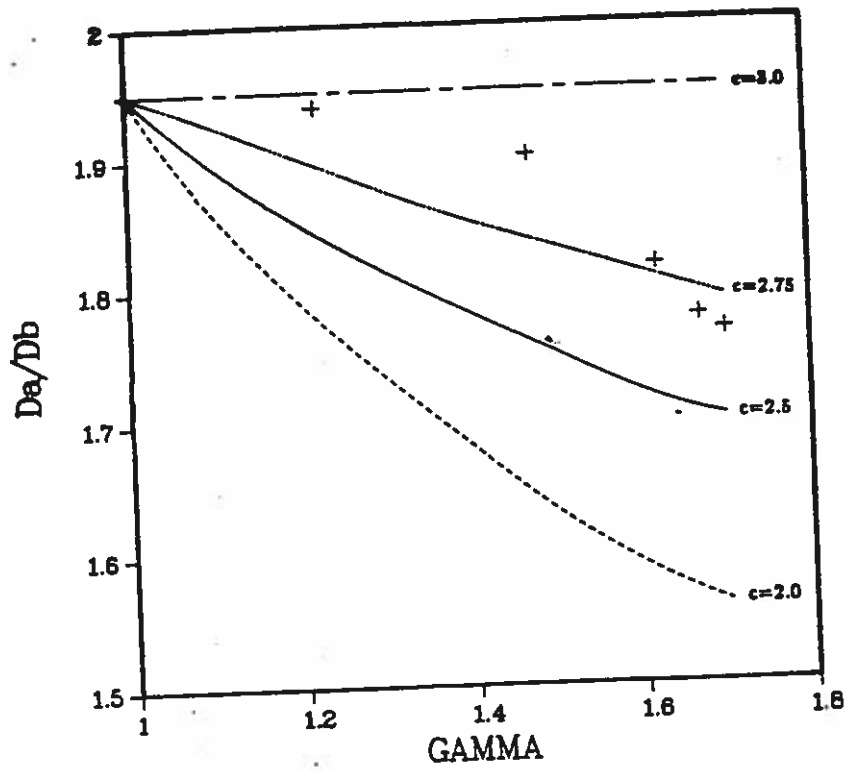


Figure 2 Variation of $\frac{D_a}{D_b}$ with γ .

Solution and Emulsion Polymerization with Partially
Neutralized Methacrylic Acid

Glenn L. Shoaf

Gary W. Poehlein*

School of Chemical Engineering

Georgia Institute of Technology

Atlanta, Georgia 30332-0100

SYNOPSIS

Polymerizations of partially neutralized methacrylic acid (MAA) were performed in both solution and emulsion systems. Polymerizations of MAA in solution were performed at an overall degree of neutralization ranging between 0 and 1. The rate of polymerization of the acid is found to decrease as the degree of neutralization increases due to increased electrostatic repulsion of the dissociated acid species (anions). The degree of neutralization of the unreacted monomer increases as the conversion increases. A kinetic model based on a copolymerization mechanism is used to describe the reaction behavior. Partially neutralized methacrylic acid was also polymerized with styrene in a seeded emulsion system. The reaction rates of both the acid and styrene decrease as the overall degree of neutralization increases. A previously developed emulsion copolymerization kinetic model is extended to account for reaction of the anions and used to investigate the overall 'terpolymerization' of the acid, anions, and styrene. Only the solution polymerization experimental and model results are presented in this brief paper.

* To whom correspondence should be addressed.

Solution Polymerization Studies

Solution polymerizations of MAA were carried out under each of the conditions listed in Table 1.

Table 1: Conditions used for solution polymerizations of both MAA and AA ($[I]_0 = 0.001 \text{ M}$)

Concentration Acid (Wt.%)	DN	Temperature (C)
20	00	85
40	00	85
70	00	85
100	00	85
70	025	85
70	050	85
70	075	85
70	100	85
70	00	70
70	00	80
70	00	90
70	00	96-98

Conversion-time curves for the natural pH (DN=0) reactions of MAA at 85°C over a range of concentrations from 2.0 to 10.0 wt.% are shown in Figure 1. The basic free-radical solution polymerization equation which has been shown to apply to many simple solution systems was used to examine the experimental data.

$$R_p = -\frac{dM}{dt} = k_p \frac{(2fk_d[I])^{1/2}}{(2k_t)^{1/2}} [M] \quad (1)$$

Integration of eq. 1, assuming that only $[M]$ varies, results in eq. 2.

$$\ln \frac{[M]_0}{[M]} = k_p \frac{(2fk_d[I])^{1/2}}{(2k_t)^{1/2}} t = Kt \quad (2)$$

Reaction samples were obtained over time, and monomer conversions were measured gravimetrically. $[I]$ can be calculated as a function of time through eq. 3.

$$[I] = [I]_0 \exp(-k_d t) \quad (3)$$

It remained essentially constant over the short reaction period (< 20 minutes) required for nearly completely conversion of MAA and AA (i.e., $[I]=0.92[I]_0$ after 20 minutes). A value of k_d of 6.89×10^{-5} was obtained from the literature [1]. A value of 1.0 was used for the initiator efficiency factor, f .

Gromov [2] assumed that the reaction rate given by eq. 1 applied to both AA and MAA solution polymerizations. (Chapiro [3] and Shoaf [4], however, showed that the mechanism for reaction of AA is more complicated than the simple solution polymerization scheme.) The value of k_p should then be independent of monomer concentration. Gromov does not specifically state the actual monomer concentrations utilized in his experiments. However, similar work which he performed with Galperina [5] involved reactions of AA at concentrations of 3.0 to 4.0 wt.%. The values for k_p based on Gromov's data were obtained by fitting an Arrhenius expression to the data (which were given for temperature ranges of 0 to 60°C) and extrapolating to 85°C, the temperature of the reactions performed in this work. These experiments as well as Gromov's were performed at natural pH (approximately 2.2 - 2.4).

Plots of $\ln[M]_0/[M]$ versus time should be linear with a slope K based on the relationship given by eq. 2. Values of $k_p/k_t^{1/2}$ can be obtained from this slope. Gromov et al. [2] reported values of k_t for MAA (0.12×10^8 L/mole s) from experiments utilizing the method of alternating illumination. The values were relatively constant over a range of temperatures from 0 to 60°C, and these values were assumed to apply also at 85° so that propagation constants could be calculated directly from $k_p/k_t^{1/2}$ ratios. Values of $k_p/k_t^{1/2}$ and k_p (L/mole s) obtained from the experimental data as well as those predicted from Gromov's data are listed in Table 2 for the range of monomer concentrations investigated.

Table 2: $k_p/k_t^{1/2}$ and k_p values for MAA and AA at 85°.

WT.%	$\frac{k_p}{k_t^{1/2}}$ (L/mole s) ^{1/2}	$k_{p\text{exp}}$ (L/mole s)	$k_{p\text{Gromov}}$ (L/mole s)
MAA			
2.0	4.37	15,200	15,900
4.0	5.24	18,200	15,900
7.0	4.89	16,900	15,900
10.0	4.34	15,000	15,900

The $\ln[M]_0/[M]$ versus time plots for MAA are shown in Figure 2. Plots of the MAA data result in relatively straight lines as predicted by the assumed first order kinetic model given by eq. 2. k_p values are plotted as a function of initial monomer weight percent for MAA in Figure 3. The data for MAA agree fairly well (within experimental error) with the k_p values predicted from Gromov's data.

Solution Polymerizations: Experimental and Model

Results with $DN > 0$

The initial rates of MAA polymerizations in solution were measured over a range of DN from 0 to 1 to check the reproducibility of the results reported by Kabanov et al. [6]. The results are shown in Figure 4 for MAA. The rates of reaction decreased with increasing DN as expected.

Additional unseeded solution polymerizations of MAA at DN between 0 and 1 were conducted to determine to what extent the DN of the unreacted monomer changed over the conversion period. The pH of these reactions was measured throughout the reaction period by inserting a pH probe and temperature probe into the reactor. The DN of the unreacted monomer could then be calculated with eq. 4 and the concentration of hydrogen ions as determined from the pH measurements.

$$DN = \frac{\frac{K_a}{[H^+]}}{1 + \frac{K_a}{[H^+]}} = \frac{\frac{10^{-pK_a}}{10^{-pH}}}{1 + \frac{10^{-pK_a}}{10^{-pH}}} \quad (4)$$

A method for predicting the actual DN of the unreacted monomer over the entire conversion period is developed as follows. Equilibrium expressions for both the monomer (1) and polymer (2) are given by equations 5 and 6.

$$K_{a1} = \frac{[H^+][A_1^-]}{[HA_1]} \quad (5)$$

$$K_{a2} = \frac{[H^+][A_2^-]}{[HA_2]} \quad (6)$$

(This analysis assumes that an average K_a value may be used for the polymer. Actually, this value depends on the chain length and chain conformation of the polymer such that a distribution of K_a values corresponding to the distribution of polymer chain lengths and chain conformations better describes the actual system.) The ratio of the K_{a1} values gives equation 7.

$$K_{a1}/K_{a2} = \frac{x(y-z)}{(M_a - x - y)z} \quad (7)$$

Here, x is the moles of dissociated monomer, y is the moles of reacted monomer, z is the moles of dissociated polymer, and M_A is the initial moles of monomer charged.

The total moles of dissociated species is

$$[A_1^-] + [A_2^-] = x + z = (DN_o)M_A \quad (8)$$

where, DN_o is the overall degree of neutralization, not the DN of the unreacted monomer.

Solving for z and substituting in equation 7 gives

$$K_{a1}/K_{a2} = \frac{x(y - (DN_o)M_A + x)}{(M_A - x - y)((DN_o)M_A - x)} \quad (9)$$

The value of x for any given value of y (obtained from the conversion) may be obtained by taking the positive root of this quadratic equation. The actual degree of neutralization of the unreacted monomer may then be obtained as a function of the moles of reacted monomer by equation 10.

$$DN(y) = \frac{x}{M_A - y} \quad (10)$$

Equation 10 is based on the assumption that a single value of K_{a2} may be used. The value of K_{a2} has a large effect on the value of DN predicted from equation 9 as revealed by Figure 5. The actual DN of the unreacted monomer does increase with conversion as expected (Figure 6), but the best fit of the experimental DN-conversion data required some modification of K_{a2} from the average value of 1.0×10^{-7} as reported by Molyneux [7]. The correct value of K_{a2} for the polymer is uncertain since there are actually many values depending on the lengths and conformations of the polymer chains. Therefore, K_{a2} was adjusted in the model to give the best fit of the data. A single value of 3.5×10^{-6} resulted in consistent fits of the DN versus conversion plots for the full range of initial DN values examined.

The next step was to predict the reaction rate of MAA at various DN accounting for the fact that the DN of the unreacted monomer does change with conversion. Kabanov et al. [6] report a value of 670 L/(mole s) for the propagation constant (k_{pCC}) of the MAA anion and $2.1E8$ L/(mole s) for the termination constant at 23°C. A value for k_{pCC} at 85°C was obtained by fitting experimental conversion data of MAA obtained at a DN of 1.0 using the basic solution polymerization equation since at a DN of 1.0, only one reaction species, the anions, will be present in the system. The best fit was obtained with a k_{pCC} of 5000 L/(mole s) (Figure 7). (The k_t value was assumed not to change significantly with temperature. Values of k_t reported by Kabanov et al. [6] for the unneutralized MAA polymerization were constant over a temperature range of 20 - 60 °C.)

The copolymer model was modified to account for the changing DN with conversion by using eq. 10. The results of the model using a K_{a2} value of 3.5×10^{-6} are shown in Figure 8. The predicted conversion-time results slightly underestimate the experimental data for all initial DN values.

A further adjustment of K_{a2} was then made in order to obtain a better fit to the conversion-time data. Figure 9 shows that a good fit of the reaction data is obtained for all initial DN values if a value of K_{a2} of 8.0×10^{-6} is used. The predicted DN was recalculated using the adjusted K_{a2} value and compared to the measured values as exhibited in Figure 10. The predicted values are close to the observed values, but in each case the observed values are slightly underestimated.

Therefore, good fits of both DN-conversion data and conversion-time data can be obtained using a solution copolymerization model which accounts for the change in DN of the unreacted monomer with conversion for a wide range of initial DN values. However, some discrepancy between the values of K_{a2} which give consistent fits of both types of data, simultaneously, still remains.

REFERENCES

1. Brandrup, J. and Immergut, E.H., Eds., Polymer Handbook, 2nd Edit., John Wiley and Sons, NY (1975).
2. Gromov, V.F., Galperina, N.I., Osmanov, T.O., Khomikovskii, P.M. and Abkin, A.D., European Polym. Journal, **16**, 529 (1980).
3. Chapiro, A. and Dulieu, J., Eur. Poly. Journal, **13**, 563 (1977).
4. Shoaf, G.L., PhD Thesis, School of Chemical Engineering, Georgia Institute of Technology, Atlanta, Ga. (1989).
5. Galperina, N.I., Gugunava, T.A., Gromov, V.F., Khomokovskii, K.I. and Abkin, A.D., Vysokomol. Soyed. A17, 1455 (1975).
6. Kabanov, V.A., Topchiev, D.A. and Karaputadze, T.M., J. Polym. Sci. Polym. Symp., **4**, 173 (1973).
7. Molyneaux, P., Soluble Synthetic Polymers: Properties and Behavior, Vol. I, CRC Press (1983).
8. Plochocka, K., J. Macromol. Sci. Rev. Macromol. Chem. **C20(1)**, 67 (1981).

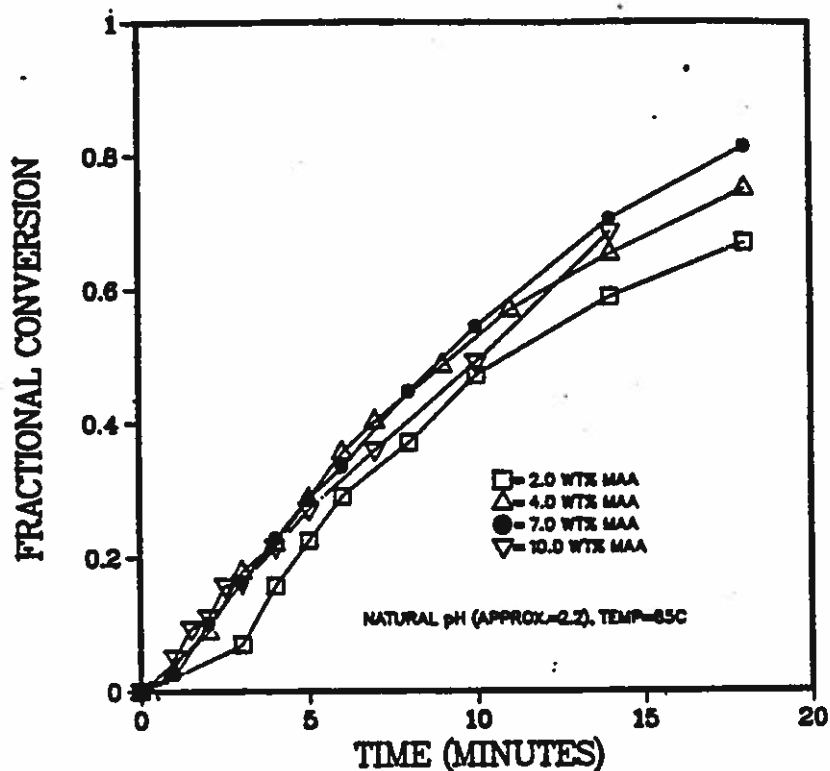


Figure 1: Conversion-time curves for the MAA solution polymerization at various initial monomer concentrations (85°C).

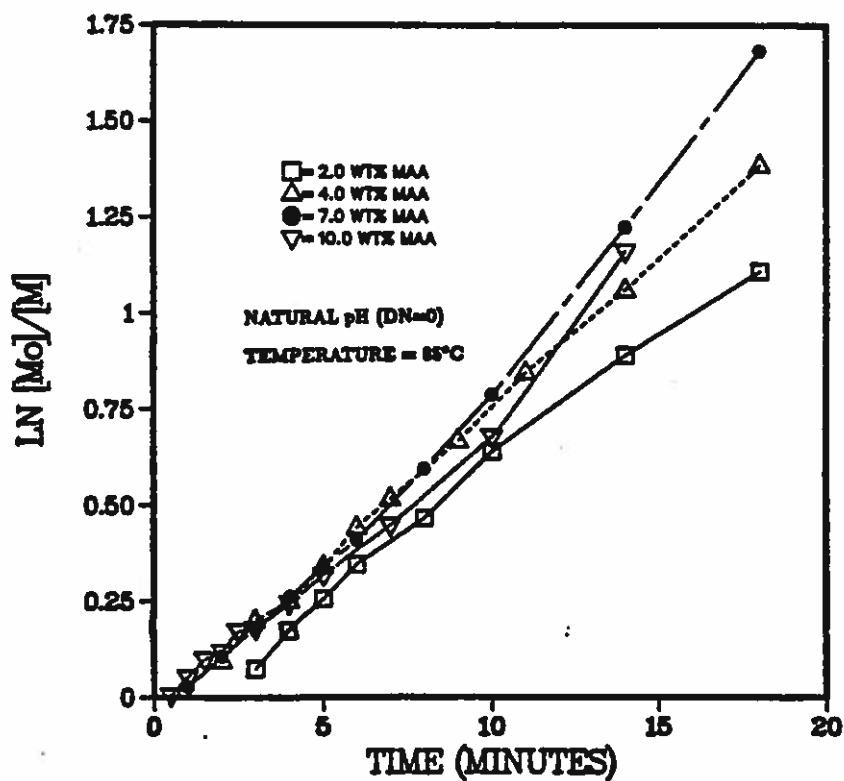


Figure 2: $\ln([M_0]/[M])$ -time relationship for 2.0, 4.0, 7.0 and 10.0 wt.% MAA solution polymerizations at 85°C and natural pH.

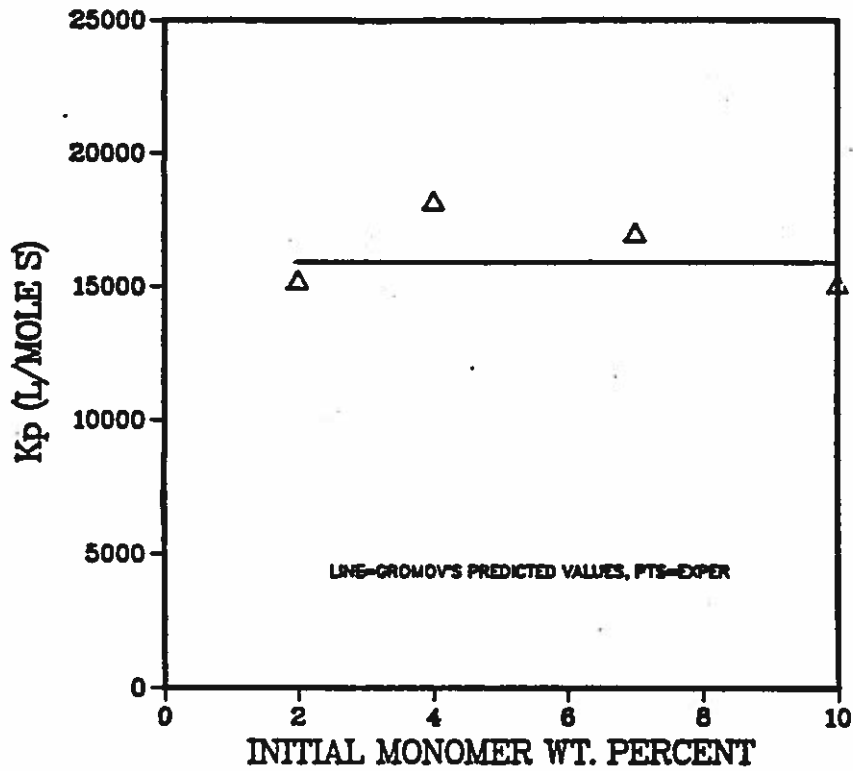


Figure 3: Dependence of k_p on initial monomer weight percent for MAA solution polymerization at 85°C.

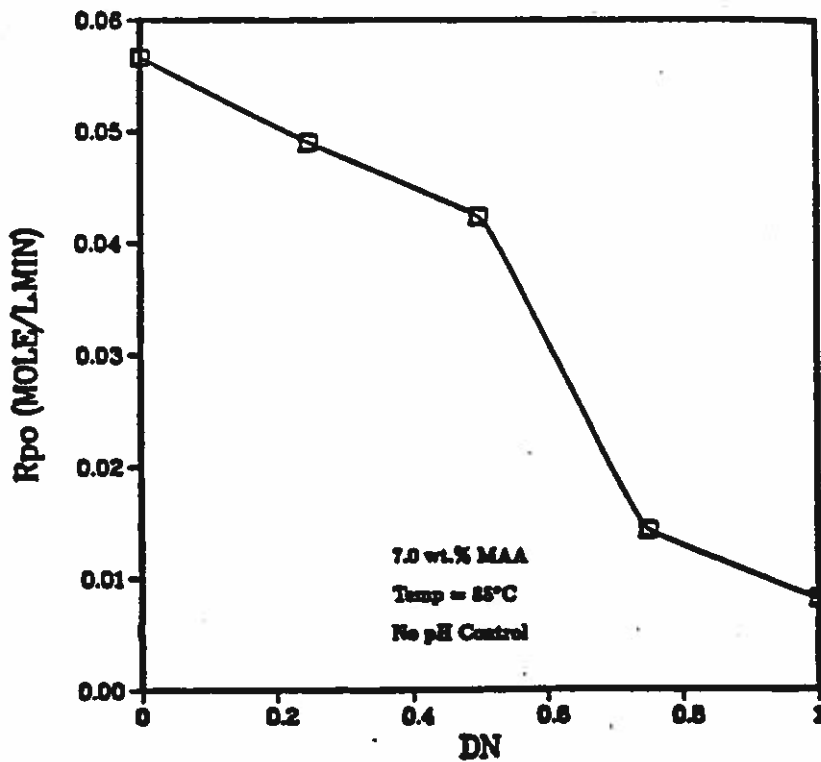


Figure 4: Initial rates of reaction as a function of DN for 7.0 weight percent MAA in solution at 85°C.

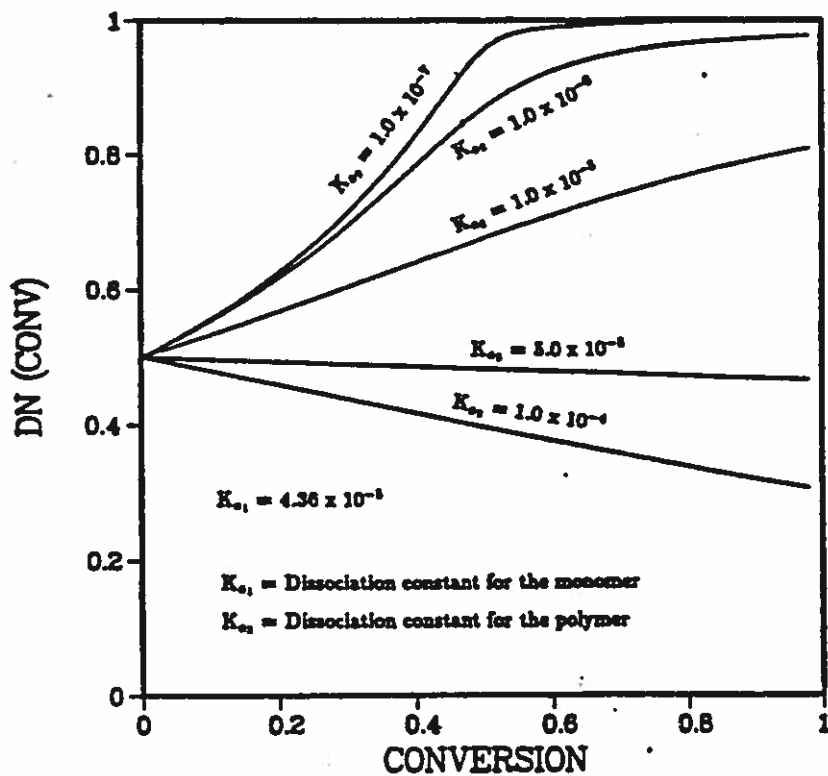


Figure 5: Effect of K_{a2} on the predicted DN as a function of conversion with an overall DN of 0.5.

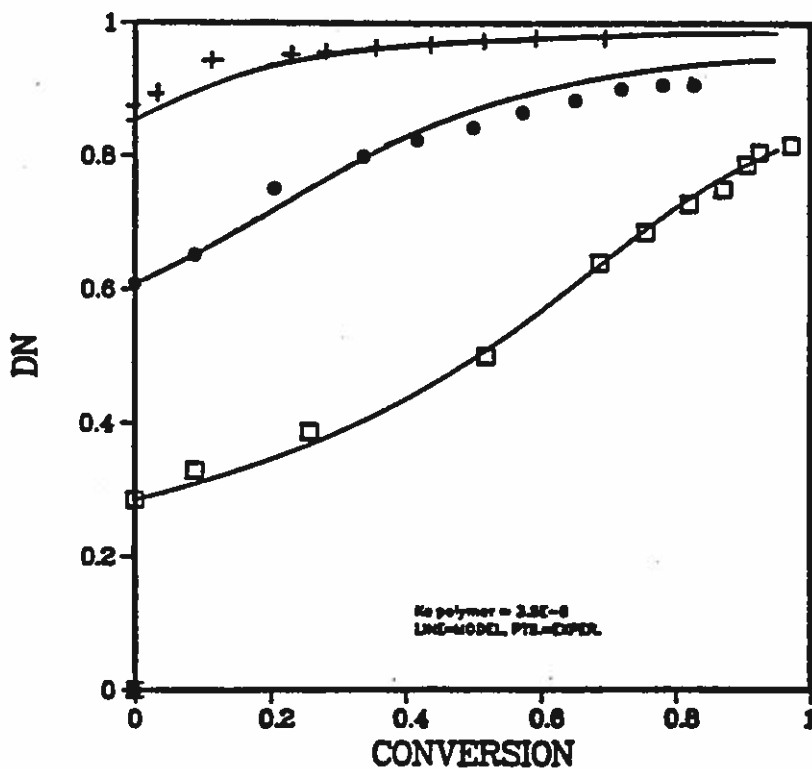


Figure 6: Comparison of predicted DN as a function of conversion with experimental values (K_{a2} of 3.5×10^{-6}).

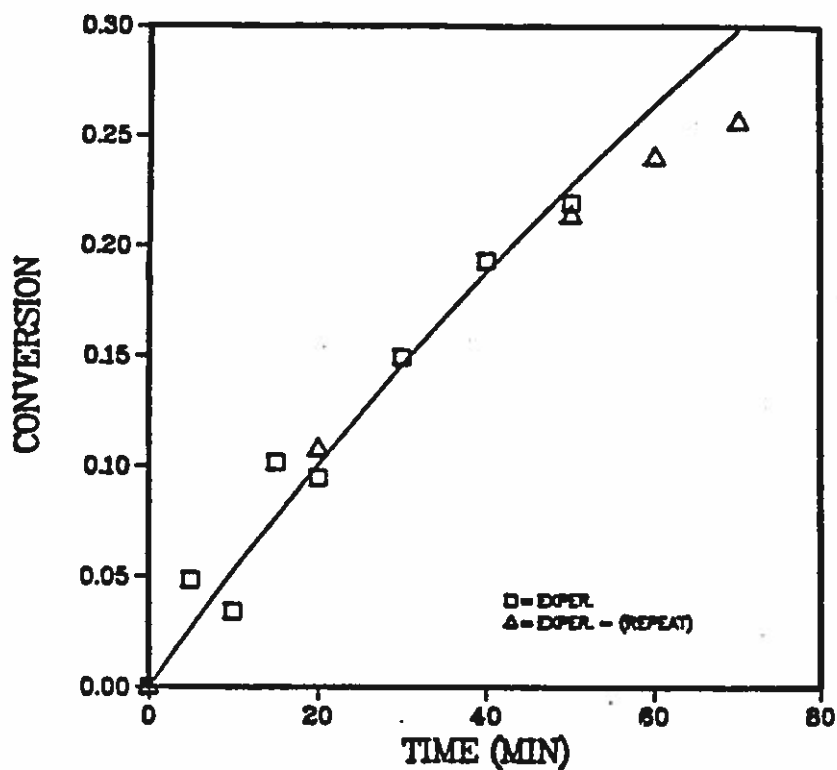


Figure 7: Fit of conversion-time data for the MAA anion at 85°C using the solution polymerization equation, a value of k_t of 2.1×10^8 (L/mole s) as reported by Plochocka [8], and an adjustable propagation constant, k_{pCC} . The best fit was obtained with a k_{pCC} of 5000 (L/mole s).

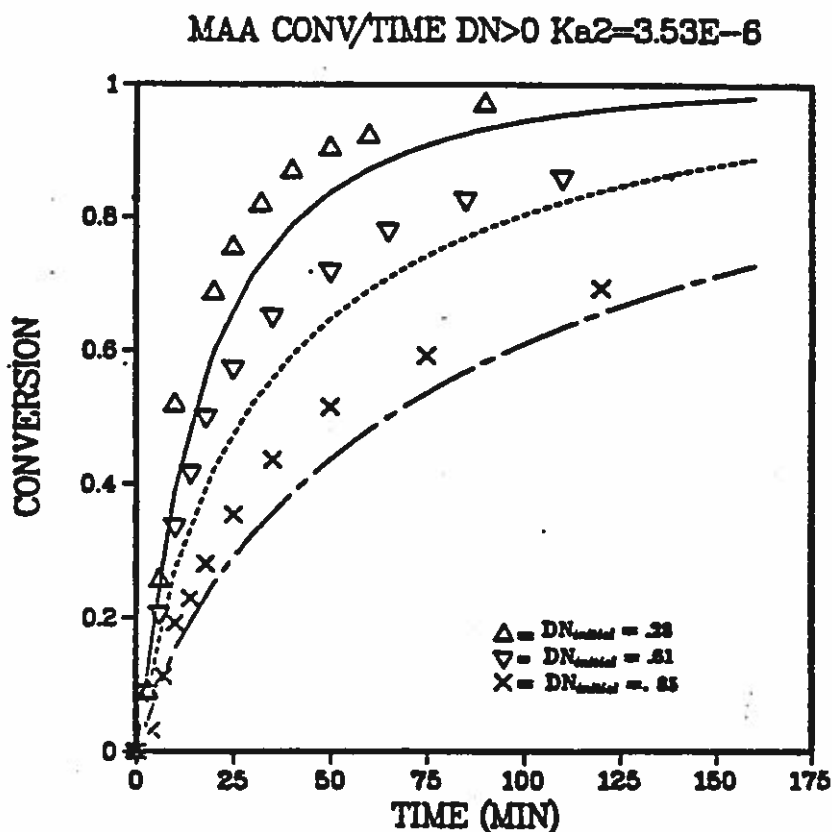


Figure 8: Comparison of solution copolymerization reaction model results to experimental data for MAA at various DN ($K_{a2}=3.5 \times 10^{-6}$).

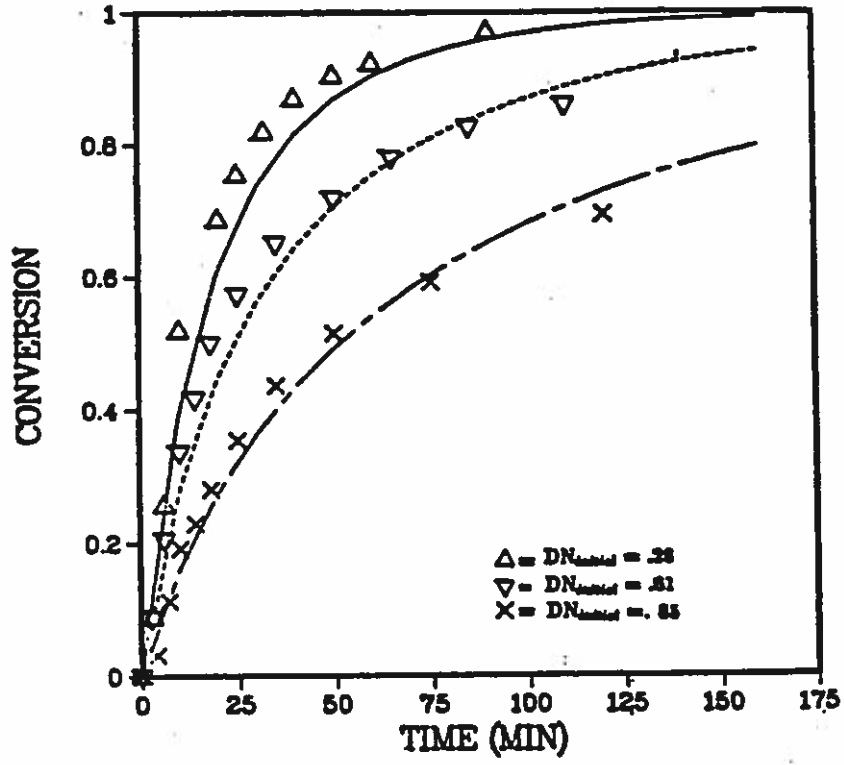


Figure 9: Comparison of solution copolymerization reaction model results to experimental data for MAA at various DN ($K_{a2}=8.0 \times 10^{-6}$).

DN/CONV Ka2=8.0E-6 MODEL/EXPER

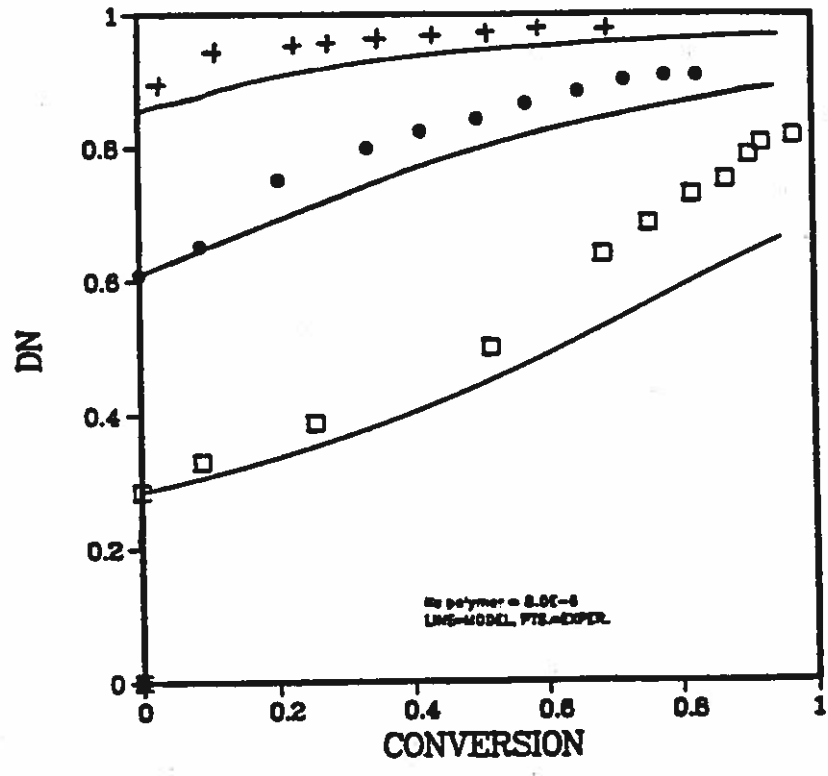


Figure 10: Comparison of predicted DN as a function of conversion with experimental values (K_{a2} of 8.0×10^{-6}).

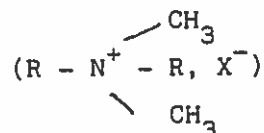
Contribution to the Polymer Colloids Group Newsletter
Spring 1990

Surface characterization of γ -irradiation crosslinked natural rubber latex
by phase transfer with cationic surfactants

P. TANGBORIBOONRAT and G. RIESS

Ecole Nationale Supérieure de Chimie de Mulhouse (France)

A phase transfer technique previously developed in our Lab (1) has been used to determine the surface charge of natural rubber latex concentrate crosslinked by gamma-irradiation. This technique involves the titration of the negatively charged latex, derived from an adsorbed layer of a protein-lipid complex, with quaternary ammonium salts



in the presence of an organic phase. At a certain concentration of the added cationic surfactants, which is just sufficient to form a hydrophobic layer, the latex particles would be transferred from aqueous phase into the organic phase. The titration end point is obtained by observing the clear aqueous phase.

The quantity of surface charge of natural latex can be calculated from the amount of the critical transfer concentration of the surfactants used. This quantity is certainly only an average surface charge for the given latex because the latex particles are not uniform in size. The results are reproducible. The critical transfer concentration depends on neither the mass of latex nor the volume of organic solvent. It depends, however, on the structure of surfactants.

This technique can also be used to isolate the rubber particles from an aqueous serum phase or to prepare polymer blends such as rubber modified polystyrene.

1) Ph. HEIM Thesis University of Haute Alsace 1987

Spring 1990

Micelle Formation of Carboxy-terminated Polyesters*

F. CUIRASSIER, Ch.H. BARADJI and G. RIESS

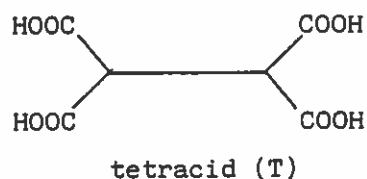
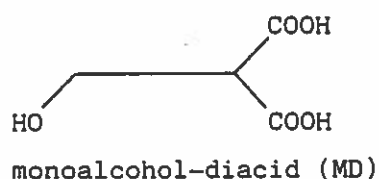
Ecole Nationale Supérieure de Chimie de Mulhouse (France)

Carboxy-terminated polyesters, based on isophthalic acid and aliphatic diols were synthesized, in a molecular weight range of M_n 1000-4000.

Such telechelic polyesters show typical surfactant behavior after neutralisation with various amines (mono- and diethanol amine, etc...). Micellization has been studied by photon correlation spectroscopy. The micelle size, typically in the range of 10-30 nm, and its structure have been examined as functions of the polyester molecular characteristics and its degree of neutralization.

Synthesis and Characterization of Carboxy terminated Polyesters

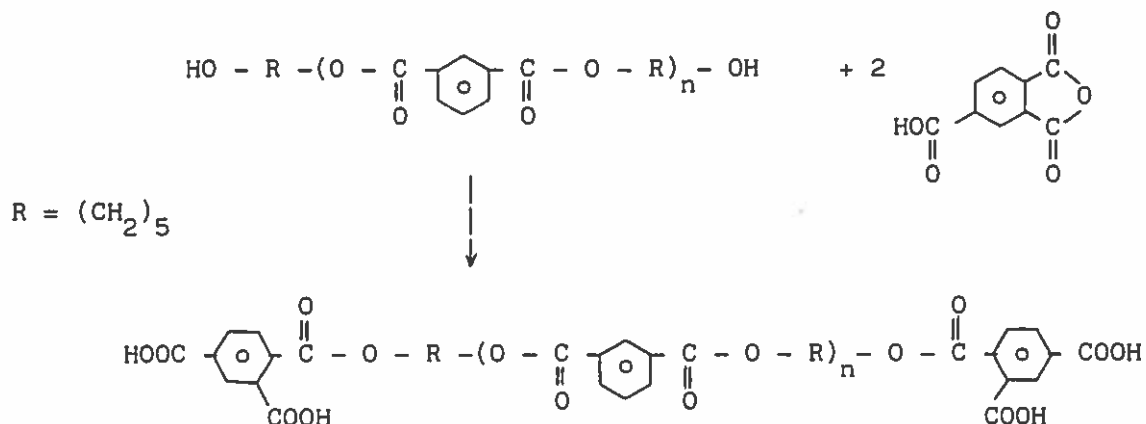
For this study we have synthesized a series of polyesters of different molecular weights having the following schematic structures :



Such polyesters are prepared by condensation in xylene of isophthalic acid with a slight excess of 1,5-pentanediol. The molecular weights are adjusted by the ratio diol/diacid. The carboxy end groups are introduced by reacting the hydroxy terminated polyesters with suitable amounts (stoichiometric amount for the tetracid) of trimellitic anhydride.

*This article is a part of the paper published in ACS Symposium Series 384 100 (1989), Ed. M.A. EL-NOKALY

For the tetracid series the reaction sequence is as follows :



The characteristics of these polyesters are given in Table 1.

TABLE 1 : Characteristics of the Carboxy Terminated Polyesters

Sample	Acid index (a)	Hydroxy index (b)	M_n (c)	M_n (d)	$[\eta]$ ml/g (e)
MD 60	61	36	1840	1820	9.3
MD 90	89	45	1260	1100	8.2
MD 120	113	69	990	/	7.0

T 60	61	/	3700	3850	13.5
T 90	100	/	2240	/	10.5
T 120	128	/	1750	1700	6.6

(a) (Milliequivalent COOH per g of polyester) x 56108. Determination by KOH titration

(b) (Milliequivalent OH per g of polyester) x 56108. Determination by acetylation

(c) M_n calculated according to the acid index

(d) M_n determined by vapor pressure osmometry

(e) Intrinsic viscosity in THF at 25°C

Micellization of Functionalized Polyesters

The carboxy terminated polyesters become water dispersable only by neutralization with a base such as amines :



As for classical surfactants, these neutralized polyesters in an aqueous phase have a tendency to form colloidal dispersions of micellar type. The size of these micelles will be a function of the molecular characteristics of the polyester (molecular weight, number of end groups).

The different amines used for neutralization of the polyesters are given in Table 2.

TABLE 2 : Amines Used as Neutralization Agents for the Polyesters

Amines	Structure	Code
Monoethanolamine (2 - amino ethanol)	$\text{H}_2\text{N} - \text{CH}_2 - \text{CH}_2 - \text{OH}$	MEA
Diethanolamine Bis (2-hydroxyethyl)amine	$\text{HN} - (\text{CH}_2 - \text{CH}_2 - \text{OH})_2$	DEA
N,N-dimethylethanol amine N,N-dimethylamino-2 ethanol-1	$\begin{array}{c} \text{CH}_3 \\ \diagdown \\ \text{N} - \text{CH}_2 - \text{CH}_2 - \text{OH} \\ \diagup \\ \text{CH}_3 \end{array}$	DMEA
N-methyldiethanolamine N,N Bis (2 hydroxyethyl) methylamine	$\text{CH}_3 - \text{N} - (\text{CH}_2 - \text{CH}_2 - \text{OH})_2$	MDEA

To achieve homogeneous colloidal systems the following technique has been used :

- Solubilizing the polyester in a water miscible solvent like THF
- Adding this organic solution to water containing the amine
- Stripping off the organic solvent under reduced pressure
- Adjusting with water the solid content of the colloidal system.

The micellar size of these colloidal dispersions is then determined by photon correlation spectroscopy (Coulter N4). Typical results are given in Figure 1, showing the variation of the particle size as a function of the neutralization degree α .

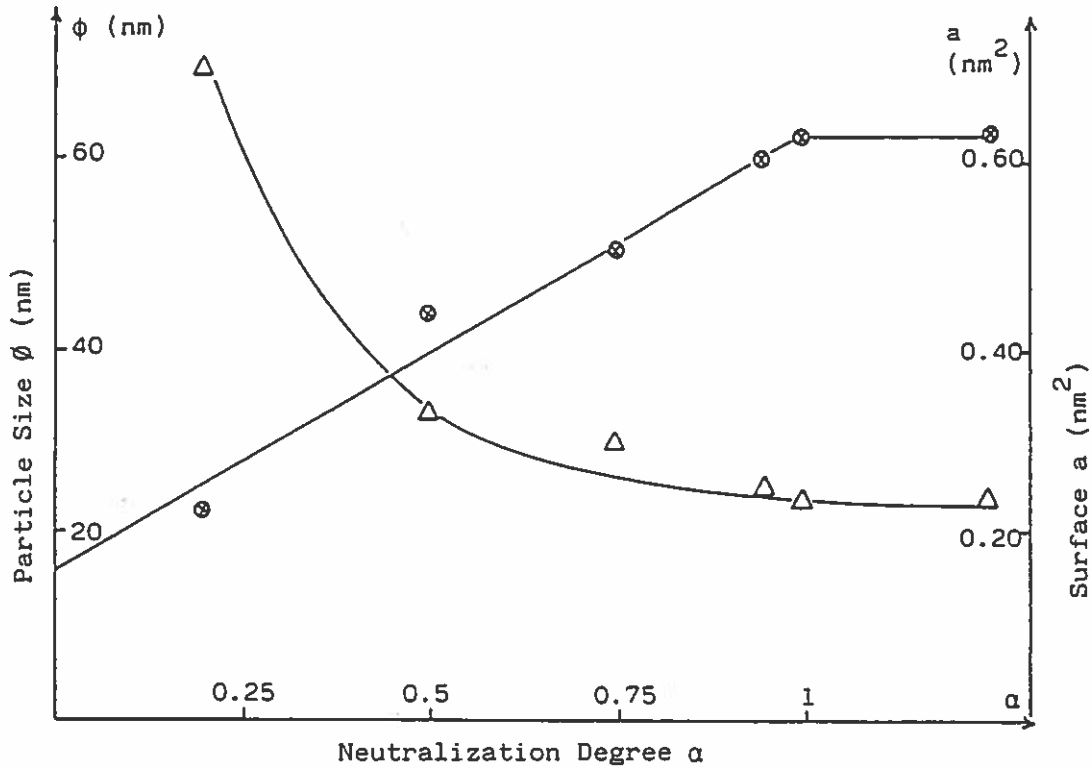


Figure 1 : Influence of the neutralization degree α on the particle size (ϕ) of the micelles and on the surface (a) occupied by one polyester chain. System MD 60 - MDEA.

$$\otimes a = f(\alpha) \quad \Delta \phi = f(\alpha)$$

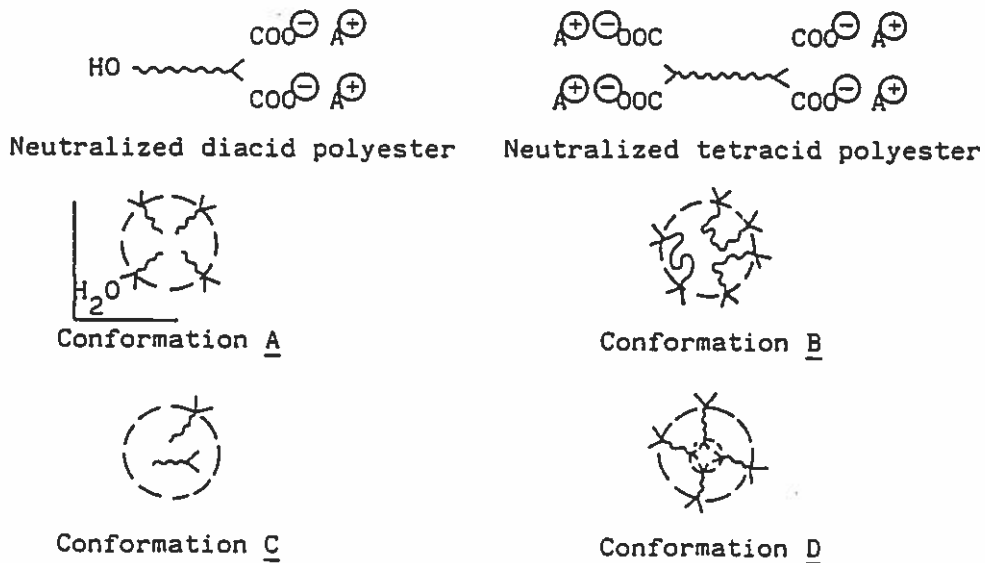


Figure 2 : Schematic representation of chain conformation in the micelles for neutralized diacid and tetracid polyesters.

This figure shows that aggregates are formed below complete neutralization of the polyester carboxy groups. The micelle size reaches a constant value above 100 % neutralization. The amine's slight volatility makes it usually necessary to work at a neutralization degree α of 1.05 to 1.25. It means an excess of 5 to 25 % amine with respect to the theoretical value.

We have systematically examined the micellar size of the different polyesters completely neutralized with the amines listed in Table 2. The size of the micelles is constant, within experimental errors, for a given completely neutralized polyester with an amine. Stable colloidal systems could be obtained with all samples (Table 3) except for sample T 60.

From the micelle size, the surface occupied by the hydrophilic part of one polyester molecule can be calculated, and thus the surface occupied by one carboxy group. This calculation is done assuming the density of the polyester in the micelle to be similar to bulk polyester and all the carboxy groups located on the micelle surface (conformation A and B given in Figure 2).

From Table 3 it appears that for the samples MD 60, MD 90, T 90 the surface occupied by one carboxy group is the same, i.e., in the range of 0.32 nm^2 . This is in agreement with the values of 0.34 to 0.51 nm^2 given by PAL et al. (1) for α , ω dicarboxylic acids.

It should be noted that the dicarboxylic polyesters (MD samples) are in fact a mixture containing theoretically 50 % diacid, 25 % tetracid and 25 % of non-carboxylated chains. If all the carboxy groups are located at the micelle surface, the average surface occupied by one carboxy groups would be 0.32 nm^2 as indicated previously. However if only one chain end of the tetracid is reaching the surface (conformation D in Figure 2) the surface occupied by one carboxy group located at the surface would be of 0.42 nm^2 .

We shall consider $a_1 = 0.32 \text{ nm}^2$ in the following, a value consistent for two diacid samples (MD 60 and MD 90) and one tetracid (T 90).

Based on this assumption and conformation C (Figure 2) we can calculate that the sample MD 120 has ≈ 15 % of the chains entrapped in the micelle. This is in agreement with the fact that this diacid sample has the highest hydroxy-to-acid index ratio and thus a slight excess of non-carboxylated chains (see Table 1).

Table 3 : Micellar Characteristics : Size, Surface occupied by Carboxy End Groups and Conformation

	Structure	Average diameter ϕ nm	a Surface per molecule nm	a ₁ Surface per carboxy group nm	Conformation*
MD 60 $\bar{M}_n = 1840$	diacid	23.7 ± 0.8	0.63 ± 0.02	0.315	A
MD 90 $\bar{M}_n = 1260$	diacid	15.9 ± 0.8	0.63 ± 0.03	0.315	A
MD 120 $\bar{M}_n = 990$	diacid	14.7 ± 1.1	0.54 ± 0.04	0.27	C 15 % of the chains entrapped
T 90 $\bar{M}_n = 2240$ $d = 1.24$	tetracid	14.0 ± 0.5	1.29 ± 0.04	0.32	B
T 120 $\bar{M}_n = 1750$	tetracid	15.6 ± 0.4	0.90 ± 0.02	0.225	40 % of chains in conformation B 60 % of chains in conformation D

* see Fig. 2 density of the polyester 1.24 ± 0.01

The same calculation for the tetracid sample T 120 indicates 60 % of the chains have only one end coming to the micelle surface (conformation D in Fig. 2). The remaining carboxy groups inside the micelle might associate in the form of clusters, as demonstrated for ionomer resins (2).

From Figure 1 (the particle size vs neutralisation degree α) we can also calculate the surface a occupied by one molecule. The variation of a vs α given in Fig. 1 shows that for $\alpha = 1$ one has a = 0.63 nm^2 , in agreement with the results given in Table 3. For $\alpha = 0$ the value of a is 0.16 nm^2 . This indicates at least a part of the non-neutralized COOH groups are located on the micelle surface. For classical surfactants, derived from fatty acids, such "mixed micelles" of neutralized and non-neutralized species are a well-established fact (3).

Acknowledgments

The authors wish to express their gratitude to "AKZO COATINGS" Montataire (France) for financial support of this work.

References

- 1) R.P. PAL, A.K. CHATTERJEE and D.K. CHATTORAJ, J. Colloid Interface Sci., 1975, 52 46
- 2) R.D. LUNDBERG, in Encyclopedia of Polymer Science Engineering, 2nd ed., Wiley New York, 1985, p. 393
- 3) A. SKOULIOS, Ann. Phys., 1978, 3, 421

ELECTROPHORETIC FINGERPRINTING FOR SURFACE CHARACTERIZATION OF COLLOIDAL PARTICLES

by

R. L. Rowell, S.-J. Shiau and B. J. Marlow
Department of Chemistry, University of Massachusetts,
Amherst, MA 01003.

PREPRINT: ACS/Boston
PMSE Div. Symposium on
Particle Size Analysis
in Polymer Science,
April 23-24, 1990.

INTRODUCTION

The zeta potential has been widely used as a characterizing parameter in colloid science (1). The zeta potential is the average potential at the surface of shear surrounding a moving colloidal particle so that it links the hydrodynamic radius with various theoretical models of the structure of the double layer. It is calculated from the measurable electrophoretic mobility $u_E = v_E/E$ which is the particle velocity under unit field strength.

In earlier work (2,3) we reported on modern instrumentation for measurement of the distribution of the electrophoretic mobility. Here we show that the average electrophoretic mobility may be represented as a function of two variables of state: the pH and the $p\lambda$ which is the negative log of the specific conductance (S/m). The representation of u_E as a function of pH and $p\lambda$ is called "electrophoretic topography" and yields a template or "fingerprint" (4,5) as well as details on the fine structure (2,3), i.e., the electrophoretic mobility distribution at a point in the pH- $p\lambda$ domain.

EXPERIMENTAL

The apparatus, a Pen Kem System 3000 Automated Electrokinetics Analyzer, is described elsewhere (2) and full experimental details may be obtained in (2,3,4 and 5).

RESULTS

In Figure 1 we show the template and fingerprint for a polystyrene latex containing acidic surface groups (carboxyl, R-CO₂H) and basic surface groups (amidine, R-C(NH)(NH₂)) so that the latex is zwitterionic. The behavior is dominated by the carboxyl group over a wide area in the pH- $p\lambda$ domain. The dashed envelope curve defines the locus in the pH- $p\lambda$ domain above which the mobility can be measured. The lower domain is shown by the curve-fitting program but it is inaccessible because changing the pH changes the conductance at the same time. Interesting features are the carboxyl-dominated ridge of stability over several orders of pH and the pronounced acid peak in mobility arising from protonation of the amidine group. The isoelectric line at pH 4 is independent of $p\lambda$ over more than two orders of magnitude giving a classic "isoelectric point." At high $p\lambda$, extrapolation of the pH- $p\lambda$ behavior predicts a migration of the isoelectric line toward more positive mobility or higher surface positive charge. Since double-layer compression acts to lower the mobility, the prediction is for specific adsorption of potassium ion at high $p\lambda$.

The fingerprint and template for the TiO₂-KCl system is given in Figure 2. Comparison of the two fingerprints (Figs. 1 and 2) readily shows the characteristic identity of each.

A set of fingerprints are shown in Figures 3 and 4 for two dispersions of carbon black which had a common ancestry. The oxidized carbon black powder, BLACK PEARLS® was manufactured by oxidation of the parent material, the non-oxidized REGAL 660®. Both materials were obtained from the Billerica, Massachusetts Research Laboratory of the CABOT Corporation. The pronounced differences in the fingerprints show the characteristic identity of each.

Finally, we note that each fingerprint is unique in this small catalog of four quite different colloidal systems.

ACKNOWLEDGEMENT

This work was supported by grants from the CABOT Foundation and a contract with the AMOCO Corporation. Technical assistance and instrument support was provided by Pen Kem, Inc. The work is based on the Ph.D. thesis of S.-J. Shiau, presently at DuPont Taiwan Ltd., 7th Fl. International Bldg., 8 Tung Hua North Rd., Taipei, Taiwan, R.O.C.

REFERENCES

1. Hunter, R. J. *Zeta Potential in Colloid Science*; Academic: New York, 1981.
2. Marlow, B. J.; Rowell, R. L. *J. Energy & Fuels* 1988, 2, 125.
3. Marganski, R. E.; Rowell, R. L. *J. Energy & Fuels* 1988, 2, 132.
4. Marlow, B. J.; Fairhurst, D.; Schutt, W. *Langmuir* 1988, 4, 776.
5. Morfesis, A. A.; Rowell, R. L. *Langmuir*, submitted.

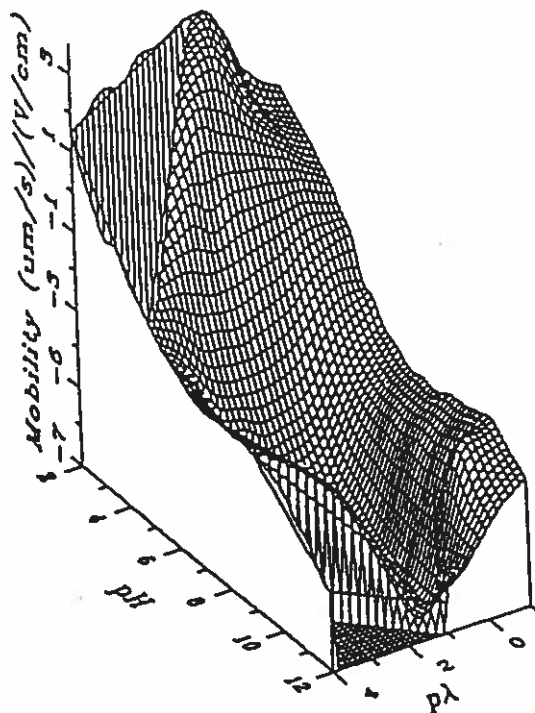
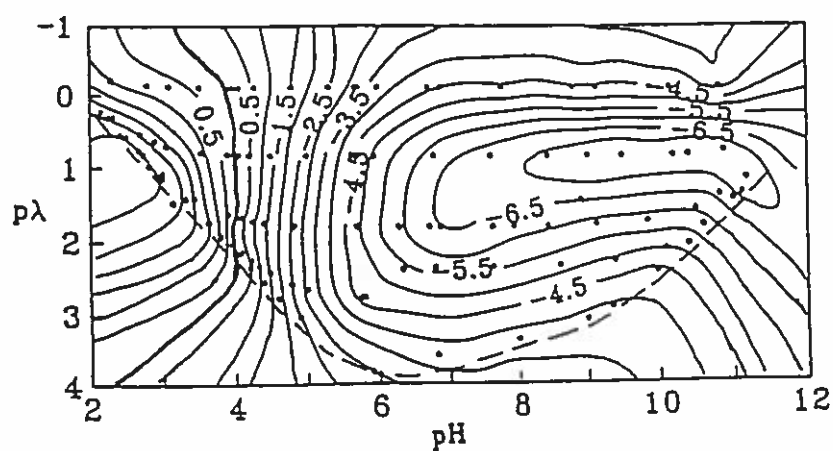


Figure1. The electrophoretic fingerprint and template of the carboxyl-amidine zwitterionic latex (PL-7).

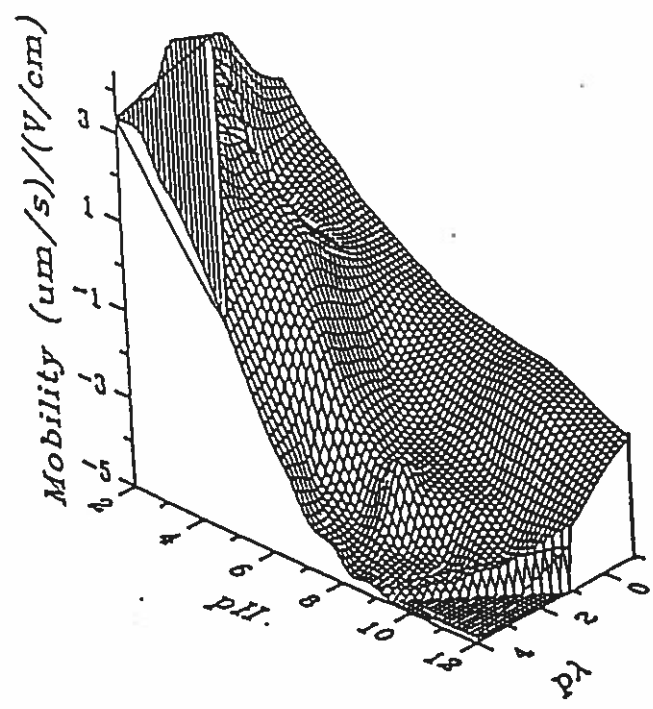
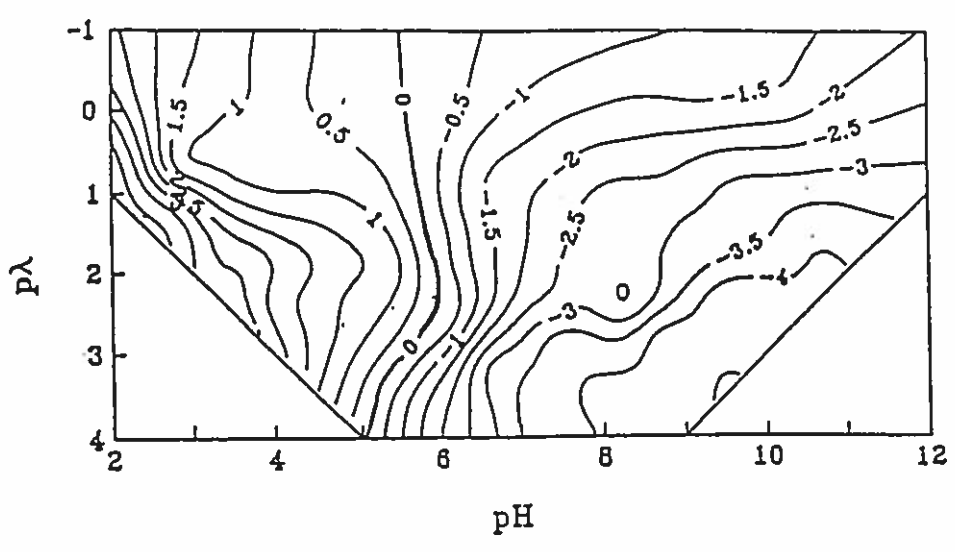


Figure 2. The electrophoretic fingerprint and template of the titanium dioxide-KCl system.

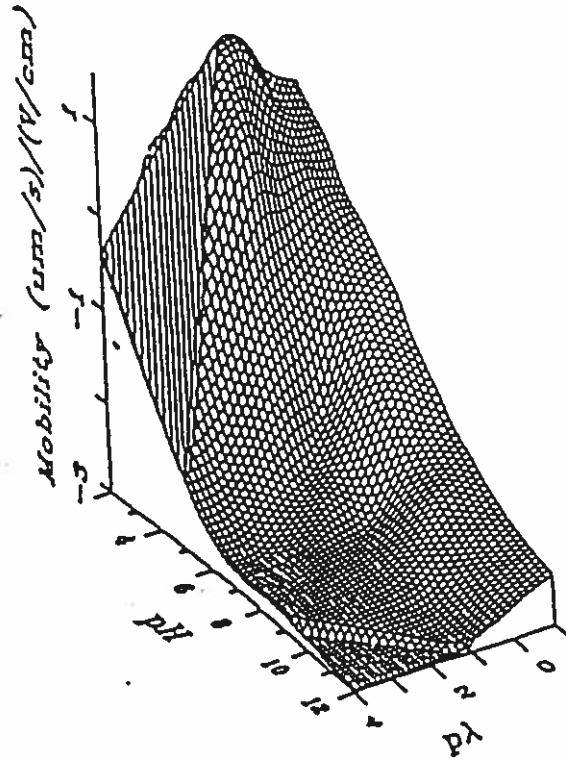
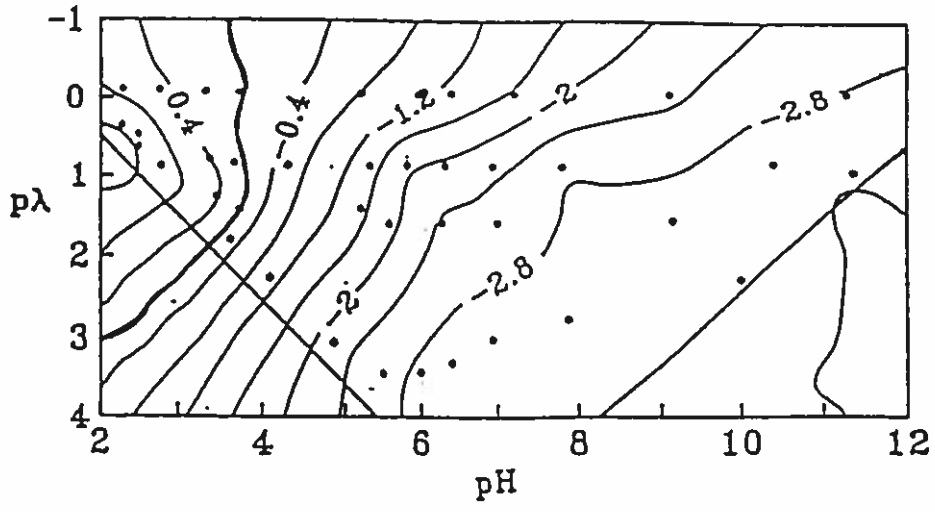


Figure 3. The electrophoretic fingerprint and template of the BLACK PEARLS® (oxidized carbon black) dispersion.

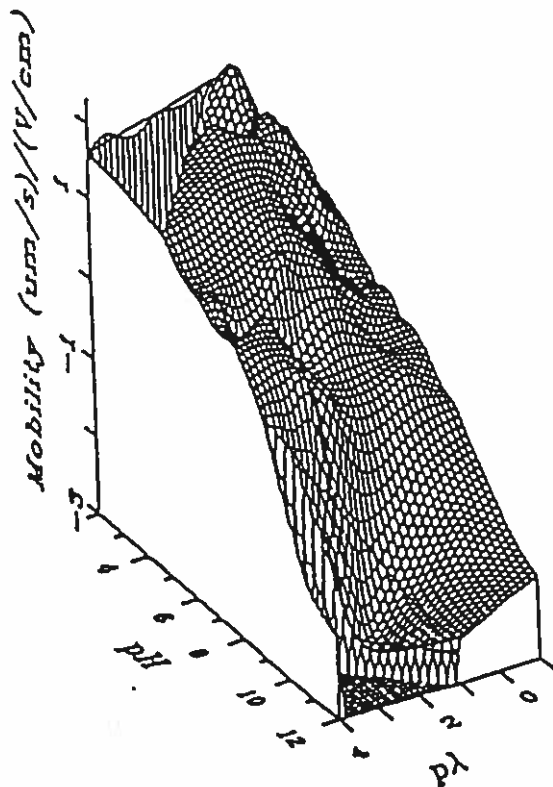
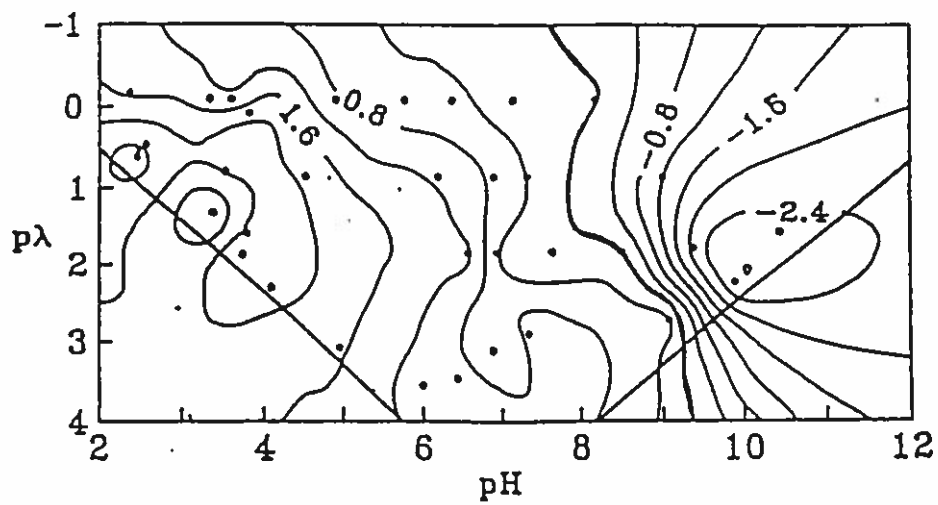


Figure 4. The electrophoretic fingerprint and template of the REGAL 660® (non-oxidized carbon black) dispersion.

Floc Coagulation in a Shear Field: Kinetics and Floc Structure

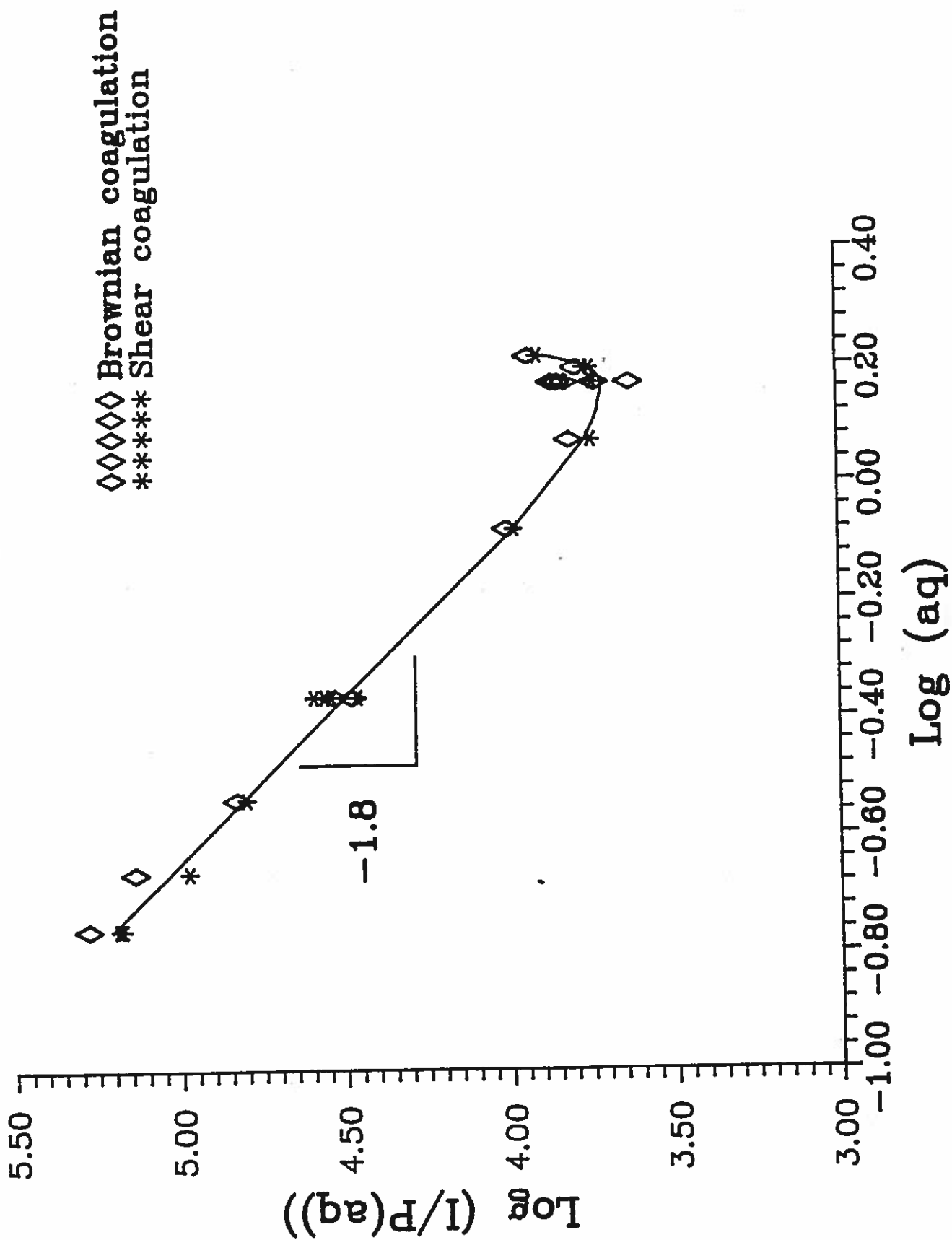
Frank E. Torres

Prof. W. B. Russel

Prof. W. R. Schowalter

Coagulation in a flowing suspension is governed by the colloidal and hydrodynamic interactions between the aggregating particles and flocs. Beyond the initial particle-particle coagulation step these interactions determine the structure of a floc being formed, and at the same time they depend on the structure of the aggregating flocs. To develop a better understanding of the coagulation process, we have examined both the internal structure and growth rate of flocs formed by rapid shear coagulation of dilute suspensions. Low surface charge polystyrene particles dispersed in 1.00 M NaCl solutions were used to ensure the formation of rigid flocs, and the suspending solvent was 36.00 % glycerol by weight to slow the coagulation to convenient rates. Floc sizes were measured by dynamic light scattering, and structure information was extracted from static light scattering spectra covering the domain $0.18 < q \cdot a < 1.7$, where q is the scattering wavenumber and a is the individual particle radius. Comparison of the results with results for flocs formed by Brownian coagulation reveals a similar structure for the two modes; in contrast, the growth kinetics for these two modes are inherently different, as expected. To model the growth behavior in a shear flow, we treat a porous floc as a body with a hydrodynamic radius which is less than the capture radius corresponding to floc-floc contact, and we compare predicted kinetics based on this model with data at several shear rates. In addition, we use our model for the growth kinetics to study the evolution of the floc structure.

Shear vs. Brownian Coagulated Aggregates



William B. Russel Department of Chemical Engineering
Princeton University
Princeton, NJ 08544-5263

Recent Publications:

Colloidal Dispersions, Cambridge University Press, 1989, 525 pp. [with D. A. Saville and W. R. Schowalter].

"Light scattering measurements of a hard sphere suspension under shear", *Phys. Fluids* A2, 491-502 (1990) [with N. J. Wagner].

RECEIVED

23 FEB 1990

Ans'd.

February 15, 1990

CONTRIBUTION TO THE INTERNATIONAL POLYMER COLLOIDS GROUP NEWSLETTER

Frank Saunders, Do Ik Lee
The Dow Chemical Company
Midland, Michigan 48874

The 22nd ACS Central Regional Meeting will be held in June 6-8, 1990 at Saginaw Valley State University with The Midland Section of American Chemical Society as a host. As part of the Meeting, Latex Symposium will be held on Thursday, June 7. Dr. Gary Poehlein, Georgia Institute of Technology, will deliver a plenary lecture for the symposium. His lecture will be followed by four presentations which are contributions from Dow Latex R&D. A tentative program for the symposium and the abstracts of the papers are as follows:

Latex Symposium

Thursday, June 7, 1990.

Symposium Chairman: Do-Ik Lee

- 9:00-10:00 AM PLENARY LECTURE---RECENT DEVELOPMENTS AND FUTURE DIRECTIONS IN EMULSION POLYMERIZATION. G.W. Poehlein, School of Chemical Engineering, Georgia Institute of Technology.
- 10:00-10:30 AM APPLICATION OF MAGNETIC RESONANCE SPECTROSCOPY TO POLYMER COLLOIDS. C.J. McDonald, The Dow Chemical Company.
- 10:30-11:00 AM DSC STUDIES OF COALESCING AID INTERACTIONS WITH LATEX FILMS. Dennis H. Guthrie, Ralph G. Czerepinski, The Dow Chemical Company.
- 11:00-11:30 AM CURING EFFECTS FROM LATEX MODIFICATION OF UREA-FORMALDEHYDE FOR FIBERGLASS MAT. James Galloway, Sally Kokke-Hall, Joan Marshall, Charles Kan, and Creig Kelly, The Dow Chemical Company.
- 11:30-12:00 AM INTERFACIAL VISCOELASTICITY OF GELATIN-SURFACTANT SOLUTIONS. Kostas S. Avramidis, The Dow Chemical Company; Tsung-Shann Jiang, Department of Chemical and Biochemical Engineering, Rutgers Univeristy.

RECENT DEVELOPMENTS AND FUTURE DIRECTIONS IN EMULSION POLYMERIZATION AND LATEX TECHNOLOGY. G. W. Poehlein, School of Chemical Engineering, Georgia Institute of Technology, Atlanta, Georgia 30332-0370.

Emulsion polymerization and latex technology could be considered a mature field. Synthetic latexes have been produced for commercial use for more than half a century and natural polymer colloids were used by early man. In spite of this rather long history the area of emulsion polymerization and latex technology continues to be a dynamic area for research and new developments. Some of the important advances and recent trends, primarily as they are related to emulsion polymerization reactions, will be reviewed in this talk. Specifically, advancements in characterization techniques and in the understanding of reaction mechanisms and kinetics will be related to developments in polymerization reaction engineering which permit production of designed latexes.

APPLICATION OF MAGNETIC RESONANCE SPECTROSCOPY TO POLYMER COLLOIDS.
C. J. McDonald, Dow Chemical Company, 1604 Building, Midland, Michigan 48674

The formation of polymer colloids has been investigated extensively, but still is subject to controversy because of limitations in the characterization data. Magnetic resonance spectroscopy is a powerful tool for examining emulsions in that it can analyze for both the specific polymer components and kinetic processes. The polymer components include the serum continuous phase, the surface and the particle structure. Each is unique because of the monomer distribution in the polymerizing emulsion.

An investigation of two emulsions polymer systems has illustrated the capability of NMR. An acrylamide modified ethyl acrylate latex was quantitatively analyzed in terms of composition and surface reactivity. Surface processes such as hydrolysis of the amide, desorption of surface components and the dynamics of the hydrated molecules at various distances away from the surface could be identified. An interpenetrating network system involving styrene, n-butyl acrylate and a crosslinking monomer, allyl methacrylate, was also studied. Here the relaxation processes involved in pulse Fourier transform NMR were valuable in the analysis of network structure. The information developed with the NMR technique was much more sensitive than that obtained from differential scanning calorimetry and electronmicroscopy. The influence of diluents, present during formation of the network, was also examined.

DSC STUDIES OF COALESCING AID INTERACTIONS WITH LATEX FILMS.
Dennis H. Guthrie and Ralph G. Czerepinski, Designed Latex Research, 1604 Building, Dow Chemical USA, Midland, Michigan 48674

Differential Scanning Calorimetry (DSC) has been used to examine the reduction in latex film glass transition temperature (T_g) caused by formulation with coalescing aids (fugitive plasticizers). For typical paint latexes, the glass transition temperature drops nearly linearly with coalescent until an apparent saturation value is approached, typically near 20 weight percent based on polymer. Beyond this apparent saturation, additional coalescent lowers the apparent T_g only slightly. Observed T_g 's correspond well with minimum film formation temperatures, and they appear to be independent of pigmentation below the critical pigment volume. In the case of coalescing aids having extremely low water solubility, and for those having extremely high water solubility, freshly dried latex films with high coalescent levels did not appear to achieve equilibrium by the time DSC measurements were made. Rationales for the various observations are presented based on solubility and transport properties of the various coalescing aids.

CURING EFFECTS FROM LATEX MODIFICATION OF UREA-FORMALDEHYDE FOR FIBERGLASS MAT. James Galloway, Sally Kokke-Hall, Joan Marshall, Charles Kan, Creig Kelley, Dow Chemical Company, 1604 Building, Midland, Michigan 48674.

Urea-formaldehyde resin is used as a binder for fiberglass mats in the roofing industry. Latex is commonly added to the urea-formaldehyde resin to improve binder performance by reducing the sensitivity of the binder to curing conditions. The purpose of this study was to determine how the latex reduces the sensitivity of the binder to curing conditions.

Electron microscopy was used to visually determine the effect of latex addition to the urea-formaldehyde resin. The resin matrix, the mat structure, and the binder location were studied. Dramatic structural differences were observed between the all urea-formaldehyde binder and the latex modified urea-formaldehyde. The addition of latex reduces the cracking and debonding, which occur upon high temperature curing of the urea-formaldehyde binder without latex.

Dynamic mechanical analysis showed that latex addition extends the modulus and loss-tangent over a broader cure range. Various types of urea-formaldehyde resins were studied alone and with latex addition levels of up to 30%.

INTERFACIAL VISCOELASTICITY OF GELATIN-SURFACTANT SOLUTIONS. Kostas S. Avramidis, Dow Chemical USA, Designed Latex Research, 1604 Building, Midland, MI 48674, and Tsung-Shann Jiang, Department of Chemical and Biochemical Engineering, Rutgers University, P. O. Box 909, Piscataway, NJ 08854

The viscoelastic behavior of a phase interface can accurately be determined using the biconical surface viscometer constructed in our laboratory. Using the balance equations for a dividing surface and the non-linear Boussinesq surface model we obtain the governing relationships for the viscometer. The rheological properties of the phase interface between air the gelatin-surfactant solutions are studied as functions of the imposed frequency of oscillation and solution temperature. For the solution at 40°C the surfaces are found to be viscoelastic with the viscous portion of the surface shear viscosity exhibiting a minimum in the neighborhood of the natural frequency and the elastic portion exhibiting a maximum. The effect of temperature on the interfacial behavior is more pronounced as the temperature increases from 38°C to 40°C than it is when the temperature increases from 40°C to 42°C.

From Ph.D. thesis: Fiber and Polymer Science Program, North Carolina State University, April 1990.

ABSTRACT

TAYLOR II, MAYLON BRUTEN. The Kinetics of Radiation-Induced Inverse Emulsion Polymerization of Vinylpyrrolidone. (Under the direction of Richard D. Gilbert and Vivian T. Stannett.)

An experimental investigation has been made of the inverse emulsion polymerization of vinylpyrrolidone. Specifically, the kinetics of inverse emulsion polymerization of vinylpyrrolidone were contrasted with radiation-induced suspension and bulk polymerization of vinylpyrrolidone.

The radiation-induced inverse emulsion polymerization of 3.0M aqueous vinylpyrrolidone in an isoparaffinic hydrocarbon oil was shown to result in PVP in viscosity average molecular weights from 1 - 2.7 million. Rapid, high conversions were obtained that had a dependency of R_p on $[I]$ or dose rate to the first power. The rate was given by the expression

$$R_p = 5.73[I] + 11.0$$

where R_p is in units of moles/liter/sec $\times 10^4$. Deviation from the expected Smith-Ewart Case II kinetics was explained on the basis of degradative chain transfer.

Variation in emulsifier composition by incorporation of a polymeric surfactant lead to substantial increases in rate of polymerization, decreases in particle sizes, and higher molecular weights of PVP to a certain compositional concentration of Hypermer B246 (ICI Corporation).

At higher levels, an essentially monodisperse particle size was also obtained which was attributed to a shorter nucleation period.

Higher molar concentrations of vinylpyrrolidone were found to gel irreversibly during polymerization due to the lack of solubility of the polymer in the monomer/water mixture.

The bulk polymerization was shown to also follow a first-order dependence of R_p on dose rate and is given by the expression:

$$R_p = 4.29[I] + 3.0$$

where R_p is in units of moles/liter/sec $\times 10^4$. For both the bulk and emulsion case, a certain contribution was noted from thermal initiated polymerization. Viscosity average molecular weights were of the order of 350,000 for the bulk polymerization.

Conversions were found to be much higher in the inverse emulsion polymerizations (90+%) over those in the bulk polymerizations (50%). Further, molecular weights for inverse emulsion polymerization were often as much as ten times higher than those of the bulk polymerizations. Procedural and characterization techniques are fully described.

CONTRIBUTIONS TO THE
INTERNATIONAL POLYMER COLLOIDS GROUP NEWSLETTER

Polymer Colloid Research at the
Institute of Polymer Chemistry (IPOC)
Academy of Sciences of GDR
Kantstr. 55, Teltow-Seehof, 1530 GDR
Reporter: Klaus Tauer

At the IPOC there has been a tradition in Polymer Colloid Research for about 15 years. In the past main topics of our investigations were several kinetic aspects of vinyl chloride emulsion polymerization (particle formation, particle coalescence, particle growth, high conversion phenomena, modeling particle size distribution) as well as preparation and properties of PVC pastes (rheology and viscosity properties of PVC pastes, PVC-plasticizer interactions, modeling steady shear viscosity of PVC pastes). Preparation and characterization of polymer dispersions are still topics at the IPOC. Nowadays the following projects are concerned with polymer colloids:

1. Emulsion polymerization in presence of polymerizable surfactants and surface active initiators

We investigate the influence of these new auxiliary materials on the mechanism of emulsion polymerization regarding particle number, particle diameter, molecular weight, rate of polymerization and application properties.

Maleic acid and acrylamido derivatives prepared in our laboratory are mainly employed as polymerizable emulsifiers. The results show until now, that it is possible to obtain stable high concentrated polymer latexes with improved properties, regarding the much lower content of residual free emulsifier, by employing monmeric surfactants.

Regarding the polymerization mechanism exist great differences between nonpolymerizable and polymerizable emulsifiers in

dependence on the initiator is water soluble or oil soluble.

Novel azo initiators prepared in our laboratory are employed as free radical generators. These initiators enable the preparation of high solid polymer dispersions without additional stabilizing agents. The influence of different initiator - emulsifier systems on latex and polymer properties are investigated by comparing emulsion polymerization with these new initiators without additional emulsifiers and AIBN or persulfate in the presence of emulsifiers.

Another topic of our investigations is the determination of decomposition rates of these new azo initiators by esr spectroscopy.

First results were presented at the Smolenice meeting "Radical Polymerizations in Heterogeneous Systems", April 10-14 1989, and will be published in "Die Makromolekulare Chemie" (Die Makromolekulare Chemie, Macromol. Symp. 31 (1990) 107-121). The investigations will be continued and progress will be reported in future.

2. Preparation, modification and characterization of special latexes for medicine and diagnostics

Procedures for the preparation, modification of latexes with special properties (dyed particles, fluorescence labelled particles, magnetic particles and activated particles) for applications in medicine and diagnostics are investigated in this project. The goal is to find better ways for preparation procedures over a wide range of particle sizes (from 50 nm up to several μm) and modification possibilities.

3. Preparation of model-latexes - Rheological and film formation studies

The dependence of viscosity of polymer dispersions on polymer volume fraction, shear rate, electrolyte content and surface charge density has been studied for nearly monodisperse electrostatic stabilized polystyrene and PMMA-latexes.

Nearly monodisperse homopolymer particles have been prepared as model-latexes over a wide range of particle sizes without

changing the kind of emulsifier and initiator, only persulfate and sodium dodecylsulfate were used. Volume fraction, surface coverage with emulsifier and ionic strength of aqueous phase can be adjusted to desired values (compare: H. Zecha, Die Makromolekulare Chemie, Macromol. Symp. 31 (1990) 169-200). Nearly monodisperse latexes with particle morphology of the core-shell type of about equal sizes with possibilities to vary the amount of core and the shell respectively as well as the composition of both have been prepared for film formation studies.

4. Film formation and film properties of emulsion polymers

The aim of this work is to study the dependence of the film forming behavior (minimum film formation temperature, MFT) and of the film properties on the size, the composition and morphology of the latex particles.

Models of film formation from polymer latexes have been reexamined and a formal criterium for interdiffusion was introduced. Expected particle size effects have been found experimentally only within a critical film formation range.

5. Preparation of aqueous macroemulsions from concentrated polymer solutions

The formation of macroemulsion by a phase inversion process has been studied for the preparation of aqueous polymer emulsions which can be used as binders for paints on the basis of concentrated solutions of chlorinated ethylen and rubber. A set of parameters has been studied to control droplet sizes and emulsion stability. Droplet sizes are strongly dependent on the amount and the HLB-value of nonionic emulsifier or the used emulsifier mixtures, on polymer solution viscosity and on "stirring"-conditions. It has been shown that a certain Reynolds number in the region of the phase inversion point is effective - independent on solution viscosity - to produce the minimal achievable particle sizes below 5 μm .

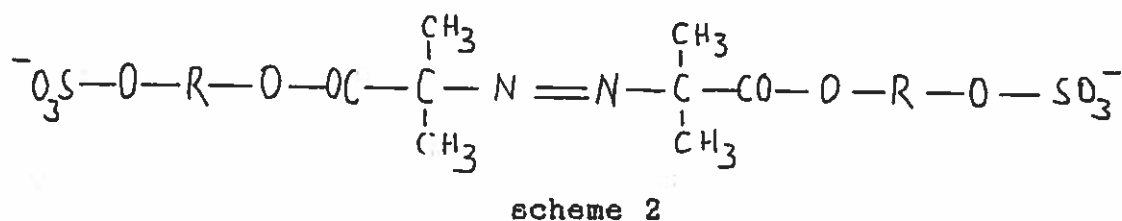
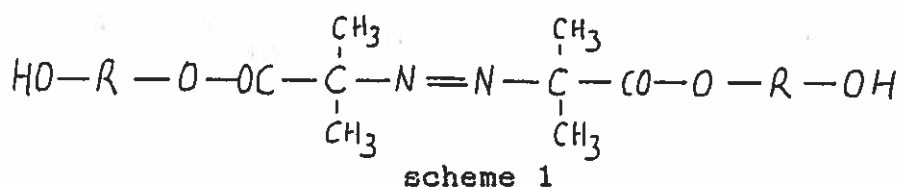
IPOC Polymer Colloid Research:

Decomposition kinetics of novel azoinitiators

Sabine Kosmella, Klaus Tauer

We started in 1985 a project concerning the synthesis and application in emulsion polymerization of novel azoinitiators. These initiators act additionally as stabilizer, e. g. emulsion polymerization can be carried out to high solid contents in the absence of common emulsifiers or stabilizer. The initiators we have investigated are the reaction products of AIBN and different α, ω -diols according to a procedure of WALZ, BÖHMER and HEITZ (1). In a second reaction step the end-standing hydroxyl groups have been converted into ionic groups, preferentially into sulfate groups.

We investigated the decomposition kinetics by esr spectroscopy in co-operation with the Polymer Institute of the Slovak Academy of Sciences in Bratislava (V. Vaskova, Z. H.Louiskova). The esr measurements were provided with a VARIAN 4 spectrometer. We investigated non sulfated (scheme 1) as well as sulfated (scheme 2) derivatives. The initiator decomposition was observed by measuring the decrease in the concentration of stable NO-radicals, which were added to the initiator solution before the reaction was started. The non-sulfated derivatives were investigated in toluene with 4-benzoyloxy-2,5-bis(dimethyl)-piperidin-N-oxide as stable radical inhibitor. The sulfated initiators were investigated in water with 4-hydroxy-2,5-bis(dimethyl)-piperidin-N-oxide stable radical inhibitor. Water was used as solvent for esr measurements although the well known problems.



By this procedure of measurements the reaction of the initiator radicals with the inhibitor radicals is detected and thus, the values of the radical gain, $2fka$, can be determined. Typical $2fka$ -values at 60 °C for sulfated and non-sulfated initiators obtained from different diols and initiator concentrations of $3 \cdot 10^{-2}$ mole.l⁻¹ are as follows:

Non-sulfated derivatives:

Diol	$2fka/s^{-1}$
AIBN	$1,16 \cdot 10^{-6}$
Poly(ethylene glycole) 200	$8,02 \cdot 10^{-7}$
Poly(ethylene glycole) 600	$1,79 \cdot 10^{-7}$
Decane-1,10-diol	$1,72 \cdot 10^{-7}$
Octadecane-1,18-diol	$9,30 \cdot 10^{-8}$

Sulfated derivatives:

Diol	$2fka/s^{-1}$
Poly(ethylene glycole) 200	$5,67 \cdot 10^{-7}$
Hexane-1,6-diol	$2,02 \cdot 10^{-7}$
Decane-1,10-diol	$9,26 \cdot 10^{-8}$

Compared with AIBN it is to see, that with increasing chain length of the different diols the $2fka$ -values become lower. The highest $2fka$ -values is estimated for AIBN.

From Arrhenius plots the following activation energies for the $2fka$ -values were calculated:

Diol	EA/kJ mole ⁻¹
Poly(ethylene glycole) 200 (sulfated)	12,11
Poly(ethylene glycole) 200 (non-sulfated)	84,94
Decane-1,10-diol (non-sulfated)	85,50

The activation energy for the sulfated Poly(ethylene glycole)

derivative is surprisingly low compared to the non-sulfated products. A satisfactory explanation of this fact can not be given at this time. Further investigations including polymerization experiments are necessary. The results concerning the esr investigations are prepared for a publication in "Die Makromolekulare Chemie".

On the progress of this work will be reported in future.

(1) R. Walz, B. Böhmer, W. Heitz

Makromol. Chem. 178 (1977) 2527-2534

IPOC Polymer Colloid Research:

Latexes for Applications in Biology and Medicine

Bernd R. Paulke

In our department of radical polymerization emulsion and emulsion co-polymerization as well as dispersion polymerization are applied for the synthesis of special polymer latexes for applications like immunological agglutination tests, particle enhanced microparticle immunoassays, phagocytosis and cell labelling studies, but also the magnetic cell labelling studies, but also the magnetic cell separation technique. This work takes place in co-operation with leading medical research departments of the G.D.R. as well as agricultural research and pesticide control utilities.

The particle size of the products ranges from 20 nm up to 10 μ m. Synthesis methods and polymerization recipes incline towards very narrow particle size distributions as a supposition for most of these applications. The microspheres synthesized consist of polystyrene or poly-methylmethacrylate modified with several co-monomers that supply the functional groups situated at the particle surface. Methods for the equipment of the particles with a magnetic core, color or fluorescence were developed. The actual investigations are concerned with the combination of different particle equipment parameters.

IPOC Polymer Colloid Research:

Emulsion Polymerization with Monomeric Emulsifiers

Karl-Heinz Goebel; Katrin Stähler

The opinions about the mechanism of emulsion polymerization initiated by AIBN are controversially. Unsolved experimental problems may be one of the reasons.

It's well known that AIBN is a strong catalyst for organic radical reactions, e. g. for oxidations /1/. May be AIBN is only in-situ converted into a peroxide catalyst /2/, combined with the change of

- the solubility in water and in the monomer droplets
- the activation energy of the initiator decomposition

Therefore the use of AIBN in EP requires the absence of oxygen.

The reproducibility of the results obtained by the usual batch polymerization in three-necked glass reactors was bad. This difficulty insufficiently should only avoided by a change of the polymerization procedure. Appropriate amounts of monomer, monomeric emulsifier (Sodium Sulfo Propyl Myristyl Maleate) and water were added to the polymerization tube, and the tube was sealed after removing oxygen by several freeze and thaw cycles (oxygen free N₂, 10⁻³ mbar).

The polymerization was carried out by tumbling the tubes end-over-end at about 50 RPM for a period of 20 hours in a water bath at a temperature of 60 °C + 0,1 °C. The series A tubes were sealed by melting under vacuum, the Series B tubes by ground stoppers. The results are shown in Fig. 1 and Fig. 2. Starting in Series A with oxygen saturated water we got a particle concentration which is twice as large as for oxygen free conditions. This shows additionally to Fig. 1 and Fig. 2 that oxygen indeed has a strong influence on the kinetics of emulsion polymerization started by AIBN.

/1/ Pohlmann, A. and Mill. Th.: J. Org. Chem. 48 (1983) 2133

/2/ Ziegler, K., Deparade, W. and Meye, W.:

Liebigs Ann Chem. 567 (1950) 141

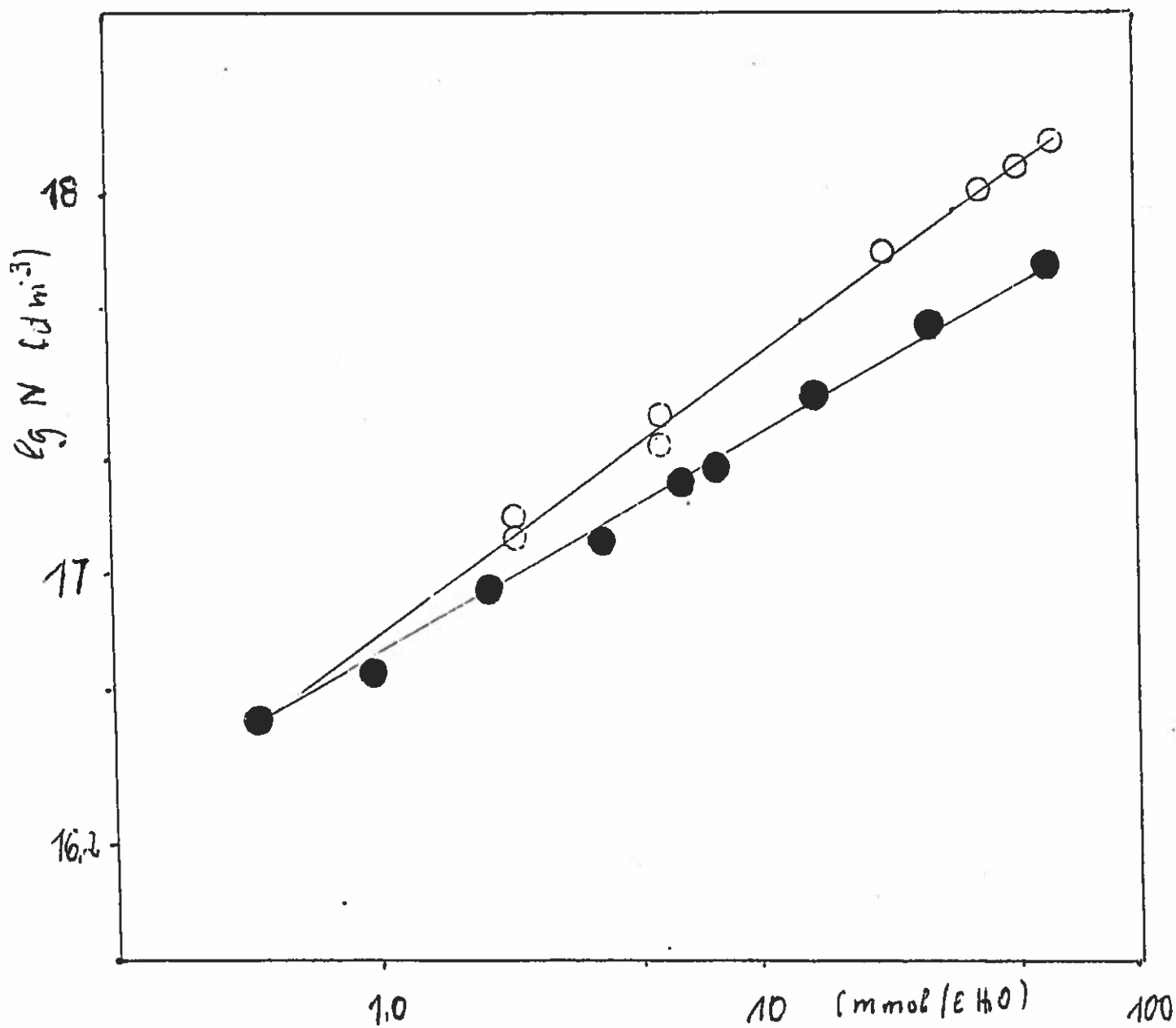


Fig. 1 Double logarithmic plot of the particle concentration versus the micellar concentration of the monomeric emulsifier SSPM

Serie A; Slope = 0,6

Serie B; Slope = 0,7

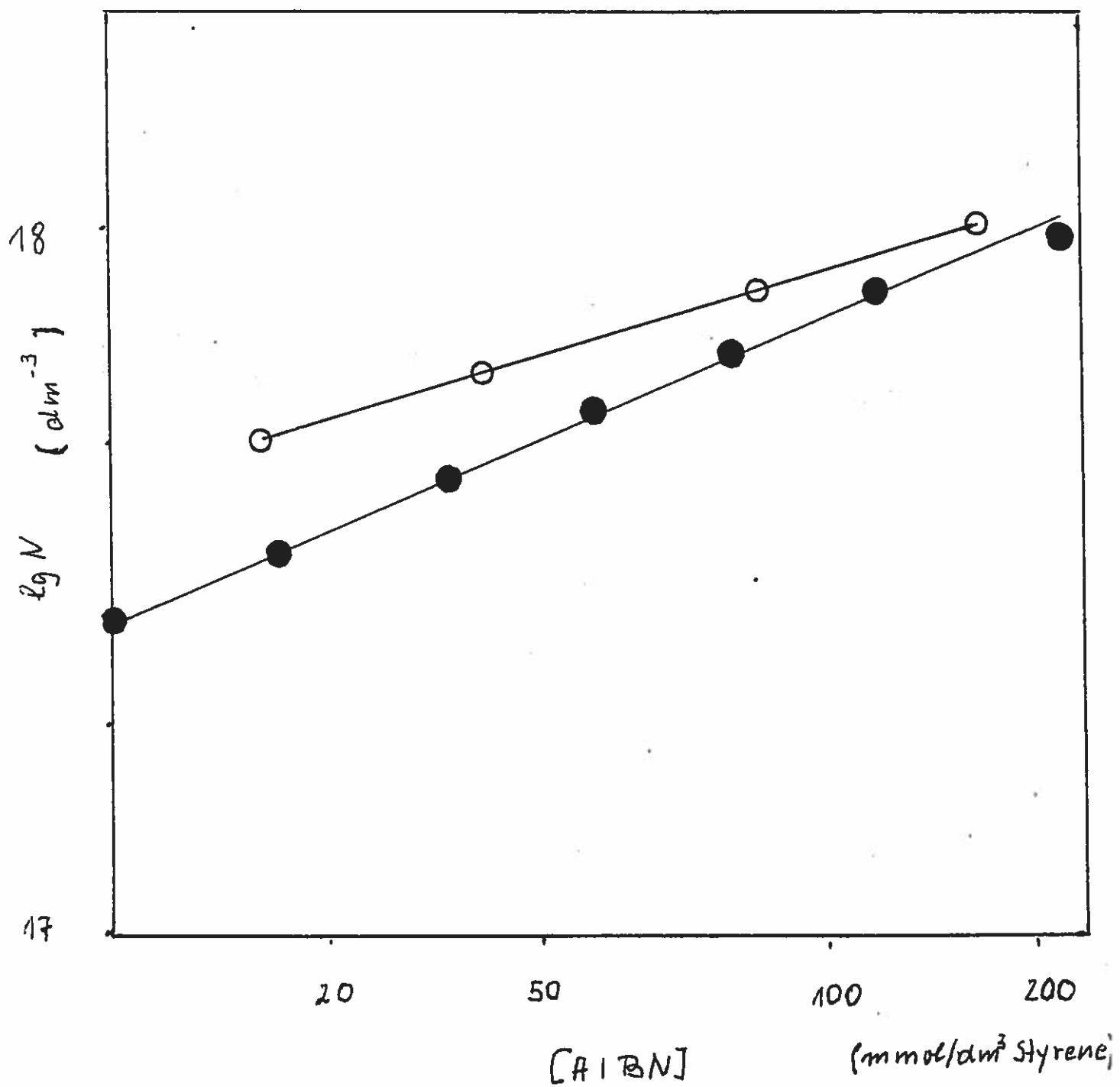


Fig. 2 Double logarithmic plot of the particle concentration versus the AIBN-concentration

Serie A; Slope = 0,5

Serie B; Slope = 0,3

IPOC Polymer Colloid Research:

Rheology of polymer dispersions

Helmut Zecha, Karl Wulf, Hartmut Schlacken, Eckhard Görnitz

- The dependence of viscosity on volume fraction and shear rate has been studied for nearly monodisperse electrostatic stabilized polystyrene latexes at high ionic strength. A particle size effect - different from hard sphere behavior - has been described assuming rotating particle clusters.

- The dynamic viscoelastic behavior of nearly monodisperse PMMA- and polystyrene latexes has been studied in dependence on volume fraction and electrolyte content. The surface potential has been calculated from shear modulus according to the model given by Goodwin et al.. It has been shown that the counter ion concentration which depends on surface charge density and volume fraction has to be taken into account to describe the experimental shear modulus data.

- Estimating the dependence of viscosity on surface charge density we found a maximum. It seems that this can be explained on the basis of the particle pair potential dependence on surface loading taking again into account the concentration of counter ions.

- A theoretical work has just been finished: On the basis of the multiple scattering theory of Freed and Muthukumar H. Schlacken has calculated the coefficient of the viscosity-concentration power series up to third order. The result for a monodisperse hard-sphere-suspension is

$$\eta_r = 1 + 2,5\phi + 4,683\phi^2 + 30,264\phi^3 + \dots$$

Furthermore the second coefficient has been discussed for a binary hard-sphere-mixture as well as for a monodisperse soft-potential suspension.

- Experimental work has been started to measure the swelling behavior of carboxylated particles in dependence on pH-value

changing polymer composition and particle morphology. First results show that the swelling (formation of a hydrodynamic effective surface layer) is restricted to a small subsurface layer of the particles, the swelling is reversible in some cases. Besides a further understanding of the complex swelling behavior of latex particles taking into account electrolyte effects the aim of this work is to correlate the swelling with the shear viscosity of concentrated latexes.

- Further work is concerned with the modeling of steady state shear viscosity in dependence on particle size distribution using bimodal systems. Aqueous and non-aqueous dispersions will be studied.

IPOC Polymer Colloids Research

Contribution to the Polymer Colloids Group News letter

Helmut Zecha

Institute of Polymer Chemistry "Erich Correns"

Kantstraße 55, Teltow-Seehof, GDR 1530

ASPECTS OF FILM FORMATION FROM POLYMER
LATEXES

Several attempts have been made to describe film formation from polymer latexes and to formulate "criteria" of film formation. Most of the derivations yield to expressions of the form first published by BROWN /1/

$$GR/\gamma \leq K(f) \quad , \quad \text{deformation} \quad f = (\pi\sqrt{2}/6)^{1/3} \quad (1)$$

$K(f) = 5,4 \dots 266$ from different approaches. The temperature dependent shear modulus was attributed to pure elastic or visco-elastic deformation. In our analysis - briefly summarized here - two driving forces are considered between particles 1 and 2 in a hexagonal close packing (Fig. 1): F_{α} , due to curvatures air/liquid g_L and particle/liquid R , and F_K , due to the curvatures a and g_K of direct particle contact:

$$F_{\alpha} = \sqrt{2/3} \pi R \gamma_F \cos^2 \psi + \sqrt{6}/6 \pi R \gamma_F \cos^2 \psi (1 + R/g_L) \quad (2)$$

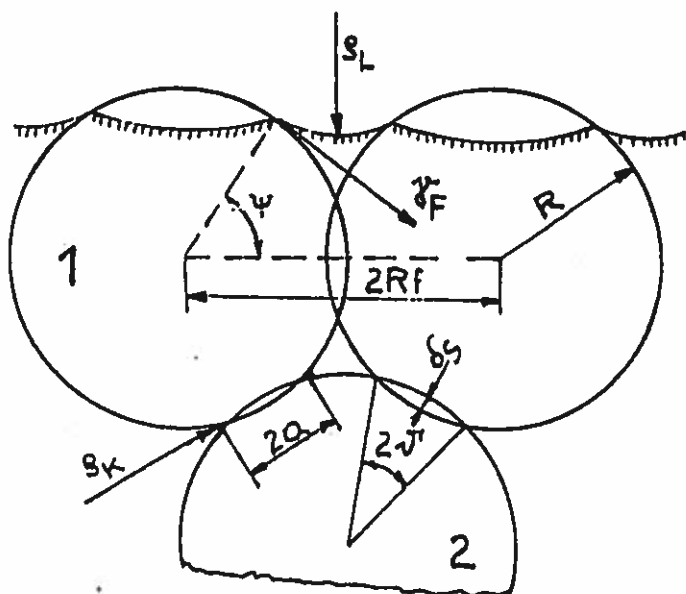
$$F_K = \pi a^2 \gamma_{sL} \left(\frac{1}{g_K} - \frac{1}{a} \right) = 2\pi R \gamma_{sL} (1-f) \left(\frac{\cos \psi}{1 - \cos \psi} - (2(1-f))^{-1/2} \right) \quad (3)$$

On the other hand two resistant forces are taken into account:

$F_{G,K}$, due to (visco)-elastic deformation, and F_D , due to the necessity of interdiffusion:

$$F_{G,K} = \frac{16}{3} a^3(t) \frac{1}{R} G^* = \frac{16}{3} G^* R^2 (2(1-f))^{3/2} \quad (4)$$

$$F_D = K \frac{kT}{D_s t} \frac{\pi a^2}{\sigma_s} (2(1-f))^{5/2} = K \frac{kT}{D_s t} \pi R (2(1-f))^{5/2} \quad (5)$$



$$S_L = R \left(\frac{1 - \cos \psi}{\cos \psi} \right)$$

$$S_K = R \left(\frac{1 - \cos \gamma'}{\cos \gamma'} \right)$$

$$\gamma' = \arctan (a/Rf)$$

$$a = (R(1-f))^{1/2}$$

$$\gamma_F = \gamma_{S,L} + \gamma_{L,g} \cos \theta$$

Fig. 1 Film formation from polymer latexes : considered parameters

Eq. 5 was derived from an expression given by GEGUSIN /2/, experimental determination of diffusion coefficients as previously published /3/ should allow to verify the constant K in Eq. 5. Following "criteria" for film formation may be defined:

$$F_{G,\alpha} \leq F_\alpha, \quad F_{G,\alpha} \leq F_K \quad \text{or} \quad F_{G,\alpha} \leq F_\alpha + F_K \quad (6)$$

$$F_D \leq F_\alpha, \quad F_D \leq F_K \quad \text{or} \quad F_D \leq F_\alpha + F_K \quad (7)$$

The criterion, Eq. 6, shows a particle size influence according to Eq. 1 whereas Eq. 7 indicates no influence of the particle dimension.

Applying Eq. 6 it is possible to describe a just published dependence of complex shear modulus G^* - measured at the minimum film formation temperature (MFT) - on particle size /4/. Conditions for calculation and results are given in Fig. 2.

From Fig. 2 it may be concluded, that the Eq. 6 criterion is only valid for the very beginning of film formation (deformation $f = 0.98$) but that even in this stadium the interfacial force F_K is effective due to direct particle contact. Further particle coalescence during film formation should be described rather by Eq. 7.

Among other things, the question arises, what deformation "f" the particles underlie during the film formation. From direct measurements of the contact circle radius "a" /4/ deformations

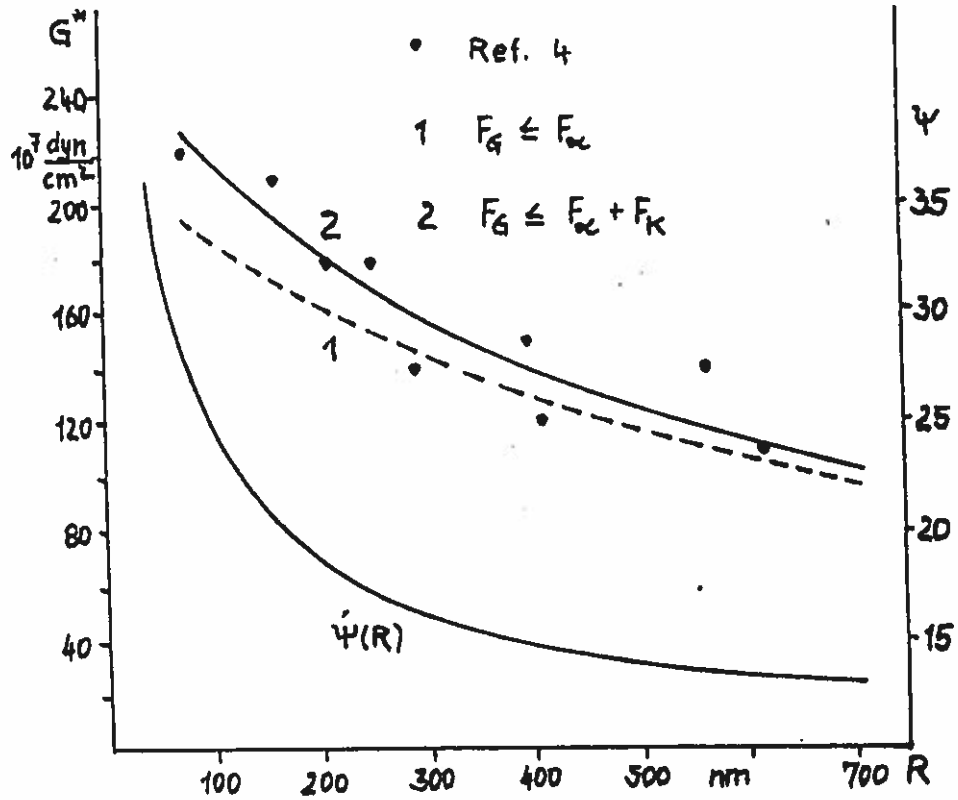


Fig. 2 Particle size dependence of G^* (MFT)
 $f = 0.98$ $\gamma_F = 60 \text{ dyn/cm}$ $\gamma_{s,l} = 30 \text{ dyn/cm}$

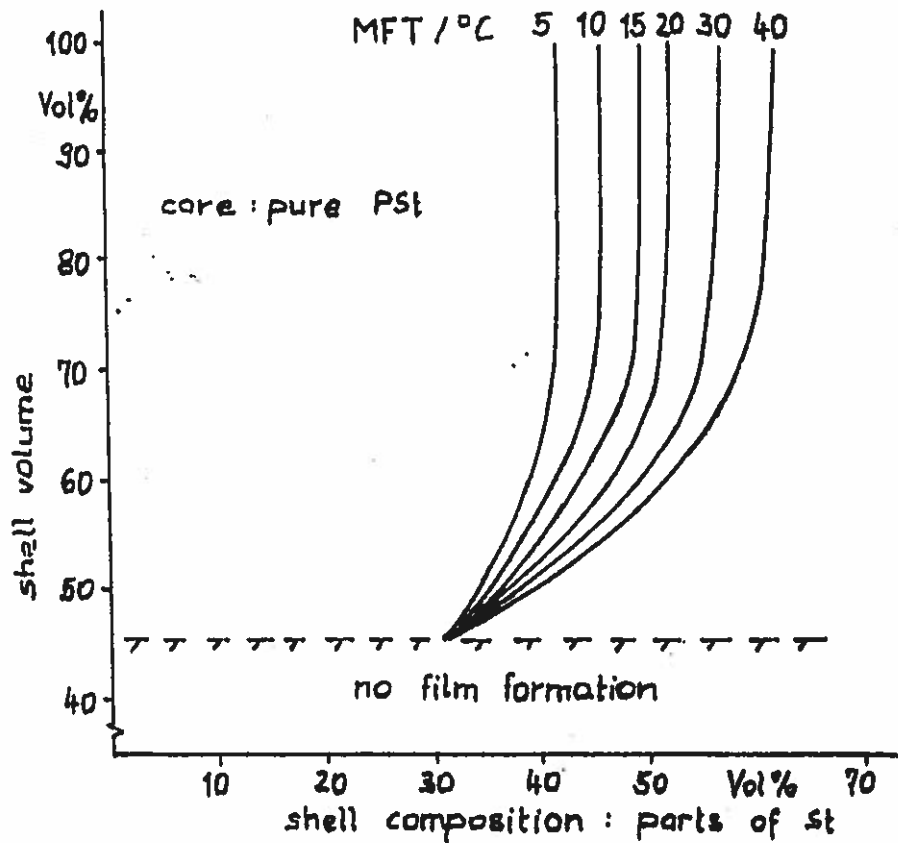


Fig. 3 MFT isotherms for film formation of St/BA core-shell-latexes

scattering between 0.69 ...f... 0.80 without dependence on particle size are found (discussion of the authors /4/ is different). Our MFT-measurements using core-shell structured particles indicate that a hard core-volume larger than 25 ... 30 Vol% already had an influence on the MFT (Fig. 3). From both facts one comes to the conclusion that much more of the particle volume is introduced in the film formation process than normally assumed from only asking for the deformation value "f" at which all holes within the particle packing disappear. Changing polymer composition and morphology as shown in Fig. 3, a region is observed where very small changes of composition or morphology will produce large differences of MFT values. A small influence of particle size on MFT could be stated only in this region.

The derivations to describe the film formation contain certain detail problems, further progress especially regarding the modeling of the MFT require new approaches such as the formulation of the inner stress state within the drying latex film.

REFERENCES

- /1/ G. L. Brown
J. Polymer Sci. 22 (1956) 423
- /2/ Compare: W. A. Bjeluj, W. A. Dowgjal, O. R. Jurkjewitsch
Polimernije Pokrijtija, Nauka i Technika, Minsk 1976
- /3/ K. Hahn, G. Ley, H. Schuller, R. Oberthür
Colloid Polymer Science 264 (1986) 1092
Colloid Polymer Science 266 (1988) 631
- /4/ S. T. Eokersley, A. Rudin
Journal of Coatings Technology 62 (1990) 89

RELATIONSHIPS FOR PREDICTING COMPOSITE PARTICLE MORPHOLOGY

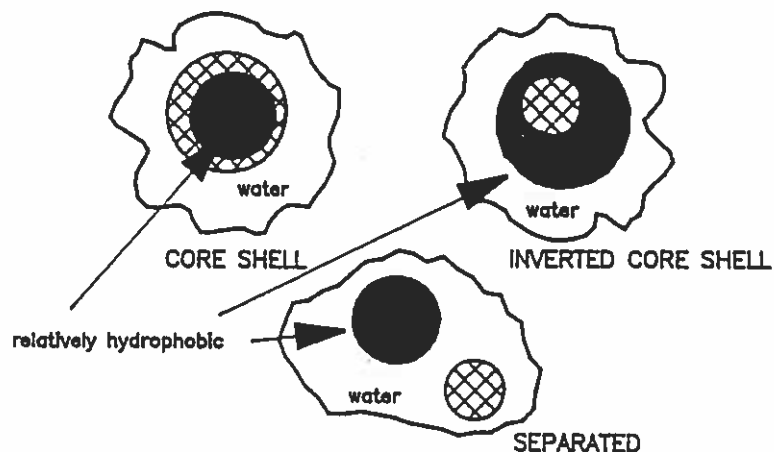
J A Waters, ICI Paints, Slough, UK

This note gives the derivation of relationships which have proved useful to show which of three extreme particle morphologies is thermodynamically preferred for a given system. The system comprises two disperse phase components in a third and continuous component. The derivation was included in a presentation at the last Gordon Conference on Polymer Colloids.

Composite latex particles comprising two dissimilar polymers have been prepared and studied over a long period (Ref.1). A variety of particle morphologies has been claimed, supported by evidence obtained with electron microscopy, surface analysis, DSC, DMA, particle sizing techniques and other methods. New particle structures and improved methods for preparing and controlling the processes continue to be published. Colloidally-stable microencapsulated particles may also be considered as composite latex particles, for example, where inorganic pigment such as titanium dioxide is enveloped by a layer of polymer and the particles are similar in size to latex particles. Particles of this sort are of increasing commercial importance.

For aqueous systems, the three extreme morphologies may be considered to be CORE-SHELL, in which the more hydrophilic component (H) constitutes a shell, interfacing with the water phase and the more hydrophobic or lyophilic (L) component constitutes the core; INVERTED CORE SHELL which is the converse with the more lyophilic component providing the shell; and SEPARATED where both components interface with the water.

The free energy for each of the three extreme arrangements differ principally in the total interfacial energy. Several workers have pointed to the importance of interfacial energy in promoting the particle morphology (Refs. 2,3).



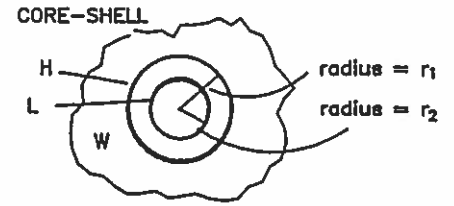
The total interfacial energy of CORE-SHELL

$$E_{CS} = 4\pi r_2^2 \gamma_{H-L} + 4\pi r_1^2 \gamma_{H-W}$$

the volume of component L = v_L
 the volume of component H = v_H
 and the total volume ($v_H + v_L$) = V

$$r_1 = (3V/4\pi)^{1/3} \quad \text{and} \quad r_2 = (3v_L/4\pi)^{1/3}$$

$$\text{and } E_{CS} = 4\pi K [v_L^{2/3} \gamma_{H-L} + v_H^{2/3} \gamma_{H-W}] \quad (I) \quad [K = (3/4\pi)^{2/3}]$$



Similarly, for the INVERTED CORE-SHELL it can be seen that

$$E_{INV} = 4\pi K [v_H^{2/3} \gamma_{H-L} + v_L^{2/3} \gamma_{L-W}] \quad (II)$$

and for the SEPARATED arrangement

$$E_{SEP} = 4\pi K [v_H^{2/3} \gamma_{H-W} + v_L^{2/3} \gamma_{L-W}] \quad (III)$$

CORE-SHELL is preferred over INVERTED CORE-SHELL if

$$E_{CS} < E_{INV}$$

and it can be seen from equations (I) and (II) that this condition is met if

$$v_L^{2/3} \gamma_{H-L} + v_H^{2/3} \gamma_{H-W} < v_H^{2/3} \gamma_{H-L} + v_L^{2/3} \gamma_{L-W} \quad (IV)$$

A fractional volume (v) may be defined such that

$$v_H = v_H / V ; \quad v_L = v_L / V \\ v_H = v_H V ; \quad v_L = v_L V ; \quad v_H + v_L = 1$$

Substituting fractional volumes into the above relationship (IV)

$$v_L^{2/3} v_H^{2/3} \gamma_{H-L} + v_H^{2/3} \gamma_{H-W} < v_H^{2/3} v_L^{2/3} \gamma_{H-L} + v_L^{2/3} \gamma_{L-W} \\ (\gamma_{L-W} - \gamma_{H-W}) > \gamma_{H-L} (v_L^{2/3} - v_H^{2/3})$$

That is, CORE-SHELL is preferred over INVERTED CORE-SHELL

$$\text{if } \frac{\gamma_{L-W} - \gamma_{H-W}}{\gamma_{H-L}} > v_L^{2/3} - v_H^{2/3} \quad (V)$$

Similarly CORE-SHELL is preferred over SEPARATED ($E_{CS} < E_{SEP}$)

$$\text{if } \frac{\gamma_{L-W} - \gamma_{H-L}}{\gamma_{H-W}} > \frac{1 - v_H^{2/3}}{v_L^{2/3}} \quad (VI)$$

These relationships between an expression for the three interfacial energies and an expression for the two fractional volumes, provide phase diagrams as in Figure 1.

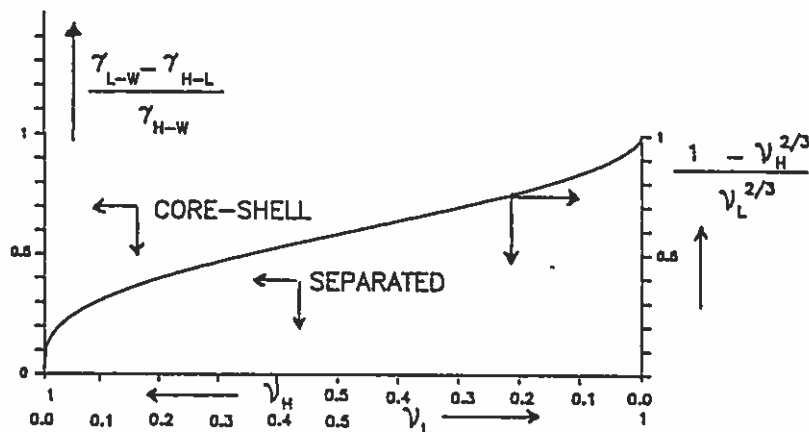


Figure 1. Phase diagram for CORE-SHELL vs. SEPARATED.

For a given system, the fractional volume expression can be calculated from the relative volumes of the two components. The interfacial energy expression may be determined at least approximately from the Young-Dupre equation, by assembling a representative model system (Figure 2) and measuring the contact angle. It is essential to include surfactants which are present in the real systems.

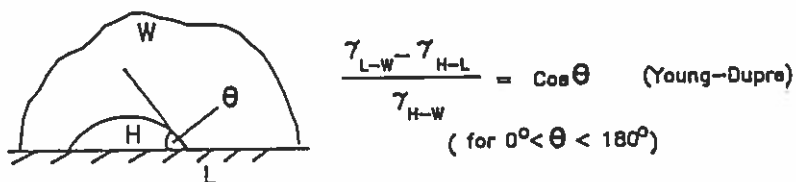


Figure 2. Measurement of interfacial energy expression.

The expression (VI) is based on an inequality, and despite errors when measuring the contact angle, it has been possible to assess the expression for a variety of systems and to predict successfully whether CORE-SHELL or SEPARATED morphology is preferred.

References

1. J C Daniel, Makromol. Chem. Suppl. 10/11 359 (1985).
2. J Berg, D Sundberg and B Kronberg. "Polym. Materials Sci. Eng." ACS Symp. series 54 (1986).
3. V L Dimonie, Y C Chen, M S EL Aasser, J W Vanderhoff. "Deuxieme Colloque International sur les Copolymerisations et les Copolymeres en Milieu Disperse", Lyon, 81 (1989).

Title: POLY(STYRENE-ETHYLENE OXIDE)
BLOCK COPOLYMER MICELLE FORMATION¹
IN WATER: A FLUORESCENCE PROBE STUDY¹

Authors: Wilhelm, M; Zhao, C-L; Wang, Y; Xu, R; Winnik, M.A.*; Mura, J-L; Riess, G; Croucher, M.D.

Abstract:

Block copolymer micelle formation was studied by a combination of fluorescent probe and quasi-elastic light scattering [QELS] techniques. The polymers, polystyrene-poly(ethylene oxide) diblock and triblock copolymers, with M_n values ranging from 8,500 to 29,000, form spherical micelles in water over the entire concentration range over which QELS signals can be detected. Pyrene [Py] in water ($6 \times 10^{-7} M$) partitions between the aqueous and micellar phases, accompanied by three changes in the pyrene spectroscopy. There is a red shift in the excitation spectrum, a change in the vibrational fine structure of Py fluorescence (I_1/I_3 decreases from 1.9 to 1.2) and an increase in the fluorescence decay time (from 200 to ca. 350 ns) accompanying transfer of Py from an aqueous to a hydrophobic micellar environment. From these data, critical micelle concentrations (range: 1 to 5 mg/L) and partition coefficients (3×10^5) can be calculated.